

HUMBOLDT-UNIVERSITÄT ZU BERLIN



**LEBENSWISSENSCHAFTLICHE FAKULTÄT
INSTITUT FÜR BIOLOGIE**

**MASTERARBEIT
ZUM ERWERB DES AKADEMISCHEN GRADES
MASTER OF SCIENCE**

*„Establishment of a method for the detection of proviral cDNA of
HERV-K(HML-2)“*

*„Etablierung einer Methode zum Nachweis von proviraler cDNA von
HERV-K(HML-2)“*

vorgelegt von
Mirjam Yasemine Langenegger

angefertigt in der Arbeitsgruppe HIV und andere Retroviren
am Robert Koch-Institut Berlin

Berlin, im Juli 2016

Table of contents

LIST OF ABBREVIATIONS	1
ZUSAMMENFASSUNG	4
ABSTRACT	5
1. INTRODUCTION	6
1.1. TAXONOMIC CLASSIFICATION OF THE HUMAN IMMUNODEFICIENCY VIRUS (HIV)	6
1.1.1. RETROVIRUSES	6
1.1.2. MORPHOLOGY AND STRUCTURE OF RETROVIRUSES	7
1.1.3. GENOMIC ORGANIZATION OF RETROVIRUSES	8
1.2. HIV AND AIDS	9
1.2.1. AIDS: HISTORY	9
1.2.1.1. Discovery	9
1.2.1.2. Origin	10
1.2.2. AIDS: EPIDEMIOLOGY	10
1.2.3. HIV: REPLICATION	11
1.2.4. HIV: PATHOGENESIS	12
1.2.5. ANTIVIRAL HOST DEFENSE AND ACCESSORY PROTEINS	13
1.2.6. HIV: ANALYSIS OF POST ENTRY EVENTS AND INTEGRATION	16
1.3. HERV-K(HML-2)	17
1.3.1. ENDOGENOUS RETROVIRUSES (ERV)	17
1.3.1.1. Human endogenous retroviruses (HERV)	18
1.3.2. INFECTIVITY AND TROPISM OF HERV-K113	19
2. OBJECTIVES OF THE MASTER'S THESIS	20
3. MATERIALS AND METHODS	21
3.1. MATERIALS	21
3.1.1. KITS	21
3.1.2. BACTERIAL STRAINS	21
3.1.3. EUKARYOTIC CELL LINES	21

3.1.4. CONSTRUCTS AND VECTORS	22
3.1.5. PRIMERS	22
3.1.6. ANTIBODIES	23
3.1.7. SOFTWARE	23
3.2. METHODS	24
3.2.1. DNA-ANALYTICS	24
3.2.1.1. Polymerase Chain Reaction (PCR)	24
3.2.1.2. Restriction digestion with help of endonucleases	31
3.2.1.3. DNA agarose gel electrophoresis	32
3.2.1.4. Purification and isolation of DNA fragments	32
3.2.1.5. Cloning into pCR4-TOPO® vector	33
3.2.1.6. Transformation	34
3.2.1.7. DNA measurement	34
3.2.2. CELL CULTURE	34
3.2.2.1. Cultivation of HEK-293T cells	34
3.2.2.2. Cultivation of CrFK cells	35
3.2.2.3. Cultivation of C8166 cells	36
3.2.2.4. Cell counting	37
3.2.2.5. Transient transfection with PolyFect® Transfection Reagent	38
3.2.2.6. Transient transfection with calcium phosphate	38
3.2.2.7. Production of pseudotyped HERV-K(HML-2) reporter viruses	39
3.2.2.8. Purification of cell culture supernatant using ultracentrifugation	40
3.2.2.9. Infection of CrFK cells	40
3.2.2.10. Infection of C8166 cells with HIV-1HIB via spinoculation	41
3.2.2.11. Cell lysis for production of genomic DNA and Luciferase Assay	41
3.2.2.12. Isolation of genomic DNA	42
3.2.2.13. Direct cell lysis for sample preparation	42
3.2.3. PROTEIN ANALYTICS	43
3.2.3.1. Luciferase assay	43
3.2.3.2. ELISA	43
3.2.4. 2^{-DDC_T} METHOD FOR CALCULATION OF RATIO BETWEEN TWO CDNA SAMPLES IN REAL-TIME QPCR	46
4. RESULTS	47
4.1. PRODUCTION OF HIV- AND HERV-K(HML-2)-REPORTER VIRUSES AND INFECTION ASSAY	47
4.1.1. PRODUCTION OF REPORTER VIRUSES	47
4.1.2. ELISA FOR NORMALIZATION OF VIRUS PARTICLE LOAD BEFORE INFECTION	48

4.1.3. LUCIFERASE ASSAY FOR DETERMINATION OF INFECTION RATE OF HERV-K AND HIV-1 REPORTER VIRUSES	49
4.2. REAL-TIME QPCR	50
4.2.1. REAL-TIME QPCR WITH SYBR GREEN I DYE OR TAQMAN PROBES	50
4.2.2. REAL-TIME SYBR GREEN QPCR FOR HIV-1 RT PRODUCTS IN CHRONICALLY INFECTED T-CELL LINE (ACH-2) COMPARED TO AN UNINFECTED T-CELL LINE (C8166) USING SYBR GREEN I DYE	51
4.2.3. REAL-TIME SYBR GREEN DUPLEX QPCR FOR RT PRODUCTS OF PLASMID-BASED HIV-1 REPORTER VIRUSES	54
4.2.4. STUDY OF HERV-K(HML-2)-POST-ENTRY EVENTS IN REAL-TIME DUPLEX QPCR AND DIGITAL DROPLET PCR	56
4.2.4.1. Measurement of HERV-K(HML-2) vDNA and 2-LTR-circles	56
4.2.4.2 Production of a positive template control (PTC) containing a mutation in the U3-region of the 5'LTR for use in real-time duplex qPCR	58
4.2.4.3. Detection of relocated mutation in 5'LTR by means of real-time duplex qPCR	61
4.2.4.4. Detection of relocated mutation in 5'LTR by means of droplet digital PCR	62
5. DISCUSSION	65
5.1. PRODUCTION AND INFECTIVITY OF PLASMID-BASED HERV-K REPORTER VIRUSES	65
5.2. ACH-2 CELLS AS VALID MODELS FOR MEASUREMENT OF HIV-1 VIRAL DNA?	66
5.3. PLASMID BACKGROUND PREVENTS ANALYSIS OF CDNA FROM PSEUDOTYPED HIV-1 REPORTER VIRUSES IN REAL-TIME SYBR GREEN DUPLEX QPCR	66
5.4. REAL-TIME DUPLEX QPCR USING TAQMAN PROBES FOR DETECTION OF HERV-K(HML-2) CDNA	67
5.5. DROPLET DIGITAL PCR FOR DETECTION OF SINGLE HERV-K(HML-2) CDNA COPY NUMBERS	68
5.6. INFECTION STUDIES OF HERV-K(HML-2) REPORTER VIRUSES	69
5.7. OUTLOOK	69
6. SUPPLEMENT	70
ACKNOWLEDGEMENT	84
DECLARATION OF AUTHORSHIP	85

List of abbreviations

AB	antibody
AIDS	acquired immune deficiency syndrome
Amp	Ampicillin
APOBEC3	apolipoprotein B mRNA-editing, enzyme-catalytic, polypeptide-like 3
ART	Antiretroviral drug
Bp	Base pair
BSA	Bovine serum albumin
CA	Capsid protein
cDNA	complementary DNA
CrFK	Crandell Rees feline kidney
CCR5	C-C chemokine receptor type 5
Conc.	concentration
CRISPR system	clustered, regularly interspaced short palindromic repeats system
ddPCR	Droplet digital PCR
DMEM	Dulbeccos Minimal Essential Medium
DMSO	Dimethylsulfoxid
DNA	Desoxyribonucleic acid
dsDNA	double-stranded DNA
dsRNA	double-stranded RNA
EDTA	Ethylenediaminetetraacetic acid
ELISA	Enzyme Linked Immunosorbent Assay
Env	envelope
ETOH	Ethanol
FCS	fetal calf serum
FDA	Food and Drug Administration (US)
FISH	Fluorescence <i>in situ</i> hybridization
g	gravitational acceleration
Gag	group specific antigen
gDNA	genomic DNA
gp	glycoprotein
h	hour

2x HBS buffer	2x Hepes Buffered Saline buffer
HEPES	4-(2-hydroxyethyl)-1-piperazineethanesulfonic acid
HERV	human endogenous retrovirus
HIV	human immunodeficiency virus
HLA	human leukocyte antigen
HS	hot start
HTLV	human T-lymphotropic virus
IL-1	interleukin-1
IN	integrase
kb	kilo base pair
LB	Luria-Broth (bacteria medium)
LTR	long terminal repeat
mM	millimolar
MMTV	Mouse Mammary Tumor Virus
min	minute
NF- κ B	nuclear factor of κ B
NK cell	natural killer cell
NTC	no template control
NTP	nucleotriphosphate
OD	optical density
PAMP	pathogen-associated molecular pattern
PBMC	peripheral blood mononuclear cell
PBS	phosphate-buffered saline
PCR	Polymerase chain reaction
pDNA	plasmid DNA
PM	2% milk in PBS
PMT	2% milk and 0.05% Tween in PBS
Pol	polymerase
PR	protease
PRR	pattern-recognition receptor
PTC	positive template control
qPCR	Quantitative PCR
RISC	RNA-induced silencing complex
RLU	Relative light unit
RNAi	RNA interference

rpm	rounds per minute
RPMI	Roswell Park Memorial Institute medium
RT	reverse transcriptase
RT/PIC	Reverse transcription- /pre-integration complex
SAMHD1	SAM-and HD-domain-containing protein 1
SHIV	Simian/Human immunodeficiency virus
SIV	simian immunodeficiency virus
TAR	trans-activation response
TAE buffer	TRIS-acetate-EDTA buffer
TE buffer	10 mM Tris-Cl, pH 7.5-1 mM EDTA buffer
T _m	temperature of melting
TM	transmembrane protein
TNF	tumor necrosis factor
TREX1	3'-reparation-endonuclease 1
TRIM5 α	tripartite motif protein 5 α
Tris	2-amino-2-hydroxymethyl-propan-1,3-diol
TU MM	TaqMan Universal Master Mix (Thermo Fisher Scientific)
U	unit
vDNA	viral DNA
VSV-G	glycoprotein G of vesicular stomatitis virus

Nucleic acid codes

A	Adenine
C	Cytosine
G	Guanine
T	Thymine

Zusammenfassung

Humane endogene Retroviren (HERVs) konnten viele Millionen Jahre lang Proviren in die menschliche Keimbahn integrieren. Jedoch führten im Laufe der Jahre Mutationen, Deletionen und Rekombinationen zu deren Inaktivierung. Heute haben alle bekannten HERV-Proviren die Fähigkeit zur Replikation eingebüßt. Jedoch wurden Transkripte und virale Partikel einer HERV-Gruppe (HERV-K(HML-2)) in verschiedenen kranken menschlichen Geweben nachgewiesen. Vorangegangene Studien mit rekonstruierten HERV-K(HML-2)-Viren konnten eine Infektion in gewissen Zelllinien nachweisen. Jedoch konnte keine Integration gemessen werden, was einen post-Entry, pre-Integrations-Block vermuten lässt. Bei welchem Schritt nach dem Zelleintritt dieser Block auftritt und welche zellulären Faktoren daran beteiligt sind ist unbekannt. In der vorliegenden Arbeit wurde versucht, in infizierten Zellen HERV-K(HML-2) cDNA nachzuweisen als Hinweis auf Reverse Transkription. Untersuchungen zum Infektionsprozess von HERV-K(HML-2) mittels Plasmid-basierenden Reporterviren wurden in der Vergangenheit bereits unternommen. Jedoch bestand das Problem, dass die cDNA, also das Produkt der Reversen Transkription, nicht unterschieden werden konnte von der kontaminierenden Plasmid-DNA. Als Lösung hierfür bot sich an, eine bestimmte Mutation in die Plasmid-DNA einzufügen, welche sich –durch intramolekulare Umlagerungen während der Reversen Transkription- verdoppelt und in der cDNA gleich zwei Mal vorhanden ist. Die cDNA unterscheidet sich so in ihrer Sequenz von der Plasmid-DNA und kann mit spezifischen Primern detektiert werden. Dieses mutierte Plasmid wurde in einer vorangehenden Arbeit hergestellt und nun als Vorlage für die Produktion von HERV-K(HML-2) Reporterviren genutzt. In der vorliegenden Arbeit wurden HERV-K(HML-2) und HIV-1 Reporterviren hergestellt, welche mit zwei unterschiedlichen Hüllproteinen, Env VSV-G und HIV-1 Δ KS, pseudotypisiert wurden. Es konnte gezeigt werden, dass mit Env VSV-G pseudotypisierte Reporterviren hochinfektios sind, während Reporterviren welche mit HIV-1 Δ KS pseudotypisiert waren, keine Infektion nachwiesen. Mittels eines Luziferase-Tests konnte ein Unterschied in der Infektion zwischen HERV-K(HML-2) und HIV-1 Reporterviren gezeigt werden, wobei das Maximum bei HERV-K(HML-2) nach 24 Stunden gemessen wurde und bei HIV-1 nach 48 Stunden. Die DNA aus den infizierten Zellen konnte isoliert und auf den Gehalt von viraler DNA untersucht werden. Hierfür wurde einerseits die real-time duplex qPCR und die droplet digital PCR angewendet. Es konnte gezeigt werden, dass sich die droplet digital PCR dank ihrer höheren Sensitivität besser für HERV-K(HML-2) Infektionsstudien eignet, da sie selbst einzelne DNA-Kopien misst. Auch konnte die Verlässlichkeit der Mutation in der U3-Region zur Unterscheidung zwischen Plasmid- und cDNA verifiziert werden.

Abstract

Over the past million years, human endogenous retroviruses (HERVs) have been inserting proviruses into the human germline, a process known as endogenization. Mutations, deletions and recombinations have since resulted in a substantial decrease in functionality of these proviruses and today all known HERV proviruses have lost the ability to replicate. However, transcripts and even whole virus particles of one HERV-group, termed HERV-K(HML-2), have since been detected in various malignant human tissues. Earlier studies with a reconstructed HERV-K(HML-2) virus have demonstrated the ability of pseudotyped HML-2-based reporter viruses to infect certain cell lines. However, no evidence of reproduction could be found, suggesting a post-entry, pre-integration block of HERV-K(HML-2). The stage after cell-entry at which this block is initiated and which cellular factors are involved remain unknown. The aim of the present work was to determine whether HERV-K (HML-2) cDNA is formed, as this would be evidence of post-entry reverse transcription. In addition, the possible integration of such cDNA into the host genome was to be investigated. The HERV-K(HML-2) infection process had already been studied using plasmid-based reporter viruses. However, using such a system it is not possible to distinguish cDNA produced during reverse transcription from plasmid contamination originating from the production of the pseudotyped virus particles. One possible solution was to insert a specific mutation into the plasmid DNA that due to intramolecular relocations during reverse transcriptions is duplicated and therefore occurs twice in the cDNA. The cDNA sequence therefore differs from that of plasmid DNA and can be detected using specific primers. This mutated plasmid had been produced in a previous work and is now used for the production of HML-2-based reporter viruses. In the present work, HIV-1 and HML-2-based luciferase reporter viruses were produced that were pseudotyped with two different envelope proteins; Env VSV-G and HIV-1 Δ KS. It could be shown that Env VSV-G pseudotyped reporter viruses were highly infectious, whereas HIV-1 Δ KS pseudotyped reporter viruses were not. Using a luciferase assay, infection by these two reporter viruses was shown to differ, with HERV-K(HML-2) showing a peak after 24 hours and HIV-1 after 48 hours. DNA from cells infected with the different reporter viruses was isolated and the amount of viral DNA was compared by real-time duplex qPCR and droplet digital PCR. The droplet digital PCR appeared to be more sensitive than classic real-time qPCR and is therefore better suited for investigating HERV-K(HML-2) infection, detecting even single copies of DNA. Furthermore, it could be shown that the mutation in the U3-region is an effective approach for distinguishing between plasmid and cDNA.

1. Introduction

1.1. Taxonomic classification of the human immunodeficiency virus (HIV)

1.1.1. Retroviruses

Retroviruses were first described by Ellermann and Bang in 1908, as they showed that fowl leukemia could be transmitted via ultra filtrates [1]. In 1911, Rous discovered that ultra filtrates from sarcomas of the fowl led new tumors in healthy, susceptible fowls [2]. The virus, responsible for these tumors was named Rous sarcoma virus. In the year 1936, Bittner could associate yet another retrovirus responsible for tumorigenesis; the mouse mammary tumor virus (MMTV), responsible for tumors in the mammary glands of mice [3]. The first human retrovirus, responsible for tumorigenesis in humans, was described by Gallo in 1980 and is known as the human T-cell leukemia virus (HTLV) [4]. In 1984, Gallo further showed that a retroviruses, HIV-1, was responsible for the human immunodeficiency syndrome AIDS (*acquired immunodeficiency syndrome*) [5].

Retroviruses (*Retroviridae*) possess a genome consisting of two single stranded (ss) RNAs in plus strand orientation. The viruses are enveloped by a membrane and use an enzyme called reverse transcriptase to translate their ssRNA into double stranded (ds) DNA. This enzyme was first described by Temin, Mizutani and Baltimore in 1970 [6]. Retroviruses possess an oncogenic potential, since they are able to integrate their translated dsDNA into the host genome. The international committee for virus taxonomy has classified retroviruses into seven independent genera based on their genetic structure: α -, β -, δ -, ϵ - and γ -retroviruses which belong to the clade *Orthoretroviridae* and the spuma viruses which belong to the clade *Spumaviridae*. Retroviruses are responsible for various diseases such as tumors, immunodeficiency and neurological defects. Retroviruses are further divided into infectious exogenous and endogenous retroviruses und infect primarily vertebrates.

1.1.2. Morphology and structure of retroviruses

All retroviruses have similar structure and a diameter of about 100-120nm. Figure 1 shows the schematic structure of HIV. Retroviruses are enveloped by a cellular lipid double membrane which contains envelope proteins. The transmembrane unit (TM) of the envelope proteins is anchored within the membrane whereas the rest of the protein is located outside of the membrane as glycoprotein (SU). The TM part of the protein is non-covalently attached to the SU part of the protein. Envelope proteins form trimers [7] and are visible in the EM as so called spikes [8]. At the inside of the membrane matrix proteins (MA) are located which are connected to the membrane by myristic acid residues and form a net-like protein layer. Inside the virus a virus capsid, consisting of capsid proteins (CA), exists. The viral genome is located inside the capsid, consisting of two ssRNAs complexed with nucleocapsid proteins (NC). Also located on the inside of the capsid are the enzymes reverse transcriptase (RT), integrase (IN) and protease (PR) (s. figure 1).

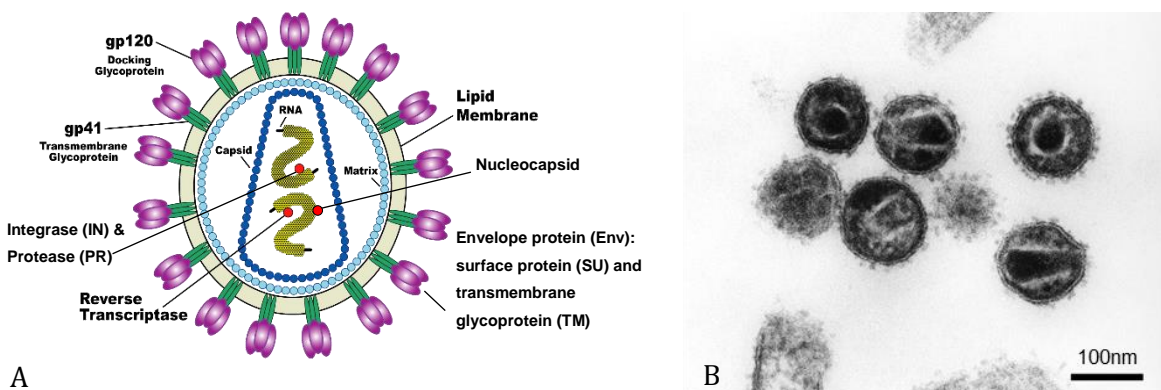


Figure 1: Schematic structure and electron microscopy of HIV

A) Schematic structure of HIV-1, *modified after* [110]. B) Electron microscopy of HIV-1 [95]

The virus consists of a lipid membrane with viral envelope proteins, consisting of a SU- and TM-unit. Matrix proteins surround the capsid. The (+)ssRNA genome is found inside the capsid together with nucleocapsid proteins, RT, IN and PR.

1.1.3. Genomic organization of retroviruses

The proviral genome of retroviruses consists of the genes *gag*, *pol*, *env* and two LTRs (long terminal repeats). Complex retroviruses furthermore possess regulatory and accessory genes such as *tat*, *rev*, *vif*, *nef*, *vpu* and *vpr*. These accessory genes can increase replication or inhibit antiviral host defense [9] [10] [11]. Simple retroviruses, in contrast, do not contain accessory genes (s. figure 2). The two identical LTRs are located at the beginning and the end of the viral genome and consist of the regions U3, R and U5. Both LTRs are important for regulatory processes of gene expression and contain cis-active sequences, promoters and enhancers. Cellular proteins bind to the U3 region and initiate transcription of integrated proviruses. The U3 and U5 regions also contain important control sequences for the RT as well as for the integration of the viral genome into the cellular DNA. The R region serves the start of transcription and contains the polyadenylation signal. Adjacent to the LTR there is the primer binding site (PB), where specific cellular tRNA binds to and RT polymerase activity starts. Subsequently the three structural genes of the virus *gag-pol-env* follow. *gag* (group specific antigen) codes for the three main structural proteins MA, CA and NC. *pol* (polymerase) codes for RT, PR, IN and RNaseH. PR processes the *gag*-preproteins to the respective MA-, CA or NC-proteins. *env* codes for the TM- and SU-unit of viral glycoproteins. The 5'-end of the viral genome consists of a cap unit whereas the 3'-end is polyadenylated and possesses one or several polypurine sites (PP) in front of the LTR, which are essential for the RT.

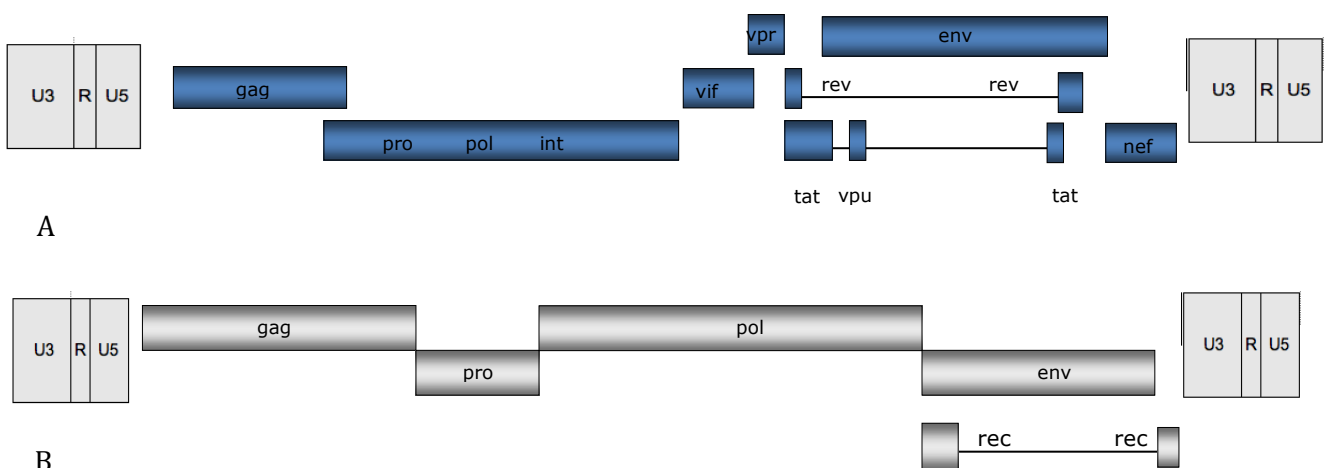


Figure 2: Genomic organization of retroviruses

A) Genomic organization of HIV, a complex retrovirus belonging to the genus of lentiviruses. B) HERV-K113, a relatively simple retrovirus belonging to the genus of betaretroviruses. All retroviruses contain 2 homologous LTR-regions (long terminal repeats) and the genes *gag*, *pol* and *env*. The more complex a retrovirus is the more accessory genes it contains. These genes play role in various functions e.g. in escape of the host immune response.. Figure after [108]

1.2. HIV and AIDS

1.2.1. AIDS: History

1.2.1.1. Discovery

In 1981 the first cases of AIDS have been clinically observed in the USA, consisting of a cluster of injection drug users and gay men who showed symptoms of *Pneumocystis carinii* pneumonia (PCP), a rare disease known to occur only in people with strongly impaired immune systems [12]. Soon after, many more cases of gay men developing PCP or other opportunistic diseases such as the rare skin cancer called Kaposi's sarcoma (KS) arose, resulting in the formation of a CDC (*Centers for Disease Control and Prevention*) task force to surveil the outbreak [13]. In the beginning, the CDC did not have an official name for the disease, which was believed to be restricted to certain communities such as homosexuals, heroin users and hemophiliacs [14] [15]. Only in 1982, after determining that AIDS was not isolated to any specific community, the CDC started using the name AIDS (*acquired immune deficiency syndrome*) [16]. Since its beginnings, the spread of HIV has developed into a pandemic having caused the death of about 39 million people worldwide [17].

HIV type 1 was first described by Luc Montagnier and Françoise Barré-Sinoussi from the Institut Pasteur from a Lymphadenopathy patient in May 1983 [18]. They named the virus LAV (*Lymphadenopathy-associated virus*) and published their findings in the research magazine Science [19]. In the same edition of the magazine Robert Gallo, head of the tumorvirus laboratory at the National Institutes of Health also published the discovery of a virus which he assumed to be the elicitor of AIDS [20]. However, he described the isolation of the *human T-cell leukemia virus type 1* (HTLV-1) from AIDS patients who by chance were present next to HIV in his samples. Only one year later he could isolate and cultivate the HI-virus and link it to AIDS. At first, he named it HTLV-III (*human T-lymphotropic virus III*) [21]. In 1986 the International Committee on Taxonomy of Viruses recommended the term *HIV* for this virus [22]. Both Montagnier and Gallo claimed to be the discoverer of HIV resulting in a long lasting legal dispute. In 2008 Luc Montagnier and Françoise Barré-Sinoussi were awarded the Nobel Prize for Medicine for their discovery of HIV [23].

In 1985 the FDA approved an ELISA which could detect antibodies against HIV-1 surface proteins as the first HIV-1-test commercially available [24]. In 1987 ZDV (zidovudine), the first antiretroviral drug became available to treat HIV [25] [26]. In 1997 a post-exposure prophylaxis to HIV shows evidence to decrease the risk of HIV infection after exposure [27].

1.2.1.2. Origin

The human HI-virus has developed from the *simian immunodeficiency virus* (SIV) which has been present in monkeys for 32'000 – 75'000 years [28]. A distinction is made between HIV-1 groups N and M, which are descendants of the African SIVcpz from chimpanzees and HIV-1 groups O and P which arose from SIVgor present in gorillas. In 2003, genetic analysis from virologists at the University of Alabama at Birmingham showed that SIVcpz is a combination of two virus strains present in redtail monkeys and collared mangabeys. Since these two monkey species are hunted by chimpanzees, a plausible explanation is, that chimpanzees got infected by both virus strains and that within their body the SI-virus cpz has formed [29].

Transmission of the SI-virus to humans occurred presumably before 1930 via injuries during hunts or the consumption of bushmeat [30]. However, SIV is a weak virus and commonly suppressed by the human immune system. Therefore, several transmission rounds are thought to have been necessary for SIV to mutate into HIV [31].

The earliest documented infection with HIV-1 dates back to 1959 in a blood sample from a man from Léopoldville (Belgian Congo). Analysis of additional blood samples, however, dates back the first transmission to the time between 1884 and 1924 [32]. One assumption is that the emergence of colonialism in Africa, with the increase of prostitution and the concomitant high frequency of genital ulcer diseases, helped the virus to establish in the human population [33].

1.2.2. AIDS: Epidemiology

About 36.9 million people worldwide are infected with HIV. Most new HIV infections occurred in Sub-Saharan Africa in 2014 (1.4 million). Nevertheless, this marks a 41% decrease of infections in this region compared to 2010. On rank two come Asia and the Pacific with 340'000 new infections (31% decrease compared to 2010), followed by Eastern Europe and Central Asia with 140'000 new infections (increase by 30% compared to 2010). Western and central Europe and North America remain fairly stable at 85'000 new infections in 2014. In regards to AIDS-related deaths, Sub-Saharan Africa shows by far the highest numbers with 790'000 (34% decrease compared to 2010), followed by Asia and the Pacific with 240'000 AIDS-related deaths (11% increase compared to 2010). Western and central Europe and North America recorded 26'000 AIDS-related deaths corresponding to a 12% decrease compared to 2010. The lowest number of AIDS-related deaths and coincidentally a three-fold increase showed Middle East and North Africa with 12'000 AIDS-related deaths in 2014. An estimated 17.1 million people worldwide living with HIV do not know they have the virus [17].

1.2.3. HIV: Replication

The replication cycle of HIV as representative of several retroviruses is initiated by the viral envelope protein Env (s. figure 3). Env binds specifically to the respective cellular receptor on the surface of the host cell. The fusion of viral membrane and host membrane is accomplished by the TM unit of the glycoprotein. This fusion leads to cell entry of the virus [34]. Inside the cytoplasm the RT transcribes the viral RNA genome into dsDNA with help of a cellular tRNA, which serves as a primer. During reverse transcription of ssRNA into dsDNA errors often happen, since the RT does not consist of a proof-reading mechanism. On the other hand the high error rate also leads to a high variability of retroviruses [35]. The viral DNA is transported into the nucleus and integrated into the host genome by the endonuclease- and ligase-activity of the IN [36]. Integration of viral DNA can be deleterious for the host, if cellular genes are switched on or off due to integration. Depending on the state of the cell the provirus either remains latent or is being transcribed [37]. Several cellular factors are involved in transcription by the cellular RNA polymerase II. The viral mRNA is spliced and transported into the cytoplasm. Subsequently translation of mRNA takes place at ribosomes or the mRNA is packaged as new viral RNA into virus particles. Gag-polyproteins are transported to the cell membrane or aggregates directly at the cell membrane. Env-precursor proteins are synthesized at the membrane of the cytoplasmic reticulum and transported to the cell surface via the Golgi apparatus. The Ψ -signal in unspliced mRNA leads to packaging of viral RNA into virus particles. Subsequently Gag-proteins interact with the viral Env-proteins and initiate the budding of the immature virus particle. After successful budding the protease is activated auto catalytically and processes the preproteins. As a consequence the viral capsid is formed and the now mature virus is able to infect another host cell.

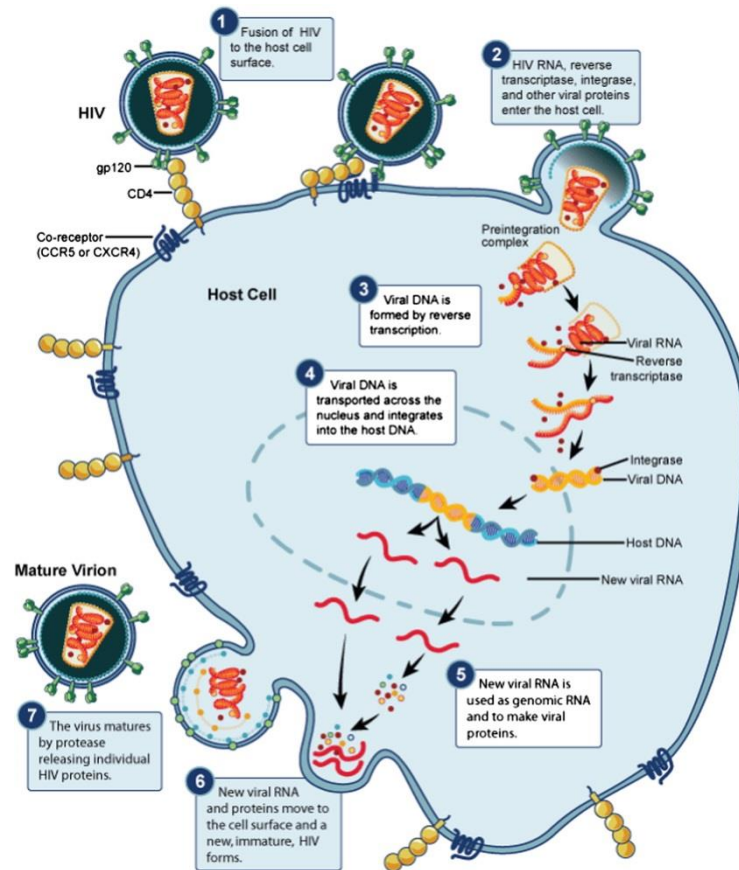


Figure 3: Schematic presentation of the replication cycle of HIV-1

Replication starts with binding to the receptor on the host cell surface via the viral surface protein Env. Subsequently fusion of virus membrane and host membrane takes place. The capsid is disintegrated and the ssRNA is reverse transcribed into dsDNA. dsDNA is then transported into the nucleus and integrated into the host genome via IN. After transcription of the provirus and splicing, viral mRNA is transported into the cytoplasm, translated into Gag-, Pro-, Pol- and Env- and other preproteins and packaged into the virus particles. After packaging of the viral genome, budding of the virus particles is initiated. Maturation takes place with proteolytic processing of the Gag-polyprotein and the virus is now able to infect new host cells. Figure after [38]

1.2.4. HIV: Pathogenesis

AIDS results from a suppression of the humoral and cell-mediated immunity. After infection with HIV some patients show flu-like symptoms such as fever, fatigue, lymphadenopathy, headache and others [39]. This so-called acute phase is followed by an asymptomatic phase (latency), during which time the virus replicates. This phase usually takes nine to eleven years but may vary strongly between individuals [40]. The final stage AIDS is characterized by low level of T-helper cells (below 200 CD4+ T cells per μl) within the body and accordingly a weak immune system. As a consequence the individual is affected by opportunistic infections and rare tumors

which would otherwise be harmless in healthy humans [41]. At this stage the course of the disease is lethal.

1.2.5. Antiviral host defense and accessory proteins

Viral infection has enormous effects on cells such as cell lysis or apoptosis. In order to combat viral infection the target organisms have developed a range of systemic and cell-based defense strategies, including immune and inflammatory processes and the induced death or suicide of infected cells [42]. Viruses in turn, have evolved different strategies to evade the host defense mechanisms. One of the earliest forms of antiviral immunity is RNA interference (RNAi). It is the predominant mechanism of antiviral defense in plants and invertebrate animals, but is also used by vertebrate animals [43]. Infection by RNA viruses leads to the generation of double-stranded RNAs (dsRNA) that differ structurally from single-stranded cellular RNAs [44]. In plants and invertebrates, this viral dsRNA is recognized by endoribonuclease Dicer which cleaves the dsRNA into small pieces, which are then loaded into the RNA-induced silencing complex (RISC).

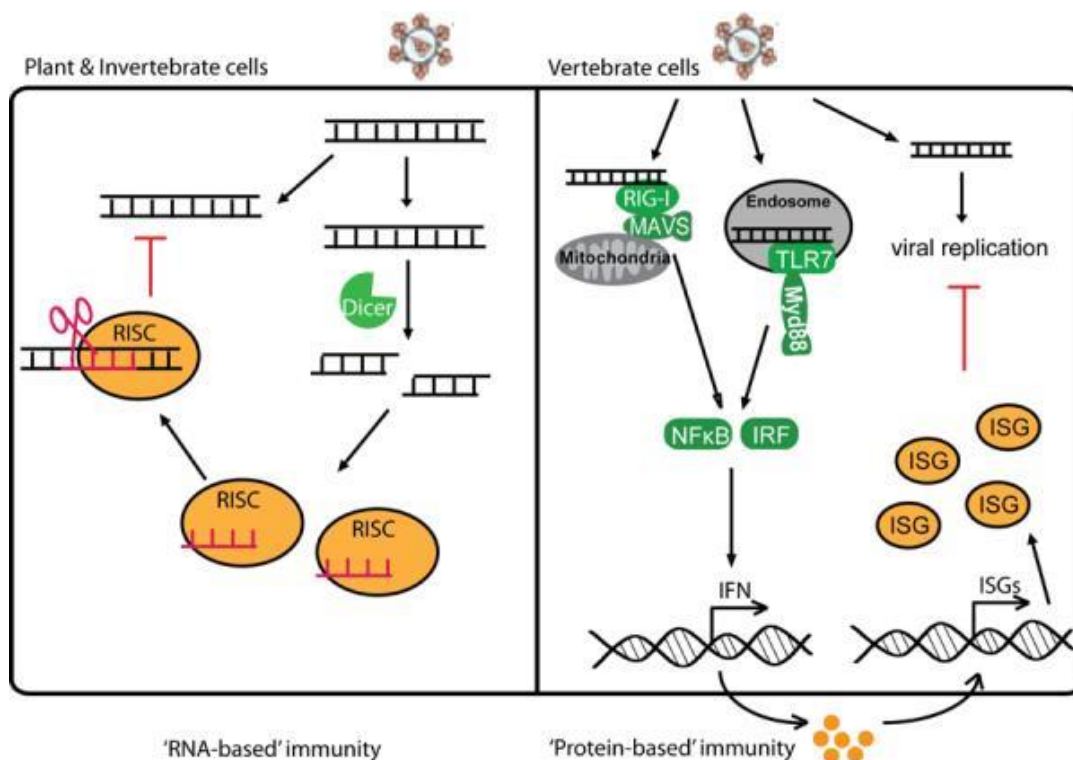


Figure 4: Scheme depicting RNA-based and protein-based immunity

The scheme depicts RNA-based immunity in plants and invertebrates (A) as well as protein-based immunity in vertebrates (B). A) Virus dsRNA is recognized by Dicer and cut into small fragments. RISC-mediated RNAi destroys the viral genome. B) In protein-based immunity, virus RNA is recognized via PRRs, which induce the signal for activation of interferon (IFN) expression. This activates further expression of interferon-like genes (ISGs), which inhibit viral replication. Figure after [43]

This complex then degrades the viral genome (s. figure 4). Another form of antiviral immunity is the clustered, regularly interspaced short palindromic repeats (CRISPR) system in bacteria and archaea, which protects them from bacteriophages and conjugative plasmids [45]. Vertebrates additionally possess protein-based antiviral defense in contrast to plants and invertebrates (see figure 3). The first line of defense against viral infection is the innate immune response [42]. Thereby, pathogen-associated molecular patterns (PAMPS), which are characteristic structural motifs of microorganisms, are recognized by pattern-recognition receptors (PRRs) in a variety of immune cells. This elicits an immediate immune reaction which leads to the elimination of the pathogen, often in an inflammatory reaction [46]. The innate immune system comprises cytokines such as interleukin 1 (IL-1) and tumor necrosis factors (TNFs), which activate and recruit macrophages, natural killer (NK) cells, and neutrophils that phagocytize and help to clear infected cells. TRIM5 α is a protein known to be crucial for the restriction of infection by lentiviruses [47]. TRIM5 α thereby inhibits RT and thus integration of lentiviruses [48] [49]. However, TRIM5 α cannot –or only weakly- inhibit HIV-1. Although the innate immune system is fast and generic, viruses are adept at escaping recognition e.g. by changing their molecular patterns [50].

In contrast, as a second line of defense, the humoral immune response is specific and can clear a host of infection as well as provide protection against future infections. It involves cytotoxic T cells, antibodies generated from B cells, which specifically recognize and bind the virus, as well as various cytokines that regulate the response [42]. Antibodies are even effective when the virus has already entered a cell. The protein TRIM21 inside cells recognizes antibodies on viruses and initiates the proteasome-process, which degrades the virus [50]. Another restriction factor, APOBEC3G deaminates the viral nucleic acids dC to dU, leading to a G-toA-hypermutation and thus damaging the viral genome (s. figure 5) [51] [52] [53]. SAMHD1 is a phosphohydrolase, which cleaves nucleotriphosphates (NTPs) into nucleosides and triphosphates thus diminishing the pool of nucleotides for the synthesis of viral cDNA [54]. This impedes viral replication.

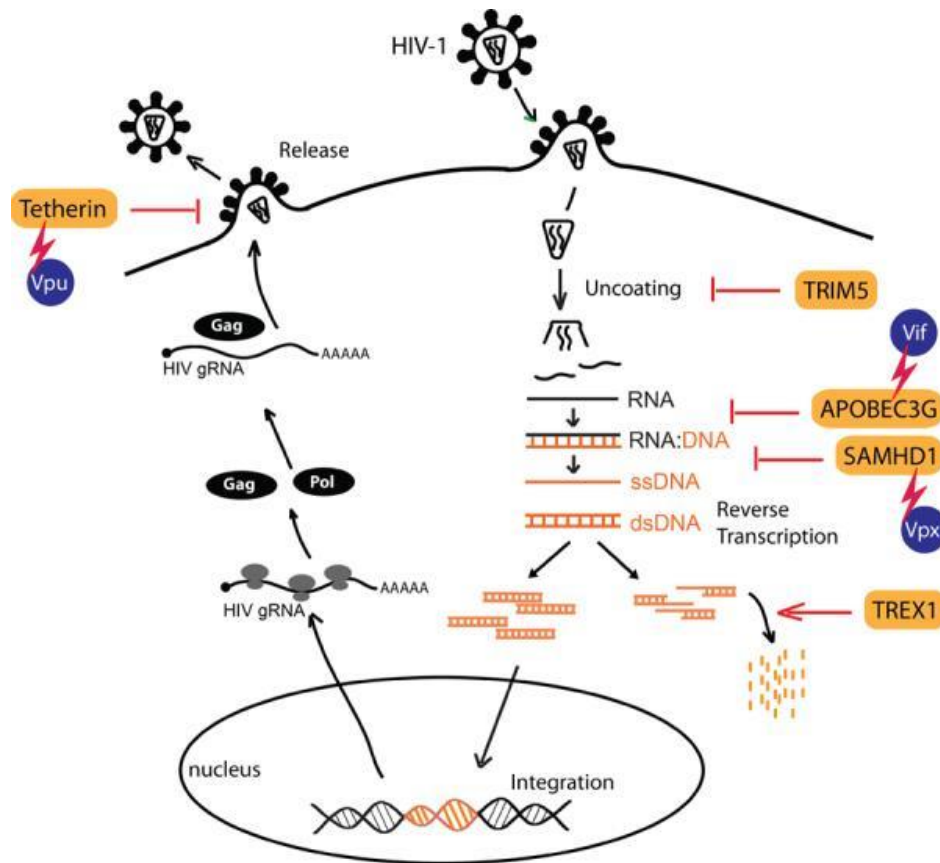


Figure 5: Scheme showing effects of restriction enzymes on the viral genome and effects of the viral accessory proteins on the restriction enzymes

The scheme depicts the process of antiviral host defense with HIV infection as an example. After HIV entry into the cell, capsid degradation can be inhibited by TRIM5 α . Action of APOBEC3G renders viral genomic RNA inoperable. Vif is an opponent of APOBEC3G, which binds and degrades APOBEC3G via the proteasomal way. SAMHD1 degrades NTPs into nucleosides and triphosphates, thus inhibiting reverse transcription. The protein Vpx binds to SAMHD1 and leads it to degradation. TREX1 degrades open 3' ends of DNAs quickly and thereby destroys open viral DNA. In the end, tetherin inhibits the budding of virus particles. Vpu is a tetherin opponent. Figure after [43]

In spite of various effective antiviral defense strategies, certain viruses such as HIV-1 have evolved numerous ways to circumvent the immune system. The successful circumvention and hiding from the immune system mainly depends on the multitude of accessory proteins: Tat, Rev, Nef, Vif, Vpr/Vpx and Vpu (s. figure 5). For example, the Nef-protein down-regulates surface MHC1, which avoids cytotoxic T lymphocyte killing of the infected cell [55]. Via the Tat-proteins HIV-1 produces TAR viral microRNA, which down-regulates cellular genes involved in apoptosis [56]. The Vif-protein inhibits APOBEC3G function [57]. The Vpr-protein of HIV-1 regulates various cellular functions such as NF- κ B suppression and cell-cycle arrest of the host cell [58]. The Vpx-protein interacts with SAMHD1 [59] and the Vpu-protein interacts with tetherins leading to their degradation in endosomes [60].

1.2.6. HIV: Analysis of post entry events and integration

Major advances in the treatment of HIV have been made possible by studying the virus and its interaction with the host cell. However, the steps from HIV-1 entry into the cell until integration of its reverse transcribed genome into the host genome still remain to be elucidated. These steps are believed to occur in so-called reverse-transcription- and pre-integration-complexes (RTC/PIC) with various host and viral proteins implicated [61]. Three models have been proposed for genome uncoating, which is defined as the loss of the viral capsid structure, consisting of homomultimers of CA proteins: i) immediate dissociation after fusion followed by reverse transcription within the remaining nucleoprotein complex; ii) gradual dissociation during reverse transcription; iii) reverse transcription in an intact capsid structure that only dissociates at the nuclear pore complex [62].

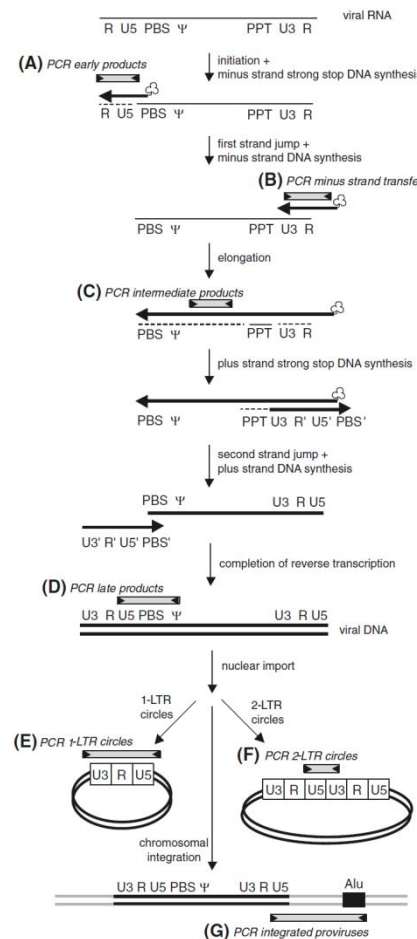


Figure 6: Schematic presentation of HIV-1 reverse transcription and integration

Real-time PCR can be used to analyze and quantify various reverse RT products as well as integrated and unintegrated (1-and 2-LTR-circles) HIV-1 viral DNA (stages A-G). Thin black lines=RNA, thick black lines=DNA, thick grey lines=chromosomal DNA, dashed lines=RNase H degradation, cloverleaf=tRNA. Figure after [63]

The model of immediate capsid dissociation, however, has recently been disfavored by multiple studies indicating that host factors interact with CA during early phase of HIV-1 replication [66] [67] and that mutations in CA as well as small molecule compounds targeting CA can affect reverse transcription and nuclear import [68]. A shielded capsid environment could prevent HIV-1 from recognition by cytoplasmic DNA sensors during reverse transcription [68]. In one study, microinjection of fluorescent nucleotides and subsequent HIV-1 infection has been done, which aimed at detection of microtubule association of a replication complex by light and electron microscopy [69]. Another study applied fluorescence in situ hybridization to visualize integrated HIV-1 cDNA [70]. However, processing steps during FISH interfered with immunostaining making detection of productive HIV-1 RTC/PIC difficult [71]. Another strategy implemented for visualizing HIV-1 RTC/PIC was the labeling of nascent DNA with a nucleoside analogue carrying an alkyne group and “click-labeling” it with a fluorophore [64]. In 2014, Tilton et al. developed a reporter virus system that measures HIV fusion with cells and viral promoter-driven gene expression and accurately determines the efficiency of early post-entry events [72]. Mbisa et al. published a method to analyze HIV-1 replication post-entry events via real-time PCR [73]. In his study, different primer sets were used that amplify distinct DNA fragments of the reverse transcription process, as well as integrated provirus (s. figure 6). This method can be used to track and quantify different stages of the reverse transcription process as well as the proviruses and the nonintegrated dead-end products of reverse transcription, 1- and 2-LTR-circles.

1.3. HERV-K(HML-2)

1.3.1. Endogenous retroviruses (ERV)

Endogenous retroviruses do not undergo a complete replication cycle, but instead remain within the host genome as a provirus. In such a way, they are able to spread vertically over the germ line and thus evade the immune system [64]. Nevertheless, completion of replication cycle and hence activation of the virus' exogenous, infectious form is possible at any time, dependent on the integrity of the provirus [64]. However, during replication of the host genome mutations occur within the proviral DNA over time, which may impair its ability to complete replication cycle [65]. The virus might therefore become unable to pass on to its exogenous form [66]. Mutations as these can even lead to complete loss of the provirus sequence [67] [68]. Van Nie *et al.* [69] first described the vertical way of infection of retroviruses. They showed that MMTV not only infected cells in the horizontal way as exogenous viruses, but were also spread as

endogenous form as part of the genome of a germ cell. Once the viral genome has integrated into the host genome, it underlies Mendelian inheritance [70].

Endogenous proviruses that have lost the ability to pass on to the exogenous form have two alternative methods of replication. One alternative is retro transposition, which only takes place intracellular [25]. The second alternative is complementation in *trans*. Thereby, co-infection of the cell with another virus leads to a gain of functionality for the inactive endogenous virus and renders it active again [26]. However, the new virus has lost its ability to replicate.

1.3.1.1. Human endogenous retroviruses (HERV)

HERVs account for about 8% of the human genome [65]. They were first described in human tissues in the 1970's by Kalter *et al.* [71] and Bierwolf *et al.* [72]. Whereas in many mammals retroviruses existed in both their endogenous and exogenous forms in parallel, no intact infectious retrovirus has been found for HERVs so far [73].

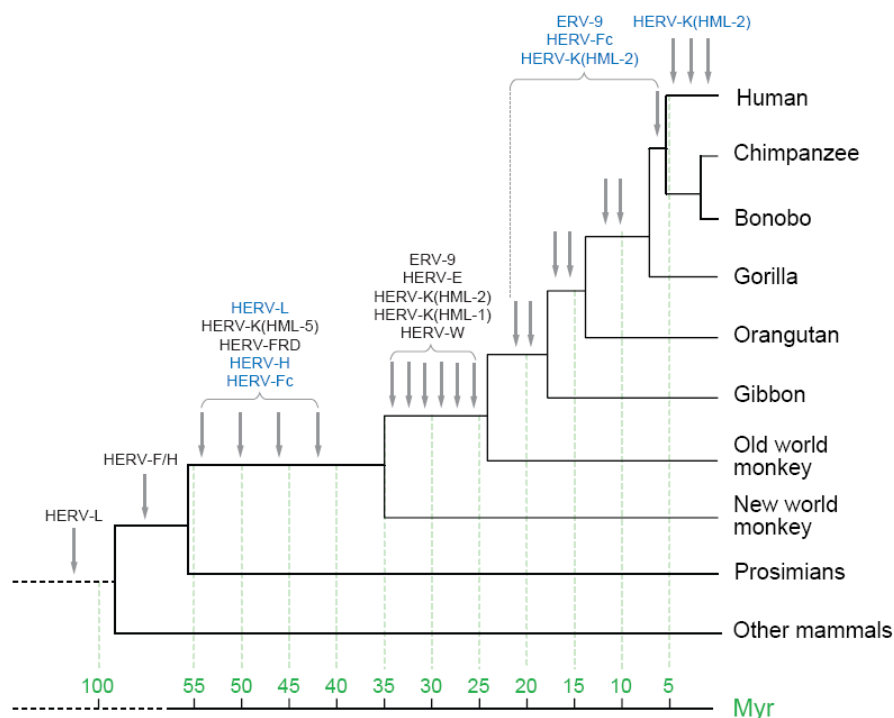


Figure 7: Time-scale of HERV-integration

The first HERVs integrated over 100 million years ago, before the divergence of the old world monkeys and the new world monkeys. Over the time, mutations, deletions and recombinations have rendered most HERVs unable to replicate. The youngest HERV-family HERV-K(HML-2) integrated about 5 million years ago [74].

Most HERVs integrated before the separation of Old World Monkeys from New World Monkeys [75] [76]. The youngest HERV-family HERV-K(HML-2), integrated into the human germ line about 5 million years ago shortly after the divergence of the human and the chimpanzee lineage [77](s. figure 7). In 2001, a HERV-sequence was discovered in a human BAC-library, which contains complete intact reading frames for all viral proteins: HERV-K113 [78]. Various studies have shown that HERV-K(HML-2) proviruses are capable of producing viral proteins [79]and even whole particles [80]. Although there are indications on the role of HERV-K(HML-2) in various diseases [81] [82] [83], its total impact on humans is still being investigated [65].

1.3.2. Infectivity and tropism of HERV-K113

The proof of infectivity of HERV-K(HML-2) pseudotyped with either Env VSV-G or a truncated HERV-K(HML-2) Env-variant, could be validated by Philipp Kramer [84]. He showed that the surface protein Env of HERV-K(HML-2) remains functional after restoration of eight non-synonymous mutations within the *env* gene [85]. He thereby used a HERV-K(HML-2) reporter construct with the *env* gene replaced by the EGFP gene. Cells were infected with various HERV-K(HML-2) reporter viruses and HERV-K(HML-2) *env* plasmids, with C termini of different sizes. The pseudotyped viruses were subsequently used for infection of various cell lines and EGFP-containing cells were studied with help of a confocal microscope. He showed that deletion of a cytoplasmic domain of HERV-K(HML-2)-Env (Env Δ C) resulted in a five-time higher infectivity compared to the full-length protein. He further compared infectivity of HERV-K(HML-2) to SHIV-particles by pseudotyping both viruses with different-sized Env proteins. As a result, a 2-log scale higher infectivity for Env Δ C pseudotyped SHIV particles could be detected compared to Env Δ C pseudotyped HERV-K(HML-2) particles. A possible explanation could be a post-entry, pre-integration-inhibition of HERV-K(HML-2) which is not valid for SHIV.

In an attempt to find the receptor for HERV-K(HML-2), different human and animal cell lines were infected with pseudotyped Env Δ C-viruses and tested for their susceptibility towards HERV-K(HML-2) [84]. This experiment showed that HERV-K(HML-2) has an amphotropic host specificity, whereby canine and feline cell lines were particularly susceptible for HERV-K(HML-2). However, no tissue specificity could be detected.

2. Objectives of the Master's Thesis

The objective target of the present work is the analysis of HERV-K(HML-2) post-entry reverse transcription by means of real-time duplex qPCR. For this purpose, HML-2-based luciferase reporter viruses (oriHERVK113*) are selected and CrFK cells used as recipient cells, as these are known to be particularly permissive for HERV-K(HML-2). For specific detection of cDNA, a luciferase-coding reporter construct (CMVoriLuc_U3Tag2) is used for production of HML-2-based luciferase reporter viruses that carries a mutation in the U3-region of its 3'LTR. Due to two intramolecular relocations, this mutation undergoes duplication during reverse transcription and is present in both the 3'LTR and 5'LTR of the resulting cDNA. This allows cDNA to be distinguished from contaminating pDNA at the molecular level.

Since no experiments had yet been performed with oriHERVK113*, an additional target of this work is to establish a real-time qPCR to quantitate DNA in cells infected with HML-2-based luciferase reporter viruses. This requires the cloning of a positive template control (PTC) that carries the mutation in the U3-region of its 5'LTR. It is then necessary to validate the functionality and sensitivity of this PTC and the respective primers and probes.

Other products of reverse transcription, such as early and late products and the two dead-end products 1_ & 2-LTR-circles, should also be investigated. This is done using TaqMan-probes to obtain results that should be as specific as possible for comparison with infection-deficient reporter viruses.

Reverse transcription of HIV-1 should be investigated in parallel, based on a publication that demonstrated detection of specific products of reverse transcription using different primer-pairs and probes. The aim here is to determine whether this method also works using the SYBR Green approach.

Finally, digital droplet PCR is used to detect the mutation in the 5'LTR of HERV-K(HML-2) cDNA. Digital droplet PCR does not require a standard and due to its high sensitivity is currently the most suitable method for detecting very low levels of DNA.

3. Materials and Methods

3.1. Materials

3.1.1. Kits

Table 1) List of kits with corresponding source of supply

Kits	Manufacturer
Endo-free Plasmid Maxi Kit	Qiagen GmbH, Hilden, Germany
Luciferase 1000 Assay System	Promega Corporation, Madison, USA
QIAprep Spin Miniprep Kit	Qiagen GmbH, Hilden, Germany
QIAquick Gel Extraction Kit	Qiagen GmbH, Hilden, Germany
QIAquick PCR Purification Kit	Qiagen GmbH, Hilden, Germany
QIAamp DNA Blood Mini Kit	Qiagen GmbH, Hilden, Germany
QuikChange® Lightning Multi Site-Directed Mutagenesis Kit	Agilent Technologies, Amsterdam, Netherlands

3.1.2. Bacterial strains

For chemical transformations chemically competent *Escherischa coli* (*E. coli*) One Shot® Top10 or *E. coli* One Shot® Stbl2 were used.

3.1.3. Eukaryotic cell lines

Table 2) List of cell lines with origin and corresponding manufacturer

Cell line	Organism	Tissue of origin	Cell culture medium	manufacturer
HEK-293T	human	kidney	DMEM, 10% FCS, 0.5% Pen/Strep	ATCC® CRL-11268
CrFK	cat	kidney	DMEM, 10% FCS, 0.5% Pen/Strep	ATCC®CCL-94
C8166	human	blood	RPMI	HPA Culture Collections

3.1.4. Constructs and vectors

Table 3) List of constructs and their corresponding vectors and manufacturer

Construct	Vector	Manufacturer
CMV _{ori} GFP	pcDNA 3.1	Oliver Hohn, FG 18
CMV _{ori} EGFP	pTH	Philipp Kramer, FG 18
CMV _{ori} Luc	pTH	Philipp Kramer, FG 18
Orico Rec_V5	pcDNA 3.1	PhD Thesis, Kirsten Hanke, FG 18, 2010
HIV packaging construct (<i>gag</i> , <i>pol</i> , <i>rev</i> , <i>tat</i>)	pS Pax 2	Addgene, provided by Didier Trono
pSVIII-KS (HIV-1 Env Δ KS)	pcDNA 3.1	Norbert Bannert, FG 18
pWPXL_Luc	pWPXL_Luc	Addgene, provided by Didier Trono, Olicer Hohn, FG 18
pWPXL_EGFP	pWPXL_EGFP	Addgene, provided by Didier Trono
VSV-G (EnvVSV-G)	pCMV	Addgene, provided by Didier Trono

3.1.5. Primers

Primers were supplied by the companies by New England Biolabs and Thermo Fisher Scientific. Primers were used at a final concentration of 10 μ M and stored at -20°C. Oligonucleotides were used for sequencing, quantitative-, amplification- and mutagenesis-PCR reactions. A detailed list of sequences and primers used can be found in the supplement.

3.1.6. Antibodies

Table 4) List of antibodies and their corresponding species and manufacturer

Antibody	Species	Manufacturer
Ag 3.1 monoclonal AB	mouse	Steve Norley, FG 18
α -HIV+ pool plasma	human	Steve Norley, FG 18
α -human conjugate	human	Sigma-Aldrich Chemie GmbH, Munich, Germany
α -rabbit IgG-HRP	goat	Sigma-Aldrich Chemie GmbH, Munich, Germany
α -tubulin (monoclonal antibody)	rabbit	Epitomics Inc., Burlingame, USA
HERMA7 monoclonal AB	mouse	K. Boller, Paul Ehrlich Institut
A-HERV Capsid serum	rabbit	Oliver Hohn, FG 18

3.1.7. Software

Table 5) List of software and corresponding source of supply

Software	Manufacturer
Adobe® Illustrator CS5.1	Adobe Systems GmbH, Munich, Germany
Berthold Luminometer Analysis Software	Berthold Technologies, Oak Ridge, USA
Clone Manager 9 Professional Edition	Sci-Ed Software, Cary, USA
EndNote	Thompson Reuters, Philadelphia, USA
Lasergene	DNASTAR Inc., Madison, USA
Microsoft Excel 2010	Microsoft Corporation, Redmond, USA
Microsoft Power Point 2010	Microsoft Corporation, Redmond, USA
Microsoft Word 2010	Microsoft Corporation, Redmond, USA
NanoDrop ND-100 v.3.3	Nanodrop, Wilmington, USA

3.2. Methods

3.2.1. DNA-Analytcs

3.2.1.1. Polymerase Chain Reaction (PCR)

PCR is used to amplify a complete DNA (deoxyribonucleic acid) strand or DNA section *in vitro*. A PCR reaction is subdivided into different stages: denaturation (D), annealing (A) and elongation (E).

All PCRs which have been used for this work are listed below.

Amplification PCR

Amplification PCR serves the amplification of a certain DNA section. Following components and conditions were used for the amplification PCR:

Table 6) Components and conditions for amplification PCR

Component	Quantity [μ l]	Cycler conditions	
Template DNA	[1-50ng]	Temperature [$^{\circ}$ C]	Duration
10 μ M Forward Primer	0.5	95	10min
10 μ M Reverse Primer	0.5	D:95	30s
10x Standard <i>Taq</i> Reaction Buffer	2.5	A: 54-55	20s
Hot Start <i>Taq</i> DNA Polymerase	0.25	E: 72	1min/kb
dNTPs	0.5	Go to 2 for 35 cycles	
10mM MgCl ₂	2	72	5min
<i>A.bidest.</i>	<i>Ad 25</i>	4	∞

The denaturation temperature and duration is dependent on the polymerase. The annealing temperature is primer-dependent and complies with its chemical properties, e.g. molecular weight and base ratio [86]. It has been calculated such that it is best suited for both primers used in the reaction. The elongation duration is dependent on the polymerase as well as the size of the DNA section to be amplified. Addition of MgCl₂ is only necessary when it is not already contained in the buffer. After DNA amplification, the fragments were separated via DNA-gel electrophoresis (s. 3.2.1.3.) and extracted. Subsequently the DNA fragments were purified (s. 3.2.1.4., section

Mini-preparation) and DNA concentration was measured (s. 3.2.1.7.). All DNA was stored at -20°C.

Fusion PCR

A fusion PCR serves the ligation of two overlapping DNA fragments and their subsequent amplification. In this method, 2 primers are used; one that binds at the “beginning” of the first-in-order-fragment and another primer that binds at the “end” of the second-in-order-fragment. The resulting fragment hence contains the combined sequence of both fragments. Following set-up was used for fusion PCR:

Table 7: Components and conditions for fusion PCR

Component	Quantity [μ l]	Cycler conditions	
Template DNA 1	4	Temperature [°C]	Duration
Template DNA 2	4	95	10min
10 μ M Forward Primer	1	D:95	30s
10 μ M Reverse Primer	1	A: 54-55	20s
10x Standard <i>Taq</i> Reaction Buffer	5	E: 72	1min/kb
Hot Start <i>Taq</i> DNA Polymerase	0.4	Go to 2 for 35 cycles	
dNTPs	1	72	5min
10mM MgCl ₂	4	4	∞
<i>A.bidest.</i>	29.6		

Mutagenesis PCR

A mutagenesis PCR serves the precise introduction of a mutation at a certain location within the DNA strand with help of mutagenesis primers. Thereby, one or multiple nucleotides can be mutated. During mutagenesis PCR, the whole DNA plasmid is amplified with the new copies containing the mutation inserted by the primers. Following set-up was used for mutagenesis PCR:

Table 8) Components and conditions for QuikChange® Lightning Site-directed mutagenesis PCR

Component	Quantity [μ l]	Cycler conditions	
Template DNA	[100ng]	Temperature [°C]	Duration
10 μ M Forward Primer	1.5	95	2min
10 μ M Reverse Primer	1.5	D:95	20s
QCLM Reaction Buffer	2.5	A: 55	30s
QCLM Enzyme Mix	1	E: 65	1min/kb
QuikSolution reagent	0.75	Go to 2 for 30 cycles	
dNTPs	1	65	5min
<i>A.bidest.</i>	<i>Ad 25</i>	4	∞

All mutagenesis reactions were performed with one primer pair/reaction, a forward primer and the corresponding reverse primer. After PCR, the methylated DNA template strand was digested with 1 μ l of the restriction enzyme Dpn1 for 1h at 37°C. Dpn1 recognizes specifically methylated DNA fragments and digests them, leaving only newly synthesized (and hence unmethylated) DNA intact. These mutated DNA fragments were subsequently transformed (s. 3.2.1.6.) into *E. coli*. The resulting colonies were purified (s. 3.2.1.4., section *Mini-preparation*) the DNA concentration measured (s. 3.2.1.7.) and an analytical digestion (s. 3.2.1.2.) and subsequent DNA gel electrophoresis (s. 3.2.1.3.) were performed to screen for potentially altered fragment sizes and numbers due to insertion of an additional Sac1-cutting site by the mutagenic primers. Plasmids showing the correct fragment numbers and sizes were consequently prepared for sequencing (see section *sequencing PCR*). All DNA was stored at -20°C.

Colony PCR

Colony PCR was performed in order to screen for colonies after fusion PCR and cloning reactions instead of the more time-consuming DNA purification from *E. coli*. The following components and conditions were used:

Table 9) Components and conditions for colony PCR

Component	Quantity [μ l]	Cycler conditions	
Template DNA	5	Temperature [$^{\circ}$ C]	Duration
10 μ M Forward Primer	0.5	95	10min
10 μ M Reverse Primer	0.5	D:95	30s
10x Standard <i>Taq</i> Reaction Buffer	2.5	A: 55	20s
Hot Start <i>Taq</i> DNA Polymerase	0.25	E: 72	1min/kb
dNTPs	0.5	Go to 2 for 35 cycles	
10mM MgCl ₂	2	72	5min
50% DMSO	2.5	4	∞
<i>A. bidest.</i>	<i>Ad 25</i>		

The template consisted of a bacterial colony dissolved in 10 μ l *A. bidest.* After colony PCR the DNA fragments were separated and analyzed via DNA gel electrophoresis (s. 3.2.1.3.). In case the DNA fragments showed the correct size, the DNA of the corresponding colony was purified by adding the remaining 5 μ l template to 2ml LB-Amp medium (1:1'000) and proceeding with the protocol for mini-preparation (s. 3.2.1.4.). The nucleotide sequence of the sample was then verified in an external sequencing lab (see section *sequencing PCR*). All DNA was stored at -20 $^{\circ}$ C for further application.

Sequencing PCR

Sequencing PCR serves the amplification of DNA strands for verification of mutagenesis PCRs, colony PCRs, ligations or DNA restriction with endonucleases. The chain-termination method was applied and the following components and conditions were used:

Table 10) Components and conditions for sequencing PCR

Component	Quantity [μ l]	Cycler conditions	
Template DNA	2	Temperature [$^{\circ}$ C]	Duration
10 μ M Primer	0.5	96	2min
5x Buffer	1.5	D:96	10s
Big Dye 3.1	1	A: 54-55	10s
<i>A. bidest.</i>	5	E: 60	1min/kb
		Go to 2 for 25 cycles	
		4	∞

The BigDye 3.1 mix consists of an *AmpliTaq*-DNA polymerase, dNTPs and a fluorescently labeled 2', 3'-Dideoxynucleotridiphosphate-mix (ddNTPs). The generated DNA fragments were sequenced in the sequencing laboratory of the Robert Koch Institute and evaluated by Lasergene DNA software.

Detection PCR

Detection PCR was performed in order to test detection primers for both mutated and non-mutated DNA vectors. Mutant-detection primers should thereby only bind to the mutant DNA site but not to non-mutated DNA. By contrast, non-mutation-detection primers should only bind to non-mutated DNA sites and not to mutated ones. After PCR, the DNA fragments were analyzed by DNA gel electrophoresis (s. 3.2.1.3.). The components and conditions used for detection PCR are according to table 7 (s. *amplification PCR*):

Real-time singleplex and duplex qPCR

Real-time quantitative polymerase chain reaction, also called real-time PCR or short qPCR, allows for quantitative DNA measurement. Real-time qPCR is based either on non-specific fluorescent dyes that intercalate with double stranded DNA or on specific DNA probes which contain fluorescently labelled oligonucleotides which permit detection only after hybridization of the probe with its complementary sequence. As the polymerase synthesizes DNA, it cleaves and displaces the probe which releases the quencher and allows fluorescence to be emitted in every amplification cycle. As a result, for each amplification cycle, the emitted fluorescence is recorded and the cycle number at which the fluorescence becomes detectable is directly correlated to the number of templates in the reaction at that cycle. However, this correlation only holds true for the exponential phase of the PCR reaction. Therefore, this technology can monitor, in real time, the progress of any PCR reaction and determine the exact DNA copy numbers per sample with a sensitivity that allows detection of 10 or fewer copies per sample [87] [88]. Real-time singleplex qPCRs only contain one primer pair and probe and therefore amplify and quantify only one target sequence. In contrast, real-time duplex qPCR use two primer pairs and probes and thus simultaneously amplify and quantify two target sequences. This can be helpful to control for e.g. the amount of cellular DNA present in each sample. Following real-time qPCR protocols were implemented:

Table 11: Components and conditions for real-time singleplex qPCR reactions

Component	Quantity [μ l]	Cycler conditions	
Qiagen SYBR Green master mix	12.5	Temperature [$^{\circ}$ C]	Duration
Forward Primer	<i>see table 14</i>	95	15min
Reverse Primer	<i>see table 14</i>	95	15-30s
MgCl ₂	1	60	1min
QuantiTect RT Mix	0.25	Go to 2 for 45 cycles	
RNase-free H ₂ O	<i>Ad</i> 17 μ l	72	1min
Template DNA	8	95	1min
Total	25	55	30s
		95	30s

Table 12: Components and conditions for real-time duplex qPCR reactions

Component	Quantity [μ l]	Cycler conditions	
TU master mix	12.5	Temperature [$^{\circ}$ C]	Duration
Forward Primer	<i>see table 15</i>	95	15min
Reverse Primer	<i>see table 15</i>	95	30s
Probe	<i>see table 15</i>	54	1min
catGAPDH_44F	0.5	Go to 2 for 45 cycles	
catGAPDH_45R	0.5	72	1min
catGAPDH_Probe	0.3		
RNase-free H ₂ O	<i>Ad</i> 17 μ l		
DNA template	8		
Total	25		

Table 13: Primers and PCR programs used for real-time singleplex qPCR

Mix	Primers and Probes	Conc.	Final Conc.	Quantity [μ l]
HIV, MM_HIV	MM_HIV1-For	10 μ M	400nM	1
	MM_HIV1-Rev	10 μ M	400nM	1
HIV, cat_Albumin	catAlb_For	10 μ M	400nM	1
	catAlb_Rev	10 μ M	400nM	1
HIV, MM_CCR5	CCR5-For	10 μ M	600nM	1
	CCR5-Rev	10 μ M	600nM	1
HIV, early products	hRU5-F2	10 μ M	600nM	1.5
	hRU5-R	10 μ M	600nM	1.5
HIV, late products	MH531	10 μ M	600nM	1.5
	MH532	10 μ M	600nM	1.5
HIV, 1-LTR- products	LA 1	10 μ M	400nM	1
	LA 15	10 μ M	400nM	1
HIV, 2-LTR- circles	SS-F4	10 μ M	600nM	1.5
	LTR-R5	10 μ M	600nM	1.5
HIV, integrated provirus	MH535	10 μ M	50nM	0.125
	SB704	10 μ M	900nM	2.25

Table 14: Primers, probes and PCR program for real-time duplex qPCR

Mix	Primers and Probes	Conc.	Final Conc.	Quantity [μ l]
HERV-K(HML- 2) U5_qPCR	HERV_U5-F	10 μ M	400nM	1
	HERV_U5_1777-R	10 μ M	400nM	1
	HERV_U5-Probe	10 μ M	200nM	0.5
HERV-K(HML- 2) 2-LTR-circles	HERVRU5_1649- 1688_For	10 μ M	400nM	1
	HERVU3_9360- 9383_Rev	10 μ M	400nM	1
	HERV_U5-Probe	10 μ M	200nM	0.5
HERV-K(HML- 2) U3-tag 2	U3tag2_F2	10 μ M	400nM	1
	U3tag2_R2	10 μ M	400nM	1
	U3tag2-Probe	10 μ M	200nM	0.5

Droplet digital PCR

Droplet digital PCR (ddPCR) is an extension of classic digital PCR which is based on water-oil emulsion droplets. Thereby, a sample is fractioned into 20'000 droplets and PCR amplification of the target molecule subsequently occurs in each individual droplet. Thereby, the droplets serve the same function as individual test tubes or wells, but at a much smaller fraction. Following PCR, each droplet is analyzed in a flow cytometer to determine the fractions of PCR-positive droplets in the original sample. Through partitioning thousands of independent amplification events within a sample can be measured, which increases sensitivity to 1 molecule/sample in theory. Following set-up was used to perform ddPCR:

Table 15: Components and conditions for the out-PCR reaction in a nested PCR

Component	Conc.	Final Coc.	Cycler conditions	
Super Mix	2x	0.5x	Temperature [°C]	Duration
U3tag2_F2	20µM	900nM	95	10min
U3tag2_R2	20µM	900nM	D:94	30s
U3Tag2_Probe	10µM	250nM	A: 55	1min
catAlb_For	20µM	600nM	E: 72	30s
catAlb_Rev	20µM	600nM	Go to 2 for 40 cycles	
catAlb_Probe	10µM	250nM	98	10min
Template DNA		300ng	4	∞
<i>A.bidest.</i>		<i>ad</i> 22.5µl		

3.2.1.2. Restriction digestion with help of endonucleases

DNA restriction digestion is performed in order to control for successful ligation, mutation, for correct vector- and gene sequences and is done with the help of endonucleases. These enzymes recognize and cut specific nucleic acid sequences. After cutting, the nucleic acid remains either with 5'-, 3'-overlaps, so called "sticky" ends, or with blunt ends. All enzymes were both provided by NEB and Fermentas and used according to the manufacturer's instructions. Following components and conditions were used:

Table 16) Components and conditions for restriction digestion with endonucleases

Component		Quantity [μ l]	Conditions	
Template DNA		5	Temperature [$^{\circ}$ C]	Duration
Fast Digest Enzyme 1		0.5	37	5-15min
Fast Digest Enzyme 2 (optional)		0.5		
10x Fast Digest Green Buffer		2.5		
10x BSA (optional)		0.25		
<i>A.bidest.</i>		<i>Ad 20</i>		

Digested DNA fragments were then separated by size via DNA gel electrophoresis (s. 3.2.1.3.).

3.2.1.3. DNA agarose gel electrophoresis

DNA agarose gel electrophoresis is used for quality control and for separation of DNA fragments according to their size and charge. The individual fragments can be analyzed and extracted (s. 3.2.1.4.). For DNA > 5kb fragments a 0.8% agarose gel was used, whereas for DNA fragments < 5kb a 1% agarose gel was used. The agarose was solubilized in 1x TAE buffer and completed with 0.5 μ g/ml Ethidium bromide (EtBr). EtBr intercalates with the nucleotides of the DNA fragments and renders them visible under UV light at a wavelength of 302nm. A 6x loading buffer was added to the DNA fragments and the fragments were hence separated in a gel chamber filled with 1x TAE buffer at a voltage of 80V. In order to determine the size of the DNA fragments, a marker suited for the expected fragment sizes was added (GeneRuler™ 1kb / 1kb Plus / 100bp / 100bp Plus ladder). Subsequently a picture of the gel was taken with a gel documentation system or the DNA fragments were extracted.

3.2.1.4. Purification and isolation of DNA fragments

PCR purification

Purification of nucleic acids from PCR reactions was accomplished with help of the “QIA PCR Purification Kit” from Qiagen. The purification was carried out according to the manufacturer’s protocol and elution was done with 50 μ l *A.bidest.*

DNA extraction from agarose gels

DNA fragments were cut out from gel on a UV-cutting plate with a scalpel. Subsequently the DNA fragments were weighed and purified by help of the “QIAquick Gel Extraction Kit” from Qiagen according to the manufacturer’s manual. Elution was done with 50µl *A.bidest.* DNA concentration was measured via NanoDrop 1000 and the samples were stored at -20°C for further use.

Maxi-preparation

Large-scale production of plasmid DNA was done in competent *E. coli* Top10 or Stbl2 bacteria. For this purpose single DNA-colonies were incubated in 5ml LB-Amp medium at 37°C, 200rpm for ca. 8h and subsequently 250µl of the suspension further cultivated with 250ml LB-Amp medium (1:1’000) in baffled flasks overnight. Purification was done with help of the “Endo-free Plasmid Maxi Kit” from Qiagen. Procedure was done according to the manufacturer’s manual and the DNA eluted with 200µl *A.bidest.* DNA concentration was measured via NanoDrop 1000 and the samples were stored at -20°C for further use.

Mini-preparation

Small-scale production of plasmid DNA was done in competent *E. coli* Top10 or Stbl2 bacteria. For this purpose single DNA-colonies were incubated in 2ml LB-Amp medium (1:1’000) at 37°C, 200rpm overnight. Purification was done with help of the “QIAprep Spin Miniprep Kit” from Qiagen. Procedure was done according to the manufacturer’s manual and the DNA was eluted with 50µl *A.bidest.* DNA concentration was measured via NanoDrop 1000 and the samples were stored at -20°C for further use.

3.2.1.5. Cloning into pCR4-TOPO® vector

TOPO® cloning reaction was performed according to manufacturer’s instructions. In order to clone a DNA fragment into the pCR4 TOPO® vector, the following reagents were added in the order shown:

Table 17: Components of a cloning reaction into pCR4-TOPO vector

Component	Quantity [µl]
Fresh PCR product	0.5-4
Salt Solution	1
<i>A. bidest.</i>	add to a volume of 5µl
TOPO® vector	1

The reaction was gently mixed and incubated for 5-15 minutes at room temperature. Subsequently, the reaction was used for transformation (s. 3.2.1.6.).

3.2.1.6. Transformation

Transformation serves the amplification of plasmid DNA, which is therefore chemically or via electroporation introduced into competent bacteria. For this work, only chemical transformation was implemented.

For chemical transformations, either competent *E. coli* Top10 or Stbl2 were used. Competent cells were stored at -80°C and thawed before the DNA was added. For re-transformations 1ng DNA-sample/50µl bacteria were used, for all other transformations 10-20ng DNA-sample was used. The sample was chilled on ice for 30min. Then, a heat shock of 42°C for 45s followed. After heat shock, the sample was chilled on ice for another 2min. Then, 250µl S.O.C. medium was added and the suspension was incubated for 1h, 650rpm at 37°C. Then, the suspension was either spread on two LB-Amp plates, with 200 and 100µl suspension per plate, respectively. Alternatively, the whole suspension was spread on one plate for reactions with low probability of success. For re-transformations, only 50µl was spread on one plate. Incubation took place either at 37°C overnight or at room temperature for 48h.

3.2.1.7. DNA measurement

DNA concentration was measured with help of a spectral photometer NanoDrop ND-1000. *A. bidest.* was used as a blank. The measurements were automatically done at a wavelength of 260nm and 280nm.

3.2.2. Cell culture

3.2.2.1. Cultivation of HEK-293T cells

“HEK cells” is the short term for *human embryonic kidney cells*, a cell line derived from human embryonic kidney cells. HEK-293T cells were derived in the 1970s from a transformation of human embryonic kidney cells and DNA pieces of the human adenovirus 5. HEK-293T cells are often used in the development of virus vaccines, chemotherapeutics and for the production of recombinant adenovirus-vectors and are a comparably easy-to-handle cell line. For this work, HEK-293T cells were used for virus production and were grown in 75cm² or 150cm² cell culture flasks at 37°C, 5% CO₂ and 98% humidity.

HEK-293T cells	ATCC® CRL-11268
HEK-293T cell media:	10ml L-glutamine: 2mM (Biochrom KG) 5ml Streptomycin, Penicillin (SP 10'000µg/ml; Biochrom KG) 7.5ml HEPES (Biochrom KG) 50ml FCS = 10% (Biochrom KG) 500ml DMEM media (Biochrom KG)
Further materials and chemicals:	Trypsin/EDTA: 25%, pH = 7.2 (DIFCO, USA) Phosphat Buffered Saline (PBS) „without Ca ²⁺ , Mg ²⁺ “, pH =7.2: 8.0g/l NaCl, 0.20g/l KCl, 1.15g/l Na ₂ HPO ₄ *2H ₂ O, 0.2g/l KH ₂ PO ₄ Cell culture flasks: NUNCLON™-Surface; Roskilde; Denmark Incubator: BBD 6220; Heraeus

HEK-293T cells form an adherent monolayer in the cell culture flask and should hence not exceed 90% confluency. If the bottom of the flask is completely covered, cells are not able to grow anymore due to contact inhibition. Therefore, HEK-293T cell were split 3 times per week 1:10. First the old media was aspirated and the cells were washed twice with 10ml (75cm²) or 20ml (150cm²) PBS. It is important that all FCS is removed, because it diminishes the activity of Trypsin, which is used for cell detachment. After washing cells were incubated with 1ml or 2ml Trypsin/EDTA, respectively, for 3minutes at 37°C. Too long incubation leads to toxic effects of Trypsin. After incubation trypsin activity was stopped by addition of 10ml or 20ml media containing FCS, respectively. The cells were singularized and split 1:10. At last, 9ml or 18ml, respectively, pre-warmed fresh media was added to the cells. Cells were then again incubated at 37°C, 5% CO₂ and 95% humidity. All work was performed under a sterile bench.

3.2.2.2. Cultivation of CrFK cells

“CrFK cells” is the short term for *crandell rees feline kidney cells*, a cell line derived from feline kidney cells. CrFK cells are extensively used for viral infectivity assays and show a high susceptibility to VSV-G pseudotyped HERV-K113 cells [89]. Therefore, in this work CrFK cells were used for infection studies and were grown in 75cm² or 150cm² cell culture flasks at 37°C, 5% CO₂ and 98% humidity.

CrFK cells	ATCC® CCL-94
CrFK cell media:	10ml L-glutamine: 2mM (Biochrom KG) 5ml Streptomycin, Penicillin (SP 10'000µg/ml; Biochrom KG) 7.5ml HEPES (Biochrom KG) 50ml FCS = 10% (Biochrom KG) 500ml DMEM media (Biochrom KG)
Further materials and chemicals:	Trypsin/EDTA: 25%, pH = 7.2 (DIFCO, USA) Phosphat Buffered Saline (PBS) „without Ca ²⁺ , Mg ²⁺ “, pH =7.2: 8.0g/l NaCl, 0.20g/l KCl, 1.15g/l Na ₂ HPO ₄ *2H ₂ O, 0.2g/l KH ₂ PO ₄ Cell culture flasks: NUNCLON™-Surface; Roskilde; Denmark Incubator: BBD 6220; Heraeus

CrFK cells form an adherent monolayer in the cell culture flask and should hence not exceed 90% confluency. If the bottom of the flask is completely covered, cells are not able to grow anymore due to contact inhibition. Therefore, HEK-293T cell were split 3 times per week 1:10. The procedure was equal to the one implemented on HEK-293T cell (s. 3.2.2.1.)

3.2.2.3. Cultivation of C8166 cells

C8166 cells are permanent lymphoid T-cells of human origin. C8166 cells are derived from primary blood cells from the umbilical cord and HTLV-1-producing cells, originating from a patient with T-cell leukemia. C8166-cells contain at least one HTLV-1 provirus but do not produce virus particles due to their lack of other necessary genes for HTLV-1. C8166 cells show a high susceptibility to HIV-1, which makes them an ideal cell line for in vitro infection studies [90]. For this work, C8166 cells were grown in 75cm² cell culture flasks at 37°C, 5% CO₂ and 98% humidity.

C8166 cells	Sigma-Aldrich 88051601
C8166 cell media:	10ml L-glutamine: 2mM (Biochrom KG) 5ml Streptomycin, Penicillin (SP 10'000µg/ml; Biochrom KG) 5ml HEPES (Biochrom KG) 50ml FCS = 10% (Biochrom KG) 500ml RPMI media (RPMI 1640 Medium 1x, Biochrom KG)
Further materials and chemicals:	Cell culture flasks: NUNCLON™-Surface; Roskilde; Denmark Incubator: BBD 6220; Heraeus

The cells were kept at sterile conditions in 75cm² cell culture flasks at 37°C, 5% CO₂ and 98% humidity. C8166 cells form cell aggregates in culture. The cells were split 3 times per week. Therefore, the cells were first transferred into a 50ml falcon tube and settled by centrifugation at 300 x g for 5min. Then, the old media was aspirated and fresh pre-warmed media was added to the cells. Then cells were then split 1:4 and additional 9ml fresh pre-warmed media was added. The cells were further incubated at 37°C, 5% CO₂ and 98% humidity.

3.2.2.4. Cell counting

Cell counting was done with help of Coulter Counter Z2 according to the manufacturer's advice. Following cell densities were used for different well plates and cell culture flasks for transfection and infection:

Table 18: Cell densities for infections or transfections for different culture formats

Culture format	Number of cells/well	Medium for infection	Medium for transfection
6-well plate	6 x 10 ⁵	2ml/well	
100mm dish	2.4 x 10 ⁶		8ml/well
150cm ² cell culture flask	60 – 80% confluency		20ml/well

3.2.2.5. Transient transfection with PolyFect® Transfection Reagent

Transient transfection was done with PolyFect® Transfection Reagent in HEK 293T cells, following the protocol “PolyFect® Transfection Reagent Handbook” from Qiagen. The following parameters were used for transient transfection:

Table 19) Parameters for transient transfection with PolyFect® Transfection Reagent

Culture format	Number of cells/well	Volume of medium [ml]	DNA [µg]	Final volume of diluted DNA [µl]	Volume of PolyFect® reagent [µl]	Volume of medium to add to cells [ml]	Volume of medium to add to complexes [ml]
100mm dish	2.4 x 10 ⁶	8.0	8.0	300	80	7.0	1.0

The day before transfection cells were seeded in appropriate growth medium and incubated overnight at 37°C, 5% CO₂ and 98% humidity. On the day of transfection, cells were sought to be around 80% confluent. DNA was dissolved in TE buffer (pH7-8) with cell growth medium containing no serum, proteins or antibiotics, since these ingredients would interfere with later complex formation. PolyFect® Transfection Reagent was added to the DNA solution and mixed. The samples were incubated at room temperature for 10min to allow complex formation. Meanwhile, old medium in the dishes was replaced by fresh growth medium, containing serum and antibiotics. After complex formation, 1ml of medium was added to the reaction and mixed. The total reaction volume was then transferred into the dishes and gently swirled. Cells were then incubated at 37°C, 5% CO₂ and 98% humidity for 48h to allow for gene expression.

3.2.2.6. Transient transfection with calcium phosphate

Transfection of HEK-293T cells using calcium phosphate is a cheap and equally effective alternative to Polyfect® Transfection Reagent and was therefore used for large-scale virus production in 150cm² cell culture flasks. The day before transfection HEK-293T cells were seeded in appropriate growth medium (20ml) and incubated overnight at 37°C, 5% CO₂ and 98% humidity. On the day of transfection cells were sought to be 80 – 85% confluent. 60µg DNA mix was filled up to a volume of 1.125ml with *A.bidest*. Then, 125µl CaCl₂ was added and the mixture was well vortexed. For each sample 1.25ml 2 x HBS buffer was prepared in a 50ml falcon tube. Subsequently, the DNA mixture was added dropwise to the 2 x HBS buffer whilst vortexing. The reaction was then incubated at room temperature for 30min. In the meantime, the medium in the cell culture flasks was renewed. After incubation, the DNA mixture was added

to the cell culture flask and then incubated at 37°C, 5% CO₂ and 98% humidity. After 12h of incubation the medium was again renewed. 48h after transfection the viruses were harvested by ultracentrifugation (s. 3.2.2.8.). A list of plasmid DNA mixes used for production of pseudotyped virus particles can be found in table 20.

3.2.2.7. Production of pseudotyped HERV-K(HML-2) reporter viruses

For production of pseudotyped HML-2-based reporter viruses HEK-293T cells were transfected with different plasmid DNA mixes containing following constituents and ratios:

Table 20: Plasmids and ratios used for viral particle production

HERV-K(HML-2) reporter virus pseudotyped with Env VSV-G		HERV-K(HML-2) reporter virus pseudotyped with HIV-1 EnvΔS	
Plasmid DNA	Ratio [%]	Plasmid DNA	Ratio [%]
CMVoriLuc_U3Tag2	60	CMVoriLuc_U3Tag2	60
CMVorico GPP	16	CMVorico GPP	16
Env VSV-G	3	Env VSV-G	3
Orico Rec V5	16	Orico Rec V5	16
HIV-1 reporter virus pseudotyped with Env VSV-G		HIV-1 reporter virus pseudotyped with HIV-1 EnvΔS	
Plasmid DNA	Ratio [%]	Plasmid DNA	Ratio [%]
pWPXL_Luc	50	pWPXL_Luc	50
PS Pax 2	37.5	PS Pax 2	37.5
Env VSV-G	12.5	HIV-1 EnvΔKS	12.5

Either 8μg or 60μg of total DNA was used to for transfection in either 75cm² or 150cm² cell culture flasks, respectively. Since EnvΔKS, originally from HIV-1, is non-functional, CMVoriLuc pseudotyped with this envelope protein was used as a negative control. The *Luciferase*-gene in the reporter viruses was under control of the EF-1α promoter. Transfection of HEK-293T cells was carried out with either PolyFect® transfection reagent (s. 3.2.2.5.) or calcium phosphate (s. 3.2.2.6.).

3.2.2.8. Purification of cell culture supernatant using ultracentrifugation

Purification of cell culture supernatants was carried out via ultracentrifugation. First, centrifuge tubes (Beckman Coulter) were sterilized in 70% EtOH under the sterile bench for 30min. The centrifuge tubes were then washed in 1x PBS and air-dried. In the meantime, cell culture media containing the transfected cells was transferred to falcon tubes and centrifuged at 1'000rpm for 10min to separate cell debris from the viruses. The supernatant was then transferred to the centrifuge tubes and the loaded centrifuge tubes were then inserted into the rotor (no. 41 for 10ml, no. 43 for 20ml) and calibrated to two decimal points. Work was done entirely under the sterile bench. The samples were then centrifuged at 34'000rpm, 4°C for 3h 15min. After centrifugation, the supernatant was discarded and the virus pellet dissolved in 100µl (for 10ml transfection volume) or 200µl (for 20ml transfection volume) 1x PBS, respectively. The solution was then transferred to a fresh Eppendorf tube and 10µl was separated for ELISA (s. 3.2.3.2.). ELISA samples were stored at -20°C, and the vital viruses were stored at -80°C for later infection (s. 3.2.2.9. and 3.2.2.10.). Rotor tubes were sterilized in disinfection reagent for 20min and then washed in 70% EtOH and air-dried afterwards.

3.2.2.9. Infection of CrFK cells

CrFK cells were infected with various pseudotyped viruses (s. table 20). Prior to infection, viruses were normalized with an ELISA (Enzyme-linked Immunosorbent Assay, s. 3.2.3.2.) to control for equal virus concentration in each infection. Thereby, max. 2/3 of normalized virus supernatant (but not less than 12ng/ml) and at least 1/3 of fresh medium were added to the cells. Cells were infected with one sort of pseudotyped virus only. In order to increase adsorption of viruses to the cell surface, 8µg/ml Polybrene® per well was added. All infection assays were done in 6-well plates and cells were lysed after 24h and 48h, respectively (s. 3.2.2.12.). Table 21 shows the reagents for infection of CrFK cells:

Table 21: Components for infections of CrFK cells

Culture format	Number of cells/well	Final volume of medium [ml]	Virus load [µg]	Volume of Polybrene® [µl]
6-well plate	1 x 10 ⁶	2.0	≥ 12ng/ml	16

3.2.2.10. Infection of C8166 cells with HIV-1IIIB via spinoculation

For infection of C8166 T-cells with HIV-1IIIB, C8166 cells were distributed in 6-well plates at 0.5×10^6 cells/well density. For the experiment, two time points post-infection were chosen to analyze: 2h and 24h post-infection. For every time-point, heat-inactivated viruses were used as negative control. Every time point was measured in duplicates

The viruses were stored at -80°C . Thawing occurred at 37°C for few minutes. The virus stocks were then kept on ice until further procedure. Heat inactivation occurred at 65°C for 1h. For infection, 2ml RPMI medium, preheated to 37°C , was added to the cells. Then 21μ Polybrene was mixed with $500\mu\text{l}$ virus suspension and the mixture was added to the cells.

Infection occurred via spinoculation at $1'200 \times \text{g}$ for 2h. After spinoculation, the cells were incubated at 37°C , 5% CO_2 and 98% humidity.

Total cellular DNA was harvested from both live virus- and heat-inactivated virus-infected cells at desired time points. Therefore, the media was transferred to a micro centrifuge tube and centrifuged at $300 \times \text{g}$ for 10min at 4°C . The supernatant was discarded and the cell pellet stored at -80°C until ready to isolate DNA (s. 3.2.2.12.).

3.2.2.11. Cell lysis for production of genomic DNA and Luciferase Assay

After infection, cells had to be lysed in order to quantify infection rate by luciferase assay (s. 3.2.3.1.) and use the genomic DNA for further analysis. Therefore, the growth medium was removed and the infected cells were washed twice with 1ml 1x PBS. Then, cells were treated with $500\mu\text{l}$ Trypsin/well of a 6-well plate and incubated for 3min at 37°C . Subsequently, Trypsin was blocked with $2 \times 500\mu\text{l}$ DMEM (+10% FCS + 0.5% P/S) and the samples were transferred to a fresh Eppendorf tube. Then the samples were centrifuged at $300 \times \text{g}$ for 5min. The supernatant was discarded and the pellet resuspended in 1ml 1x PBS. $750\mu\text{l}$ was used for production of genomic DNA (s. 3.2.2.12.) and $250\mu\text{l}$ was used for luciferase assay. These $250\mu\text{l}$ were centrifuged again at $300 \times \text{g}$ for 5min and the supernatant discarded. Then, $200\mu\text{l}$ 5x Passive Lysis Buffer was added and the reaction was incubated at room temperature for 10min. Then, the cells were vortexed for 10-15s and again centrifuged at $12'000 \times \text{g}$ for 30s. The supernatant was transferred into 4 PCR-tubes, $50\mu\text{l}$ each and stored at -80°C until further use.

3.2.2.12. Isolation of genomic DNA

Isolation of genomic DNA was performed according to the manufacturer's instructions with help of the "QIAamp DNA Blood Mini Kit" from Qiagen. 750µl of infected cells suspended in PBS (s. 3.2.2.11.) were centrifuged at 300 x g for 5min. Then, the supernatant was discarded and the pellet softly patted dry. If isolation was not continued immediately, the dried cell pellet was stored at -20°C until proceeding. The pellet was dissolved in 200µl 1x PBS. Then 20µl Proteinase K was added. 200µl Buffer AL was added to the mixture and the sample was pulse-vortexed for 15s. Then, the sample was incubated at 56°C for 10min. After incubation the samples were shortly spun down to ensure no droplets were inside the lid. Then, 200µl Ethanol (98%) was added and the samples again pulse-vortexed for 15s. Again, they were spun down shortly before transfer to a 2ml spin column provided by the manufacturer. The samples were centrifuged at 6'000 x g for 1min. Then the column was washed with 500µl Buffer AW1 and centrifuged again for 1min at 6'000 x g. The column was again washed with 500µl Buffer AW2 and centrifuged at 20'000 x g for 3min. After every washing step the 2ml collection tube was replaced by a new one. In order to get rid of residual buffer the sample was centrifuged again at 20'000 x g for 1min. Then, the column was placed into a fresh 1.5ml microcentrifuge tube and 200µl elution buffer AE was added to the sample and the samples were incubated at room temperature for 1min. Finally, the samples were centrifuged at 8'000 x g for 1min and the column discarded. DNA concentration was measured and the samples were stored at -20°C until further use.

3.2.2.13. Direct cell lysis for sample preparation

In order to prepare DNA samples after infection, two methods were applied: DNA isolation (s. 3.2.2.12.) and direct cell lysis. It has been shown that during isolation of genomic DNA, some of the DNA gets lost, an unwanted side effect which is absent in direct cell lysis [91]. For direct cell lysis, following protocol was performed with dry cell pellets:

Table 22: Protocol for direct cell lysis

Step	Temperature [°C]	Duration
Freezing	-80	20min
Thawing	60	5min
Repeat 3 times		
Lysis	60	3h
	95	1h

Lysis was performed with 200µl/pellet Lysis buffer containing proteinase K (1:100). After lysis, the sample was used directly for PCR.

3.2.3. Protein Analytics

3.2.3.1. Luciferase assay

Luciferase activity was quantitatively measured with help of an Illuminometer. A bioluminescence producing gene served as a reporter. This gene, called *firefly-Luciferase*, originates from the lightning bug (*Photinus pyralis*) and serves the purpose of light generation. For measurement of Luciferase activity pseudotyped viruses were produced which expressed the *Luciferase-gene* (s. 3.2.2.7.). The amount of firefly-Luciferase in the cell lysate is thereby proportional to the light emission measured; hence a direct indication for the amount and infection rate of luciferase-viruses in the cell lysates can be drawn. Preparation of luciferase-virus lysates was done according to the manufacturer's instructions. The arithmetic mean of Luciferase activity was determined using one infection assay which was repeated 3 times.

3.2.3.2. ELISA

In order to normalize virus particles before infection, an ELISA (Enzyme-linked immunosorbent assay) was performed. Therefore, a 96-well plate was covered with capture antibody and incubated at 4°C overnight. On the next day, the supernatant was discarded and the plate rinsed three times with 0.05% Tween. Then, the plate was blocked with PM and incubated at 37°C for 45 – 60min. In the meantime, virus samples were inactivated with 0.2% Tween for 5 – 10min at room temperature. After incubation, the PM was discarded and the plate firmly tapped but not rinsed. Then, the samples were applied (s. figure 8) and incubated at 37°C for 45 – 60min. After incubation, the plate was rinsed three times with 0.05% Tween. Subsequently, the primary antibody was applied and the plate was incubated 45 – 60min at 37°C. Afterwards, the plate was rinsed three times with 0.05% Tween and the secondary antibody was applied and the plate was again incubated at 37°C for 45 – 60min. After this last incubation step, the plate was rinsed three times with 0.05% Tween. In the next step, the stain was added and the plate incubated for 10 – 15min at room temperature until staining became clearly visible. The reaction was finally stopped with H₂SO₄. The plate was then read in an ELISA reader system. All reagents used and their volumes are listed in table 23.

ISN	1	2	3	4	5	6	7	8	9	10	11	12
A	Sample 1: 1:25 in PMT ; 75µL/well			Sample 2: 1:25 in PMT ; 75µL/well			Sample 3: 1:25 in PMT ; 75µL/well			Sample 4: 1:25 in PMT ; 75µL/well		
B	Dilution 1:9			Dilution 1:9			Dilution 1:9			Dilution 1:9		
C	Dilution 1:27			Dilution 1:27			Dilution 1:27			Dilution 1:27		
D	Dilution 1:81			Dilution 1:81			Dilution 1:81			Dilution 1:81		
E	Dilution 1:243			Dilution 1:243			Dilution 1:243			Dilution 1:243		
F	Dilution 1:729			Dilution 1:729			Dilution 1:729			Dilution 1:729		
G	100ng/ml Standard	Dilution 1:3	Dilution 1:9	Dilution 1:27	Dilution 1:81	Dilution 1:243	Dilution 1:729	Dilution 1:2187	Dilution 1:6561	Dilution 1:19683	Dilution 1:59049	blank
H												

Figure 8: Scheme showing an ELISA plate set up

Scheme showing the application of samples on an ELISA plate. Lanes B – H were filled with 50µl/well PMT as background. The samples were added 1:3 diluted in PMT in lane A (75µl). Then the samples were titrated; 25µl were transferred from one well to the next in the following lane (A to F) and pipetted 5x up and down. In lane F, 25µl were removed and discarded. Lanes G and H contained the standard. Starting from 75µl pure standard in G1 and H1, titration was performed as for the samples, but down the lane (G1/H1 to G11/H11). Wells G12 and H12 were left blank (only PMT). Lane A did not contain PMT as background.

Table 23) Components and respective volumes used in an ELISA

Component	Dilution	Volume per well [μ l]
Capture antibody	HERV-K113: HERMA7 1:100 in carbonate buffer HIV-1: Ag 3.1 in carbonate buffer	50
0.05% Tween	1:200 10% Tween stock solution in 1x PBS	<i>wash</i>
PM	2g milk powder in 100ml 1x PBS	200
PMT	0.4ml 10% Tween stock solution in 80ml PM	<i>Diluent</i>
Primary antibody	HERV-K113: K140 (rabbit), 1:400 in PMT; HIV-1: HIV+ pool plasma, 1:10'000 in PMT	50
Secondary antibody	HERV-K113: α -rabbit, 1:2000 in PMT; HIV-1: α -human, 1:1000 in PMT	50
Virus sample	<i>s. figure 8</i>	<i>s. figure 8</i>
Stain	5mg OPD pill in 12.5ml phosphate citrate buffer & 12 μ l H ₂ SO ₄	50
H ₂ SO ₄	-	25
Standard p27 or BG1	<i>s. figure 8</i>	<i>s. figure 8</i>

3.2.4. $2^{-\Delta\Delta C_T}$ method for calculation of ratio between two cDNA samples in real-time qPCR

Real-time qPCR measures C_T -values for target and reference genes of two different samples. Formula 1.1. was implemented to calculate the normalized C_T -value for a sample:

$$\Delta C_{T,q} = C_{T,Xq} - C_{T,Rq} \quad (1.1)$$

Where: $\Delta C_{T,q}$: normalized C_T for sample

$C_{T,Xq}$: C_T of target in sample

$C_{T,Rq}$: C_T of reference in sample

Calculation of normalized C_T -value for the calibrator sample was done with formula 1.2.:

$$\Delta C_{T,cb} = C_{T,Xcb} - C_{T,Rbc} \quad (1.1)$$

Where: $\Delta C_{T,cb}$: normalized C_T for calibrator

$C_{T,Xcb}$: C_T of target in calibrator sample

$C_{T,Rcb}$: C_T of reference in calibrator sample

Calculation of the ratio was done by equation 1.3., where $\Delta\Delta C_T$ is from formula 1.4.:

$$Ratio = 2^{-\Delta\Delta C_T} \quad (1.3)$$

$$\text{With } \Delta\Delta C_T = \Delta C_{T,q} - \Delta C_{T,cb} \quad (1.4)$$

Since all values were measured in duplicates or triplets, standard deviation and arithmetical mean of the ratio values could be calculated.

4. Results

4.1. Production of HIV- and HERV-K(HML-2)-reporter viruses and infection assay

4.1.1. Production of reporter viruses

Viruses are produced artificially by help of various plasmids carrying the necessary genes for structural proteins, enzymes and, last but not least, the virus genome. pWPXL_Luc is a lentivirus vector which carries both LTRs and the packing signal and the *firefly luciferase* gene under the EF1 α promoter. Luciferase signal from viruses inside cells can later be detected by means of a Luciferase assay, enabling a quantitative measurement of infectivity. pS Pax 2 is a vector containing the HIV *gag*, *tat* and *rev* genes. Env VSV-G (glycoprotein G of Vesicular Stomatitis Virus) codes for an envelope protein known to infect a broad range of cells [92], whereas HIV-1 Env Δ KS codes for a non-functional envelope protein from HIV-1. In order to produce pseudotyped luciferase HIV-1 reporter viruses, human HEK 293T cells were transfected with pWPXL_Luc together with pS Pax 2 and either Env VSV-G or HIV-1 Env Δ KS. In contrast, pseudotyped HML-2-based luciferase reporter viruses were produced using 4 plasmids. CMVoriLuc contains –next to the *firefly luciferase* gene under the EF1 α promoter- the HERV-K (HML-2) genome. In order to be able to distinguish between plasmid DNA and cDNA in later infection studies, a CMVoriLuc plasmid carrying a mutation in the U3-region of the 3'LTR was used and the respective reporter particles were termed oriHERVK113*. HML-2-based luciferase reporter viruses produced with the non-mutated CMVoriLuc plasmid were termed oriHERVK113. CMVoricogpp contains the genes *gag*, *pro* and *pol* of HERV-K(HML-2). Orico Rec_V5 is necessary for the exit of the RNA genome from the nucleus during replication. As for HIV-1, HML-2-based luciferase reporter viruses were pseudotyped with Env VSV-G (VSV-G) or HIV-1 Env Δ KS (Δ KS). These reporter viruses were used for infection studies, where Δ KS-pseudotyped reporter viruses served as negative controls due to their inability to infect.

4.1.2. ELISA for normalization of virus particle load before infection

Viruses were normalized prior to infection by means of an ELISA. Both HIV-1 and HML-2-based luciferase reporter viruses were produced and either pseudotyped with VSV-G or Δ KS. Transfection with 60ng DNA resulted in 1.08×10^5 ng/ml p24 CA VSV-G-pseudotyped HIV-1 reporter viruses and 3.75×10^4 ng/ml p24 CA Δ KS-pseudotyped HIV-reporter viruses (s. figure 9). Slightly less HML-2-based luciferase reporter viruses were produced with 1.5×10^4 ng/ml p27 CA VSV-G-pseudotyped and 3.2×10^4 ng/ml p27 CA Δ KS-pseudotyped particles (s. figure 10). In conclusion, particle production worked well for both HIV-1 and HML-2-based luciferase reporter viruses.

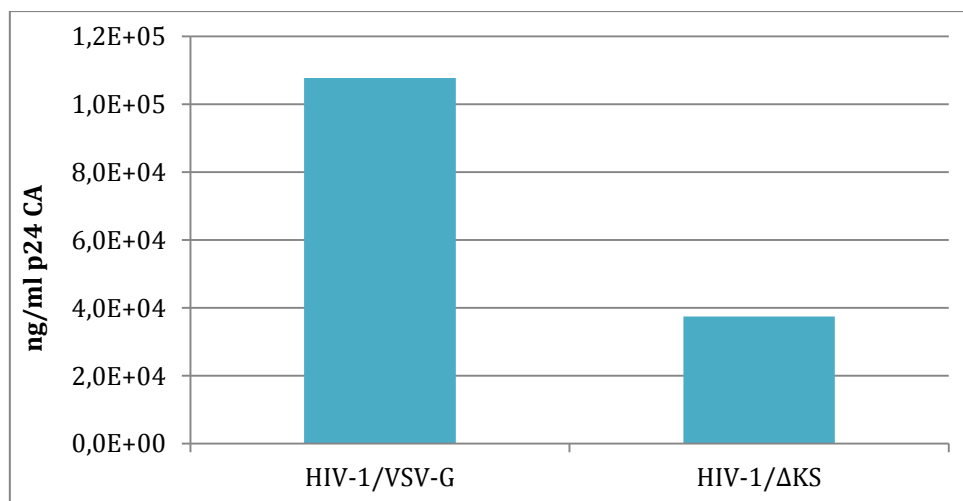


Figure 9: ELISA for HIV-1-reporter viruses after transfection of 293T cells for 48h

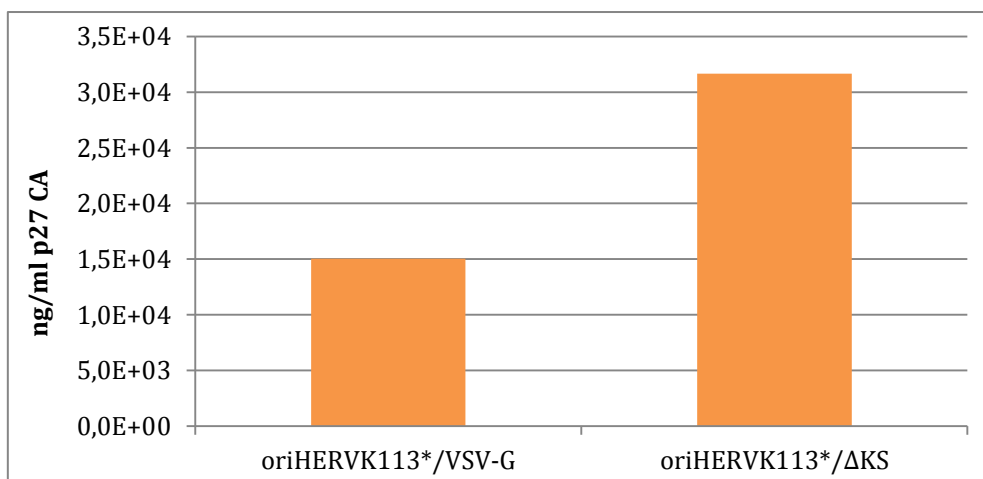


Figure 10: ELISA for tagged HERV-K(HML-2)-reporter viruses (oriHERVK113*) after transfection of 293T cells for 48h

4.1.3. Luciferase assay for determination of infection rate of HERV-K and HIV-1 reporter viruses

After normalization, virus particles were used for infection of CrFK cells. CrFK cells are particularly permissive for HERV-K(HML-2) [93] and neither contain a copy of HERV-K(HML-2) nor HIV-1 in their genome, which makes them well suited for infection studies of both viruses. Infected cells were lysed 24h and 48h post- infection. Infection rate for both reporter viruses was measured in a Luciferase assay. It was of particular interest, whether the mutation in the 3'LTR had any negative effects on infectivity of HML-2-based luciferase reporter particles. Therefore, infection rate was compared to non-mutated HML-2 based reporter viruses. As can be seen in figure 12, no particular effects of the mutation on infection rate were seen. The RLU signal for oriHERVK113 pseudotyped with VSV-G (6.5×10^3) is about equal to the one for oriHERVK113* (1.2×10^4 24h post-infection and 3×10^3 48h post-infection). A difference in infection could be measured comparing VSV-G-pseudotyped HIV-1 and HLM-2-based luciferase reporter viruses: whereas HLM-2-based luciferase reporter viruses had their peak 24h post-infection, HIV-1 reporter viruses had their peak 48h post-infection (5.32×10^6 24h post-infection compared to 1.47×10^7 48h post-infection, s. figure 11). In contrast, pseudotypization with Δ KS strongly reduced infectivity for both reporter viruses. These results support the expectations that a) pseudotypization with VSV-G enhances infectivity of reporter viruses; whereas Δ KS impedes infectivity and that b) the mutation has no measurable side effects on HML-2-based luciferase reporter viruses.

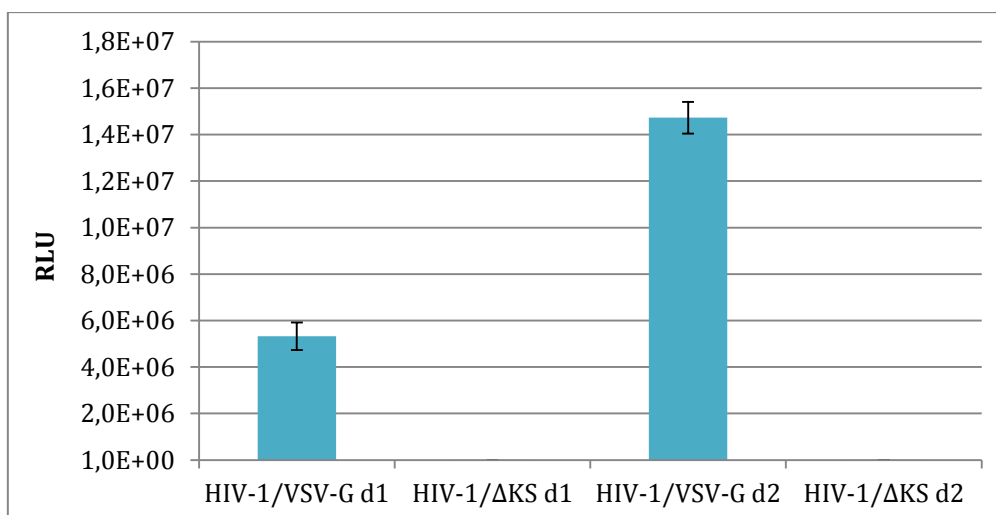


Figure 11: Luciferase assay for HIV-1 reporter viruses in CrFK cells

Luciferase assay for HIV-1 reporter viruses after infection of CrFK cells 24h (d1) and 48h (d2) post-infection. Bars represent average means of four replicates. Error bars represent standard deviations of four replicates.

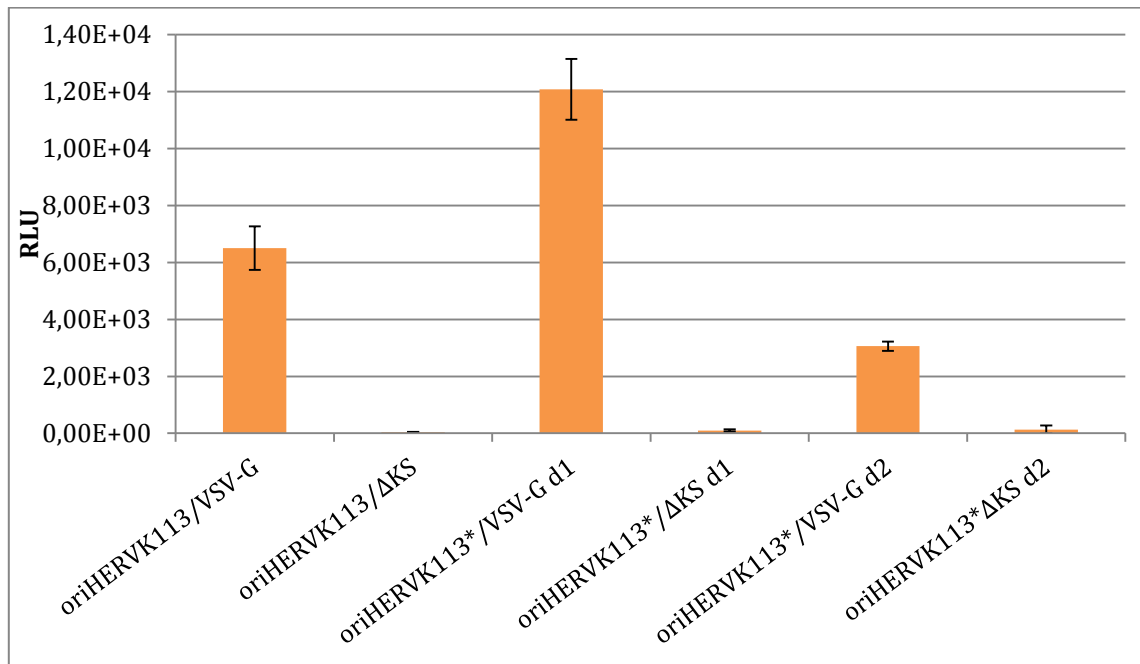


Figure 12: Luciferase assay for non-tagged and tagged HERV-K(HML-2) reporter viruses in CrFK cells

Luciferase assay for HERV-K(HML-2) reporter viruses after infection of CrFK cells 24h (d1) and 48h (d2) post-infection. Bars represent average means of four replicates. Error bars represent standard deviations of four replicates.

4.2. Real-time qPCR

4.2.1. Real-time qPCR with SYBR Green I dye or TaqMan probes

After infection, retroviruses normally undergo reverse transcription followed by nuclear import and integration of the viral cDNA genome into the host genome. Real-time qPCR is sensitive enough to detect even low amounts of DNA in a sample. Therefore, this method has been chosen to search for and track post-entry events of HIV-1 and HML-2-based luciferase reporter viruses. In order to detect and quantify various products of reverse transcription and integrated provirus, primer-sets have been used which bind specifically to distinct RT products. Thereby, two different qPCR techniques have been applied: for real-time qPCR with HIV-1 reporter viruses, SYBR Green I dye has been used, a moderately priced dye which is universally applicable to all PCR reactions. For HML-2-based luciferase reporter viruses, real-time qPCRs with TaqMan probes have been performed. Although more costly, these probes provide a greater level of specificity and are hence generally preferred over SYBR Green for real-time qPCR. The primers for HIV-1 have been adapted from a paper published in 2009 by Mbisa *et al.* [88] where the same assay has been performed for different HIV-1-reporter viruses (except for the control primers,

which are taken from yet another paper published by Malnati *et al.* [94]). The primers for HERV-K have been designed in-house.

4.2.2. Real-time SYBR Green qPCR for HIV-1 RT products in chronically infected T-cell line (ACH-2) compared to an uninfected T-cell line (C8166) using SYBR Green I dye

The different primer-sets (s. supplement) for HIV-1 real-time qPCR were first applied in a set-up with ACH-2 and C8166 cells. Figure 6 in the introduction gives an overview over the different primer binding sites. ACH-2 is a cell line derived from a HIV-1 latent T cell clone which contains one integrated proviral copy. It is known, that apart from integrated proviruses stable forms of unintegrated 1- and 2-LTR-circles form also part of the HIV DNA-pool within these cells [95] [96]. C8166 cells, in contrast, do not contain a proviral copy of HIV-1. The aim was to assess the suitability of SYBR Green as alternative to TaqMan probes.

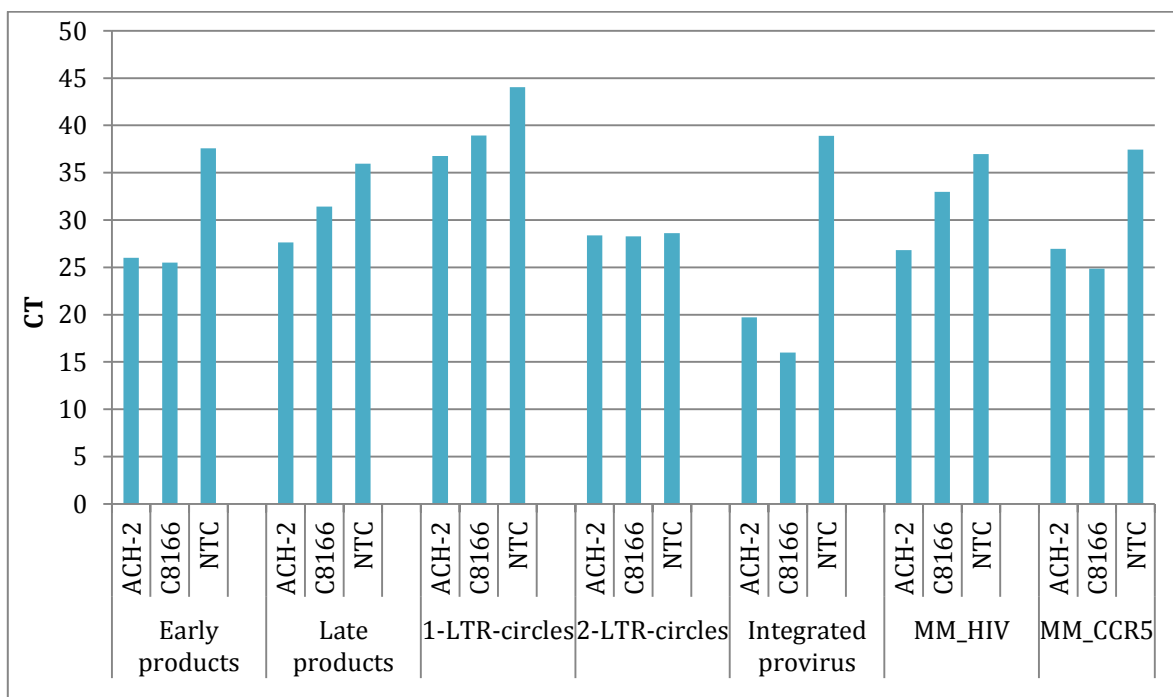


Figure 13: SYBR Green real-time qPCR of ACH-2 and C8166 cells for detection of different HIV-1 RT products

CT values for early and late RT products, 1- & 2-LTR-circles and integrated provirus in ACH-2 and C8166 cells. Early products: CT=25.99 for ACH-2 cells, CT=25.51 for C8166 cells and CT=37.58 for NTC. Late products: CT=27.63 for ACH-2 cells, CT=31.42 for C8166 cells and CT=35.95 for NTC. 1-LTR-circles: CT=36.76 for ACH-2 cells, CT=38.93 for C8166 cells and CT=44.03 for NTC. 2-LTR-circles: CT=28.36 for ACH-2 cells, CT=28.28 for C8166 cells and CT=28.62 for NTC. Integrated Provirus: CT=19.73 for ACH-2 cells, CT=15.99 for C8166 cells and CT=38.89 for NTC. HIV-1 DNA (MM_HIV): CT=26.82 for ACH-2 cells, CT=32.98 for C8166 cells and CT=36.97 for NTC. Bars represent average means of the duplicates. NTC=no template control.

As can be seen in figure 13, a higher HIV-DNA content in ACH-2 cells (CT=23.61) compared to C8166 cells (CT=29.58) could be measured (primer pair MM_HIV) which corresponds to a 308.69-fold change calculated by the $2^{-\Delta\Delta C_T}$ method (s. figure 14). The dissociation curve clearly shows a different product in ACH-2 cells compared to C8166 cells, indicating HIV-1 amplification only in ACH-2 cells (s. figure 15 D). Early products and 2-LTR-circles show almost no difference in CT-signal between ACH-2 and C8166 cells (CT=25.99 and CT=25.51 for early products and CT= 28.36 and CT=28.28 for 2-LTR-circles, respectively) and the difference for integrated provirus is rather small (0.32-fold change, not shown) indicating either unspecific primer binding on genomic DNA, primer-dimerization or contamination. The dissociation curve for early products shows the same fragment for ACH-2 & C1866 cells and the NTC though, making primer dimerization or contamination more likely to be the cause for the generated CT (s. figure 15 A). By means of the $2^{-\Delta\Delta C_T}$ method a distinct 59.71-fold change for late RT products for ACH-2 cells compared to C8166 cells could be calculated (CT=27.63 for ACH-2 cells compared to CT=31.42 for C8166 cells, s. figure 14). Although CT-signals for both ACH-2 and C8166 cells were quite similar for 1-LTR-circles (CT=36.76 for ACH-2 cells and CT=38.93 for C816 cells), their difference in signal in relation to DNA quantity corresponded to a 19.43-fold change (s. figure 14). Furthermore, the dissociation curve shows a clear difference in peaks between the two cell lines, with one C8166-sample being completely negative after all (s. figure 15 C).

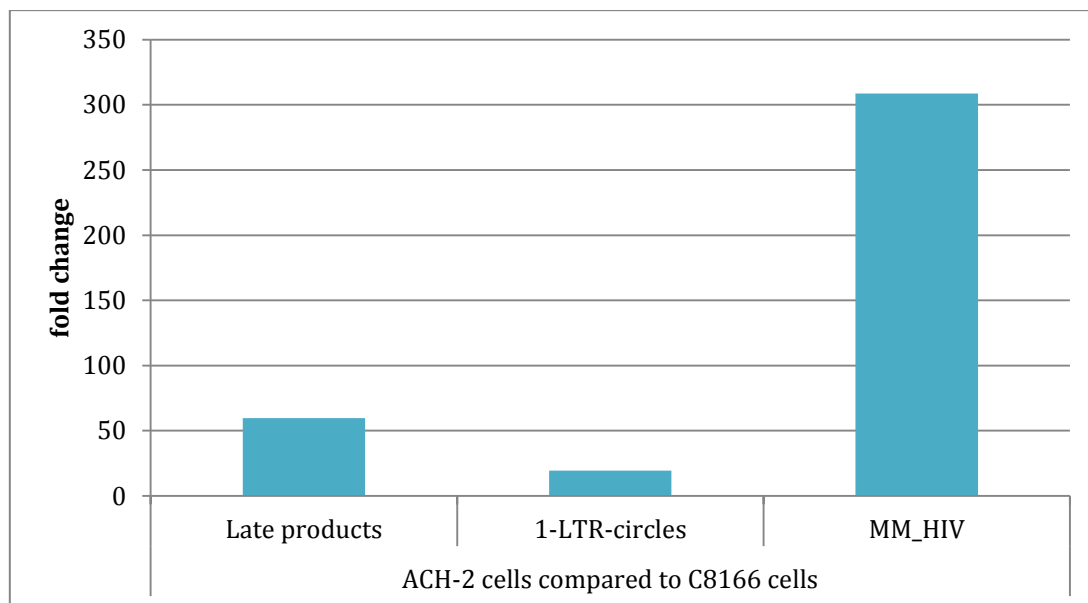


Figure 14: Fold change in difference of HIV-1 vDNA between ACH-2 and C8166 cells after real-time qPCR of genomic DNA using the $2^{-\Delta\Delta C_T}$ method

Numbers are corrected for amount of DNA measured in each sample. For HIV vDNA a 308.69-fold change was measured in ACH-2 cells compared to C8166 cells. For late RT products, a 59.71-fold change and for 1-LTR-circles a 19.43-fold change was measured.

In conclusion, CT-signals for C8166 cells and the NTC were present with all primer-pairs applied and noticeable differences in relative signal intensity could only be evaluated for less than half of the primer-pairs. The differences in CT-signal for 1- and 2-LTR-circles and for integrated provirus are fairly smaller than expected with C8166 supposed to be completely negative after all. Admittedly, no predictions could be made concerning early and late products, since it is not known if at all and to what extent these forms exist in HIV-1 latent T-cells. Nevertheless, these data suggest that SYBR Green creates unspecific signals, probably by binding redundantly to double stranded DNA and by primer-dimerization. ACH-2 cells are probably not very suited as a model to study infection, since replication might not take place in these cells.

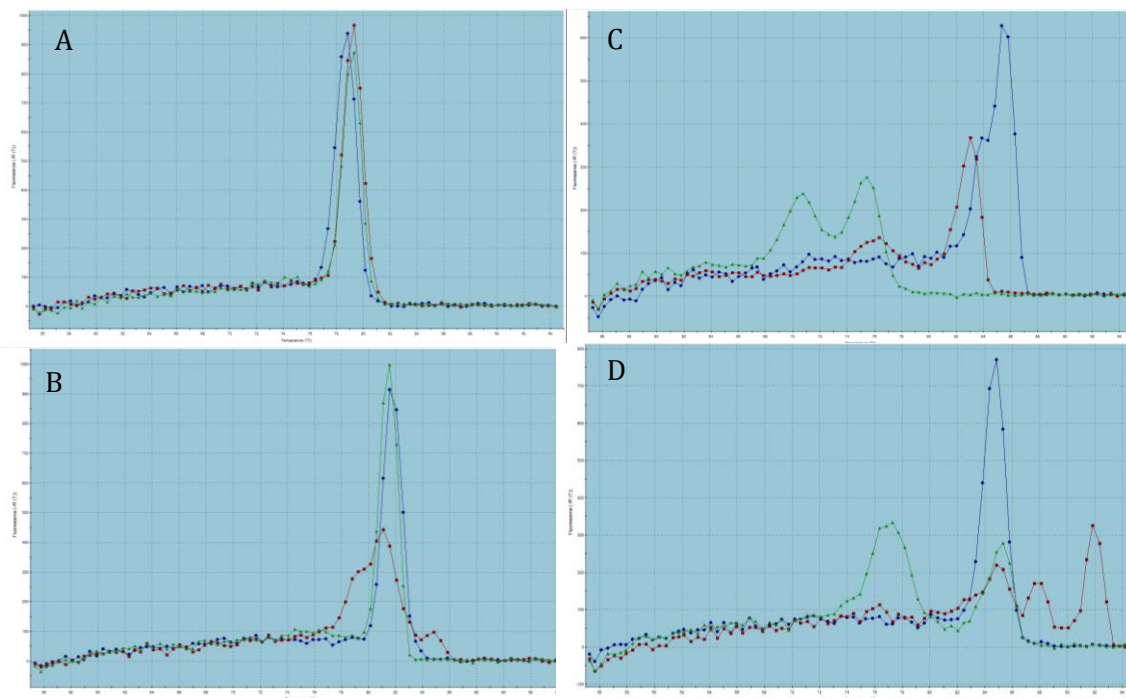


Figure 15: Dissociation curve of HIV-1v DNA for ACH-2 and C8166 cells and NTC in real-time qPCR of genomic DNA

Blue Lines= ACH-2 cells, red lines=C8166 cells, green lines=NTC. A=Early products, B=Late products, C=1-LTR-circles, D=HIV-1 DNA. NTC=n -template control

4.2.3. Real-time SYBR Green duplex qPCR for RT products of plasmid-based HIV-1 reporter viruses

CrFK cells were infected with pseudotyped plasmid-based HIV-1 reporter viruses and the DNA isolated 24h and 48h post-infection. gDNA was subsequently analyzed in real-time SYBR Green qPCR. The same primer-pairs as in the assay for ACH-2 cells were used (s. 4.2.2.).

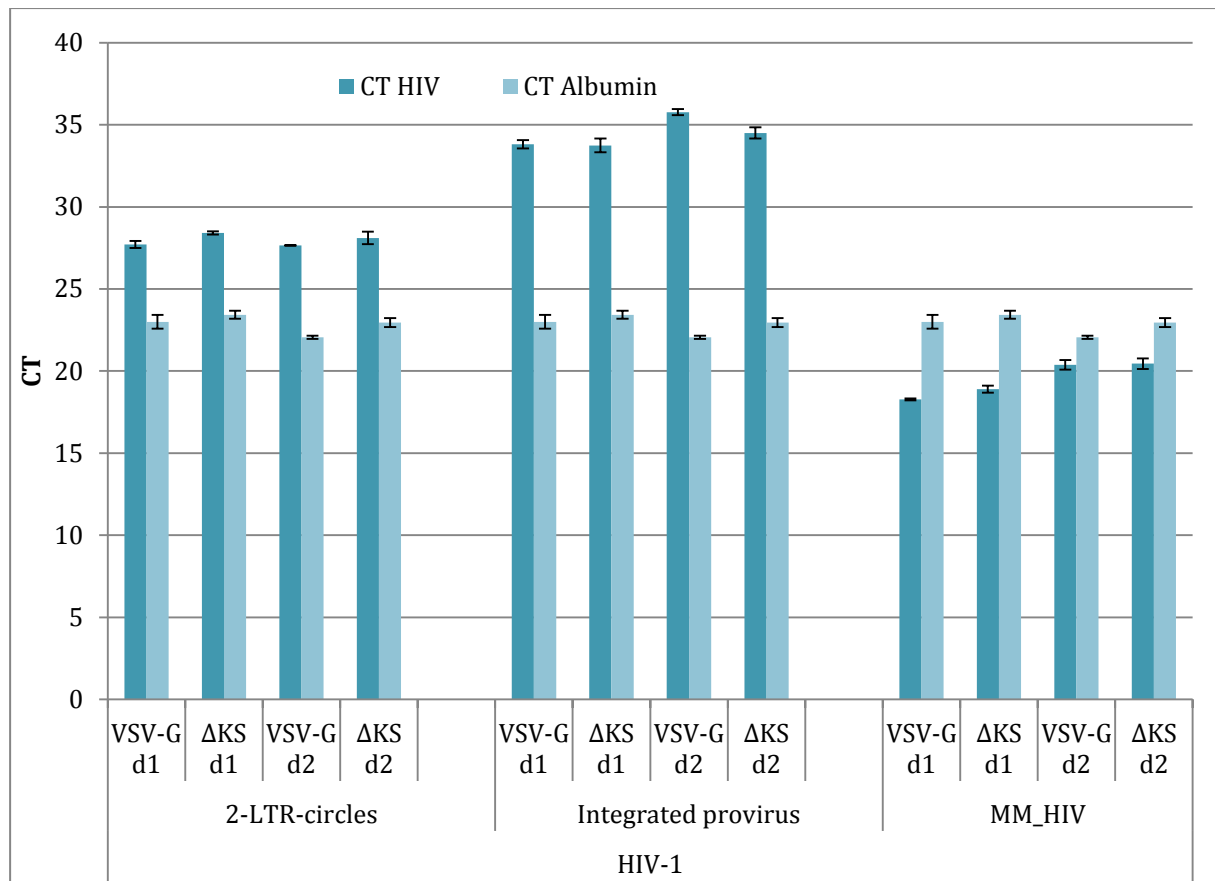


Figure 16 SYBR Green real-time duplex qPCR of CrFK cells infected with VSV-G- or ΔKS-pseudotyped HIV-1 reporter viruses for detection of HIV-1 vDNA, 2-LTR-circles and integrated provirus

CT values for 2-LTR-circles and integrated provirus in C8166 cells infected with HIV-1 reporter viruses. VSV-G-pseudotyped viruses, cells lysed 24h post-infection: 2-LTR-circles=27.71, integrated provirus=33.82, HIV-1 DNA=18.28. ΔKS-pseudotyped viruses, cells lysed 24h post-infection: 2-LTR-circles=28.41, integrated provirus=33.74, HIV-1 DNA=18.9. VSV-G-pseudotyped viruses, cells lysed 48h post-infection: 2-LTR-circles=27.65, integrated provirus=35.77, HIV-1 DNA=20.38. ΔKS-pseudotyped viruses, cells lysed 48h post-infection: 2-LTR-circles=28.11, integrated provirus=34.5, HIV-1 DNA=20.45. Albumin (CT Albumin) was measured as internal control for amount of genomic DNA present in the sample. Bars represent average means of three replicates. Error bars represent standard deviations of three replicates. d1=cells lysed 24h post-infection. D2=cells lysed 48h post-infection. NTC=no template control.

These two assays differed in two regards: First, whereas viral replication is uncertain in HIV-1 latent ACH-2 cells, it is definitely expected for HIV-1 reporter viruses, which guarantees the presence of various RT products such as early and late products. Second, whereas the assay for ACH-2 cells was performed in a plasmid-free context, pDNA contamination was predicted to be one major drawback of plasmid-based HIV-1 reporter viruses, since it provides a template for certain primer-pairs. The experiment with HIV-1 reporter viruses nevertheless provided a means of comparison of suitability between SYBR Green and TaqMan probes, which were used by Mbisa *et al.* [63]. In parallel to HIV vDNA, albumin was measured as internal control for the content of cellular DNA. As can be seen in figure 16, CT-signals were measured in all samples, and values differed little between Δ KS- (non-infectious) and VSV-G- (infectious) pseudotyped HIV-1 reporter viruses. By fact, an earlier CT-value was measured for early and late products as well as for 1-LTR-circles in samples from Δ KS-pseudotyped HIV-1 reporter viruses, voiding these data (not shown). For 2-LTR-circles, integrated provirus and HIV-1 vDNA minor differences in favor of VSV-G-pseudotyped HIV-1 reporter viruses could be calculated (fold change 24h and 48h post-infection: 2-LTR-circles= 1.21 and 0.74; integrated provirus= 0.7 and 0.22; HIV-1 vDNA= 1.14 and 0.57, s. figure 17).

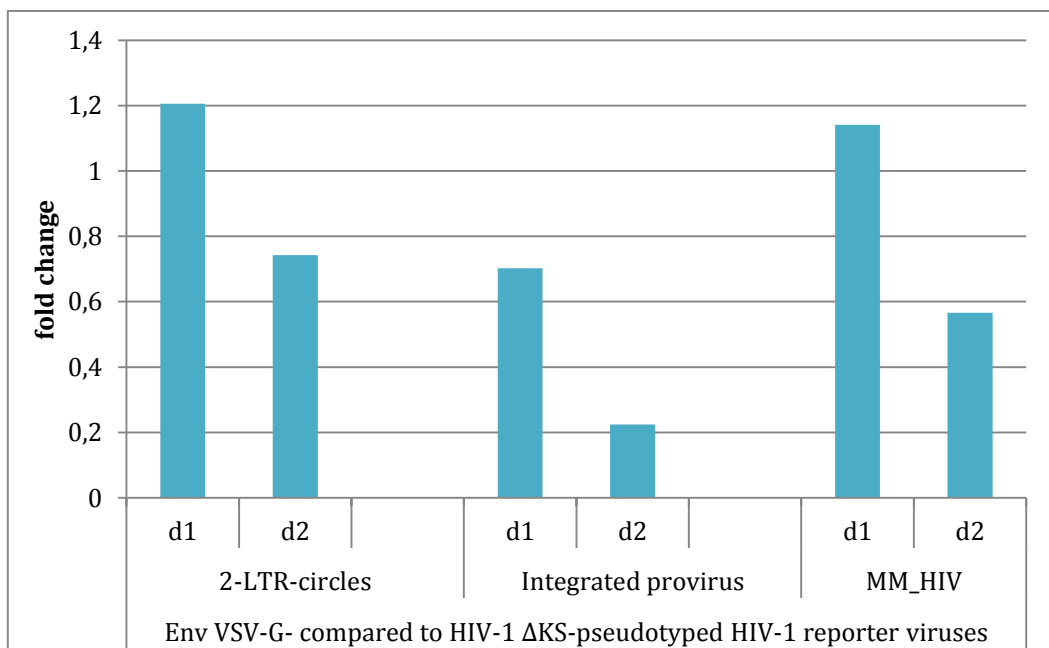


Figure 17: Fold change in difference between samples from VSV-G- and Δ KS-pseudotyped reporter viruses after SYBR Green real-time duplex qPCR of genomic DNA from CrFK cells infected with HIV-1 reporter viruses using the $2^{-\Delta\Delta C_T}$ method

Numbers are corrected for amount of DNA measured in each sample. 24h post-infection (d1) a 1.21-fold increase and 48h post-infection (d2) a 0.74-fold increase in cDNA from HIV-1 2-LTR-circles was measured in samples from VSV-G pseudotyped viruses compared to samples from Δ KS pseudotyped viruses. For DNA of integrated provirus, a 0.7-fold change was measured 24h post-infection and a 0.22-fold change 48h post-infection. For HIV vDNA a 1.14-fold change was measured 24h post-infection and a 0.57-fold change 48h post-infection.

In conclusion, these data suggest that the absence of specific probes in the real-time SYBR Green qPCR seems to have the negative effect of primer dimers generating false positive signals. Although positive signals for all NTCs could be measured, the signals were later in time compared to infectious and even non-infectious viruses, suggesting yet another negative effect of unspecific primer binding on genomic DNA. As a consequence, specialized probes are necessary to avoid unspecific primer binding and primer dimers and thus to obtain meaningful results.

4.2.4. Study of HERV-K(HML-2)-post-entry events in real-time duplex qPCR and digital droplet PCR

4.2.4.1. Measurement of HERV-K(HML-2) vDNA and 2-LTR-circles

Pseudotyped HML-2-based luciferase reporter viruses were produced and infected in CrFK cells. After 24h and 48h, respectively, the cellular DNA was isolated and analyzed by real-time duplex qPCR. Primers and corresponding probes were designed to specifically detect vDNA and viral 2-LTR-circles (s. figure 18A and B, respectively). Whereas pDNA served as a target for vDNA-detecting primers (targeting the U5-region), CT-signals for 2-LTR-circles should solely be attributed to newly produced cDNA.

PCR for vDNA



PCR for 2-LTR-circles

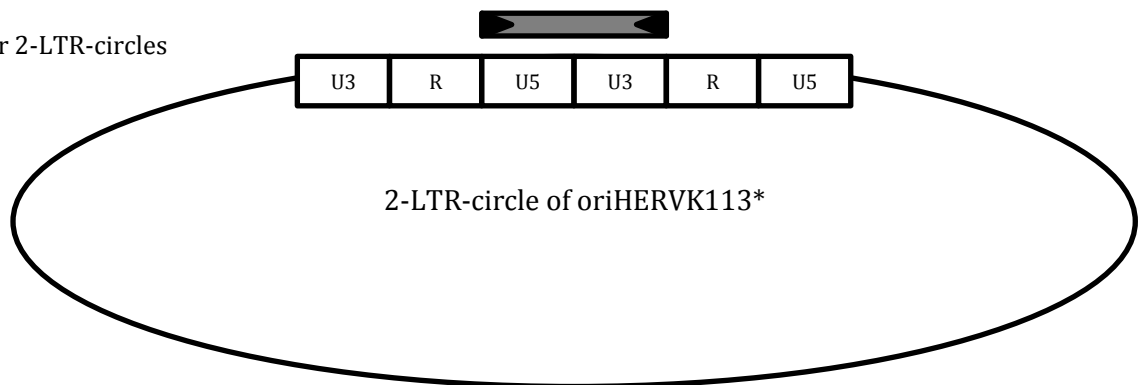


Figure 18: Amplified fragments in real-time qPCR for RT products of HML2-based luciferase reporter viruses

A) Fragments for detection of vDNA. B) Fragment for detection of 2-LTR-circles.

In this regards, it was interesting to see if the ratio of vDNA and 2-LTR-circles would allow for suggestions concerning the amount of contaminating pDNA present in the sample. In a paper published by Brady *et al.* [97] the amount of 2-LTR-circles measured represented 8% of total vDNA in the sample which confirms that HERV-K(HML-2) 2-LTR-circles are produced *in vitro*.

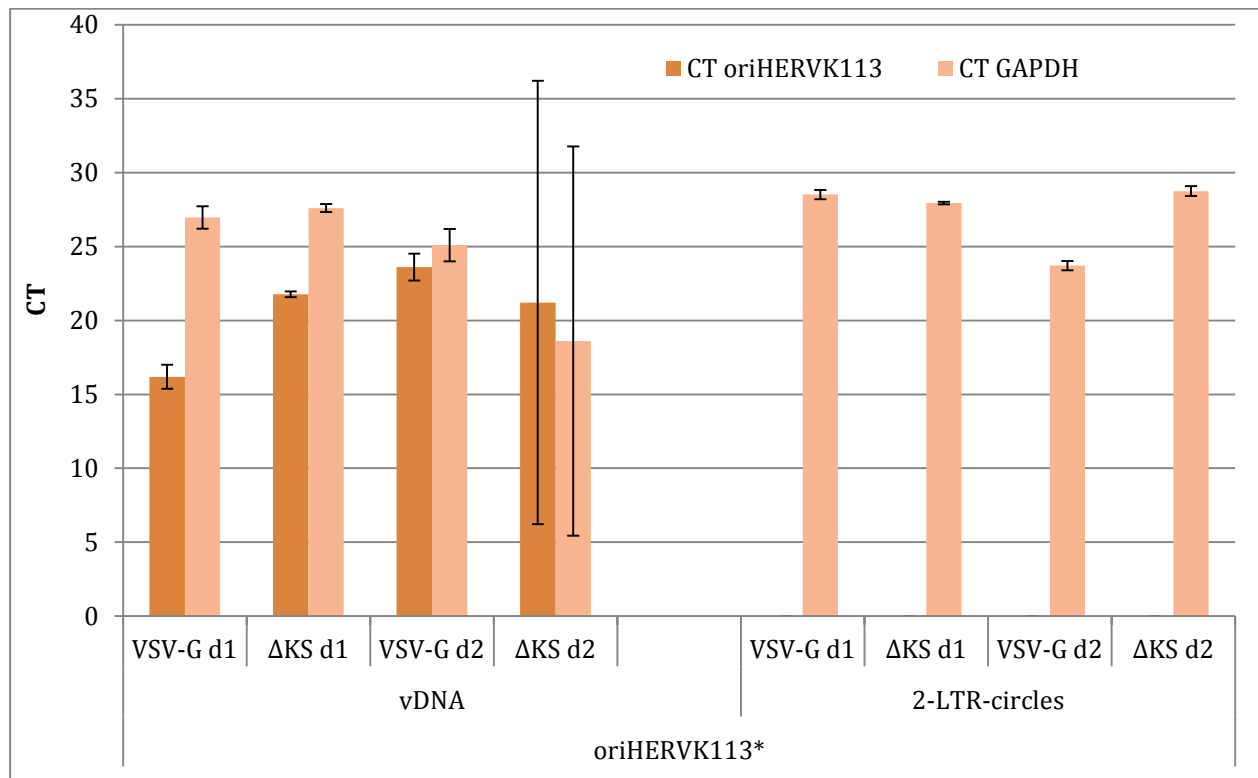


Figure 19: real-time duplex qPCR of CrFK cells infected with VSV-G or ΔKS pseudotyped HML-2-based luciferase reporter viruses for detection of HERV-K(HML-2) vDNA and 2-LTR-circles

CT values for HERV-K(HML-2) vDNA and 2-LTR-circles in CrFK cells infected with HML-2-based luciferase reporter viruses. All samples were completely negativ for 2-LTR-circles. HERV-K(HML-2) vDNA: VSV-G pseudotped viruses, cells lysed 24h post-infection=16.19, ΔKS pseudotped viruses, cells lysed 24h post-infection=21.77. VSV-G pseudotped viruses, cells lysed 48h post-infection=23.6, ΔKS pseudotped viruses, cells lysed 48h post-infection=21.21. GAPDH (CT catGAPDH) was measured as internal control for amount of genomic DNA present in the sample. Bars represent average means of three relicates. Error bars represent standard deviations of three replicates. d1=cells lysed 24h post-infection. D2=cells lysed 48h post-infection.

Parallel measurement of GAPDH served as control for the cellular DNA content of the samples. As can be seen in figure 19, CT-signals for vDNA were measured in samples from VSV-G-pseudotyped reporter viruses 24h (CT=16.19) and 48h (CT=23.6) post-infection. However, no CT-signals were measured for 2-LTR-circles in these samples, despite presence of cellular DNA (CT= 28.51 24h post-infection and CT=23.70 48h post-infection). Taken together with the fact, that the CT-value for vDNA was comparable between VSV-G- and ΔKS-pseudotpyed reporter viruses these data suggest, that pDNA might be largely responsible for the generated CT-signals.

4.2.4.2 Production of a positive template control (PTC) containing a mutation in the U3-region of the 5'LTR for use in real-time duplex qPCR

Since HML-2-based luciferase reporter viruses were produced from plasmids, there was a potential for unwanted plasmid background, when HERV-K(HML-2) DNA was measured. To circumvent this problem, a HERV-K(HML-2) reporter construct was produced which carries a discrete mutation in the U3-region of the 3'LTR. During reverse transcription, which takes place after the virus has entered the cell, the U3 region of the 3'LTR is duplicated due to two intramolecular relocations. In the cDNA, the U3 region carrying the mutation is thus present not only in the 3'LTR but also in the 5'LTR. This way, the cDNA of this reporter construct contains a DNA sequence different from that of the pDNA (s. figure 20). cDNA from reporter viruses produced with this mutated plasmid, termed CMVoriLuc_U3Tag2 should thus be distinguishable from the plasmid background which is inevitably present in the samples [94].

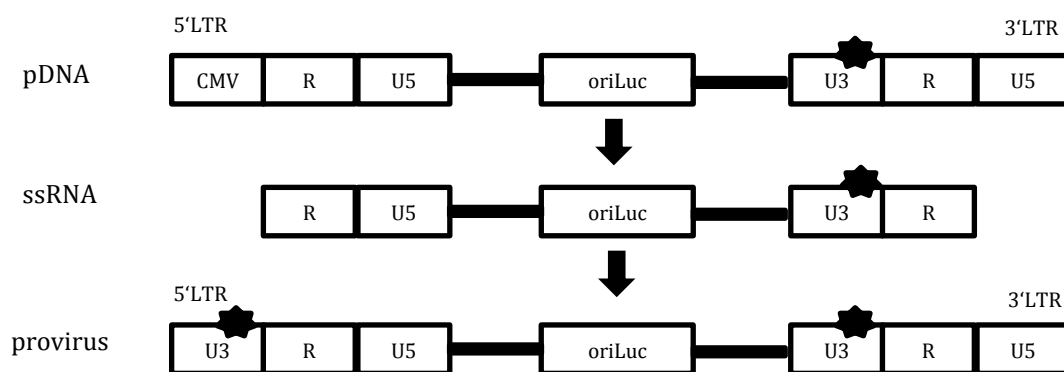


Figure 20: Scheme of the duplication and relocation of the mutation in the U3-region from pDNA CMVoriLuc_U3Tag2 to cDNA of HML-2-based luciferase reporter virus oriHERVK113*

In the plasmid, the mutation is only present in the U3-region of its 3'LTR. In the cDNA of HML-2-based luciferase reporter viruses, the mutation has duplicated and is present in the U3-region of the 3'LTR and 5'LTR. Black star=mutation

As a matter of fact, the reliability of the test results depends on a positive control (PTC) which ensures that the primers used to detect the mutation in the 5'LTR effectively work. Since there was no plasmid at stock containing this mutation in its 5'LTR, the respective region had yet to be constructed (s. figure 21). For this purpose, the mutated U3-region of CMVoriLuc_U3Tag2 was amplified and at the same time a fragment from CMVoriLuc (non-mutated) consisting of the 5'LTR and part of the *gag* gene (s. figure 22B). Those two fragments were then combined in a fusion PCR (s. figure 22A).

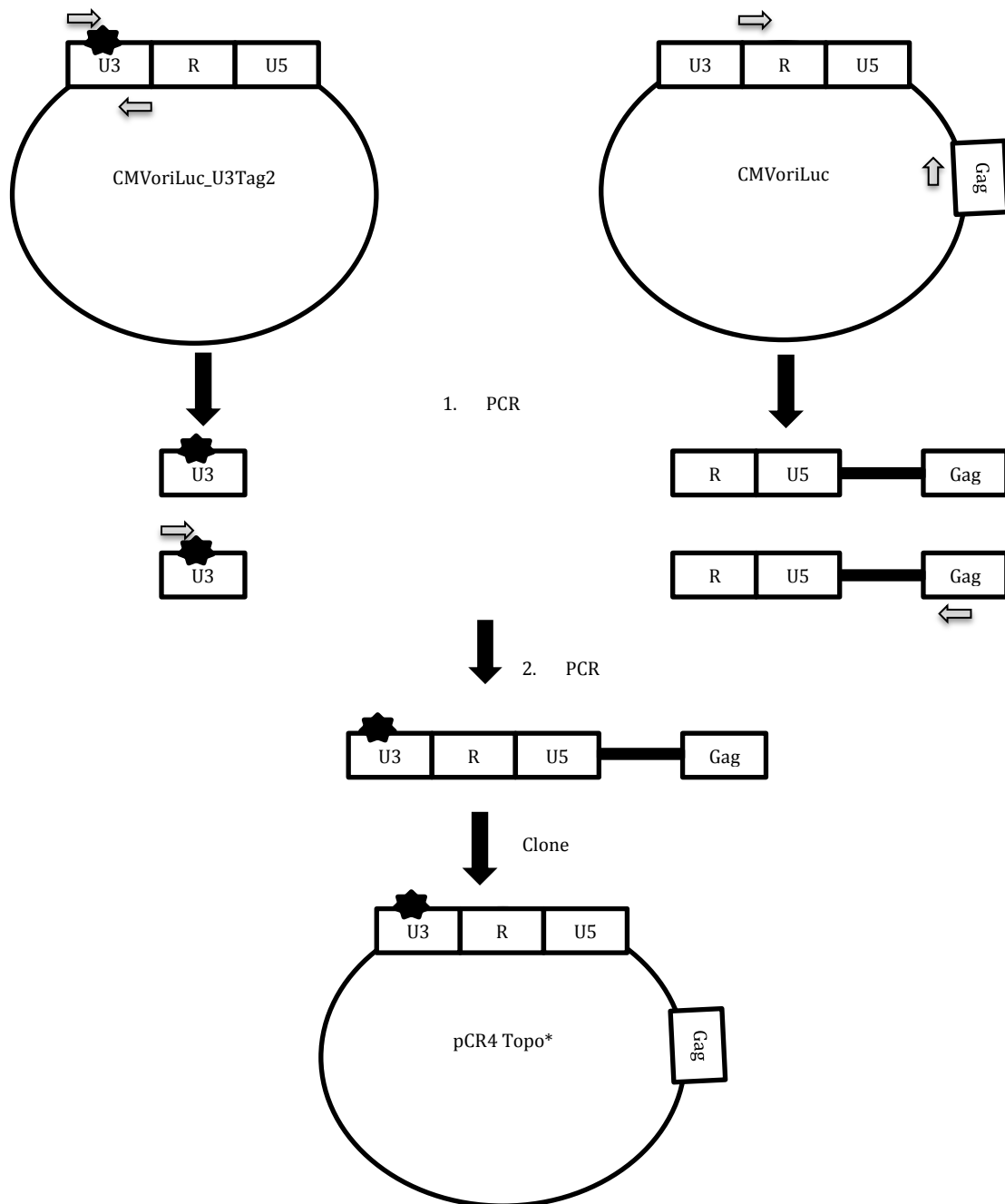


Figure 21: Scheme showing the construction of the positive template control (PTC) pCR4 Topo*

HML-2-based luciferase reporter viruses produced with plasmid CMVoriLuc_U3Tag2 should carry the relocated mutation U3Tag2 in the U3-region of the 5'LTR of their cDNA. In real-time qPCR aiming at detection of the relocated mutation, a positive template control (PTC) is needed. The PCT was constructed by ligation of the mutated U3-region from CMVoriLuc_U3Tag2 and the R-U5-*gag*-region from CMVoriLuc. The ligated fragment was then cloned into a pCR4 Topo vector. Black star=mutation

The resulting fragment consisted of the *gag* gene and the 5'LTR carrying the mutation in the U3 region. This fragment was then ligated into a pCR4 Topo vector (s. figure 22 C).

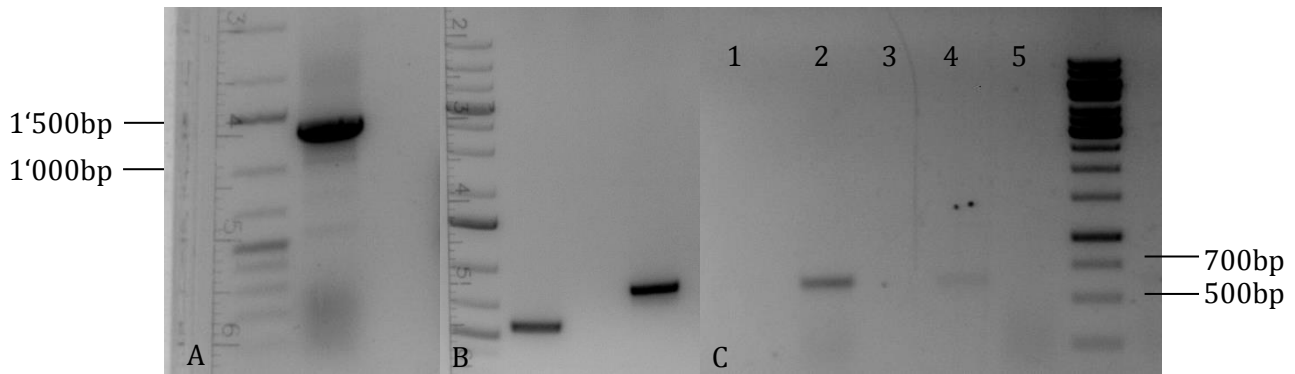


Figure 22: PCR fragments of mutated U3 region and 5'LTR-*gag* (A) as well as fused fragment (B) and colony-PCR with primers 2-For-U3-tag and VL1 Rev for pCR4 Topo* (C)

A) Lane 1=marker; Lane 2=Fused fragment U3-R-U5-*gag*. A) Lane 1=marker; Lane 2=mutated U3 region from CMVoriLuc_U3Tag2; Lane 3= NTC; Lane 4= R-U5-*gag* fragment of CMVoriLuc C) Lane 1=clone 1; Lane 2=clone 2; Lane 3=clone 3; Lane 4=clone 4; Lane 5=clone 5; Lane 6= marker. Expected fragments: mutated U3 region from CMVoriLuc_U3Tag2=560bp, R-U5-*gag* fragment of CMVoriLuc=785bp, Fused fragment U3-R-U5-*gag*=1'323bp. NTC=no template control. *Marker: GeneRuler™ 1kb Plus DNA ladder (1st) & 1kb DNA ladder (2nd and 3rd)*

The PTC sequence was approved by sequencing and verified in a *SacI*- and *XhoI*-digest (s. figure 26).

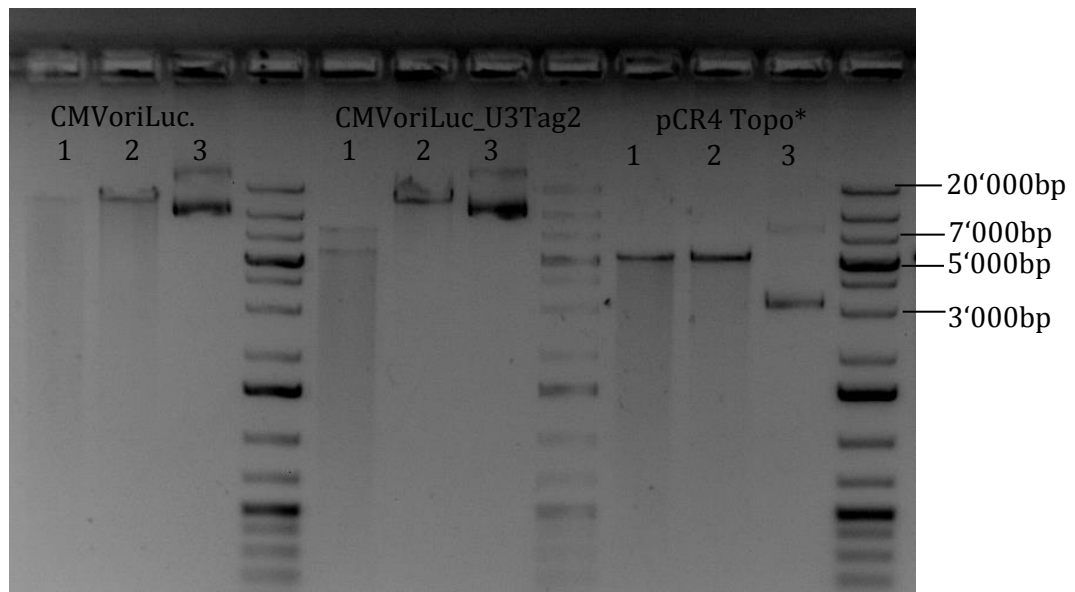


Figure 23: Restriction digests of Topo*, CMVoriLuc and CMVoriLuc_U3Tag2

1=restriction digest with *SacI*, 2=restriction digest with *XhoI*, 3=undigested plasmid

Lanes 1-3: CMVoriLuc digested with *SacI*, *XhoI* and undigested, respectively. Lanes 5-7: CMVoriLuc_U3Tag2 digested with *SacI*, *XhoI* and undigested, respectively. Lanes 9-11: The PTC pCR4 Topo* digested with *SacI*, *XhoI* and undigested, respectively. Lanes 4, 8 and 12: marker. Expected fragments for CMVoriLuc: 1: 13'653 bp (lin.) 2: 13'653 bp (lin.) 3: 13'653 bp. Expected fragments for CMVoriLuc_U3Tag2: 1: 7'933 bp, 5'720 bp 2: 13'653 bp (lin.) 3: 13'653 bp. Expected fragments for pCR4 Topo* (PTC): 1: 5'279 bp (lin.) 2: 5'279 bp (lin.) 3: 5'279 bp. *Marker: GeneRuler™ 1kb Plus DNA ladder*

4.2.4.3. Detection of relocated mutation in 5'LTR by means of real-time duplex qPCR

Measurement of the mutation in the 5'LTR of HML-2-based luciferase reporter viruses as proof of the presence of cDNA was performed by real-time qPCR and droplet digital PCR. The primers were specifically designed to bind to the mutated U3-region (forward-primer) and the *gag*-region (reverse-primer) to ensure that only the mutation within the 5'LTR –and not within the 3'LTR- is amplified (s. figure 24).

PCR for mutation in 5'LTR

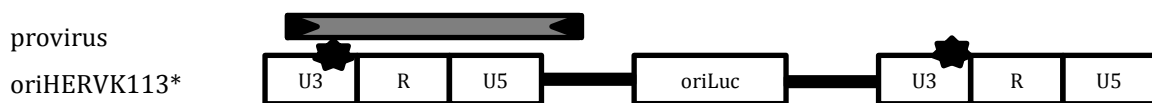


Figure 24: Amplified fragment in real-time qPCR detecting the relocated mutation in the 5'LTR of HML2-based luciferase reporter viruses

Black star=mutation

The PTC was measured in serial dilutions from 1×10^6 to 1×10^1 copies per sample to control for sensitivity level of the PCR reaction. GAPDH was measured in every sample to control for genomic DNA content. As can be seen in figure 25 for real-time duplex qPCR, no genomic DNA was measured in the PTC as expected. The titration of the PCT could nicely be measured (CT=22.2 for 1×10^6 copies, CT= 27.39 for 1×10^5 copies, CT=32.96 for 1×10^4 copies, CT=36.99 for 1×10^3 copies, CT=38.01 for 1×10^2 copies, no CT signal for 1×10^1 copies). Despite the fact, that there was a measurable amount of genomic DNA present in samples from VSV-G-pseudotyped HML-2-based luciferase reporter viruses (CT= 25.32 24h post-infection and CT=25.29 48h post-infection), a CT-signal for mutation in the 5'LTR was not measured in any of these samples. These data might suggest that although real-time qPCR generally is sensitive enough to detect small amounts of vDNA, the parameters applied might not have been optimal and therefore the few copies presumably present in the sample could not be detected by this protocol.

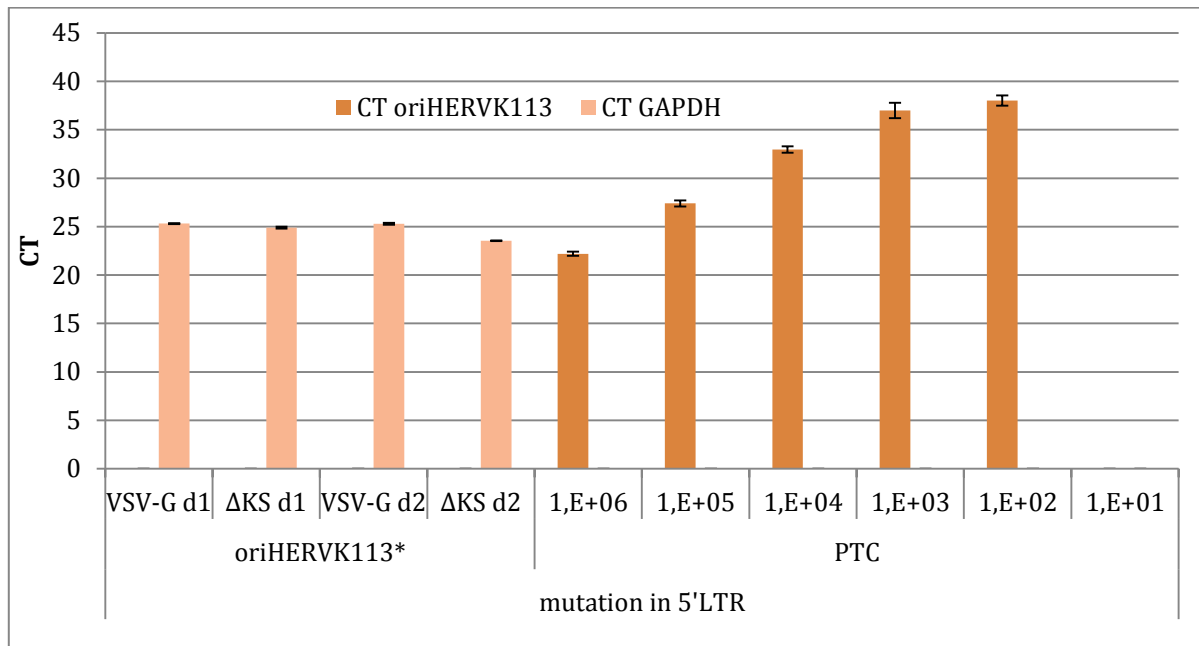


Figure 25: Real-time duplex qPCR for CrFK genomic DNA infected with HML-2-based luciferase reporter viruses for detection of the mutation in the 5'LTR of cDNA

HML-2-based luciferase reporter viruses were either pseudotyped with VSV-G or Δ KS and two different time-points were measured: 24h post-infection (d1) and 48h post-infection (d2). The PTC was measured in serial dilutions from 1×10^6 copies to 1×10^1 copies. GAPDH (CT catGAPDH) was measured to control for genomic DNA content of the sample. Presence of HERV-K(HML-2) cDNA signal (CT HERV-K) indicated presence of the relocated mutation. All oriHERK113*-samples were completely negative for viral cDNA.

4.2.4.4. Detection of relocated mutation in 5'LTR by means of droplet digital PCR

Droplet digital PCR was used to detect the few copy numbers of HERV-K(HML-2) cDNA, presumably present in the DNA-samples from HML-2-based luciferase reporter virus-infected CrFK cells. The same samples and the same primers as in the real-time duplex qPCR (s. 4.2.4.3.) were tested and the output compared. In contrast to real-time duplex qPCR, where no signals for HERV-K(HML-2) cDNA could be detected, single copy numbers could be measured with droplet digital PCR in samples from VSV-G-pseudotyped viruses 24h post-infection (s. figure 26 & table 24). In contrast, almost no copies could be detected in comparable samples from Δ KS-pseudotyped viruses. The PTC was measured in parallel in serial dilutions from 1×10^3 to 1×10^1 copies. As can be nicely seen in table 24, the 10-fold change in copy number between two serial dilutions could be monitored in the experiment albeit the measured copy number differs from the copy number estimated by Nanodrop Spectrophotometer (which was the basis for the preparation of the serial dilution). These clear findings differ from the ones obtained by real-time duplex qPCR, where all samples (except the PTC) were completely negative. In conclusion,

droplet digital PCR is more sensitive compared to real-time qPCR and thus a valuable method to detect even lowest copy numbers of DNA.

Table 24: Copy numbers of HERV-K DNA in sample as measured in ddPCR

Sample	Total cells/sample	Copies HERV-K DNA/sample
HERV-K/VSV-G	6'503	97
HERV-K/HIV-1 Δ KS	6'570	18
PTC, estimated 1×10^1 copies	0	25
PTC, estimated 1×10^2 copies	0	243
NTC	0	0

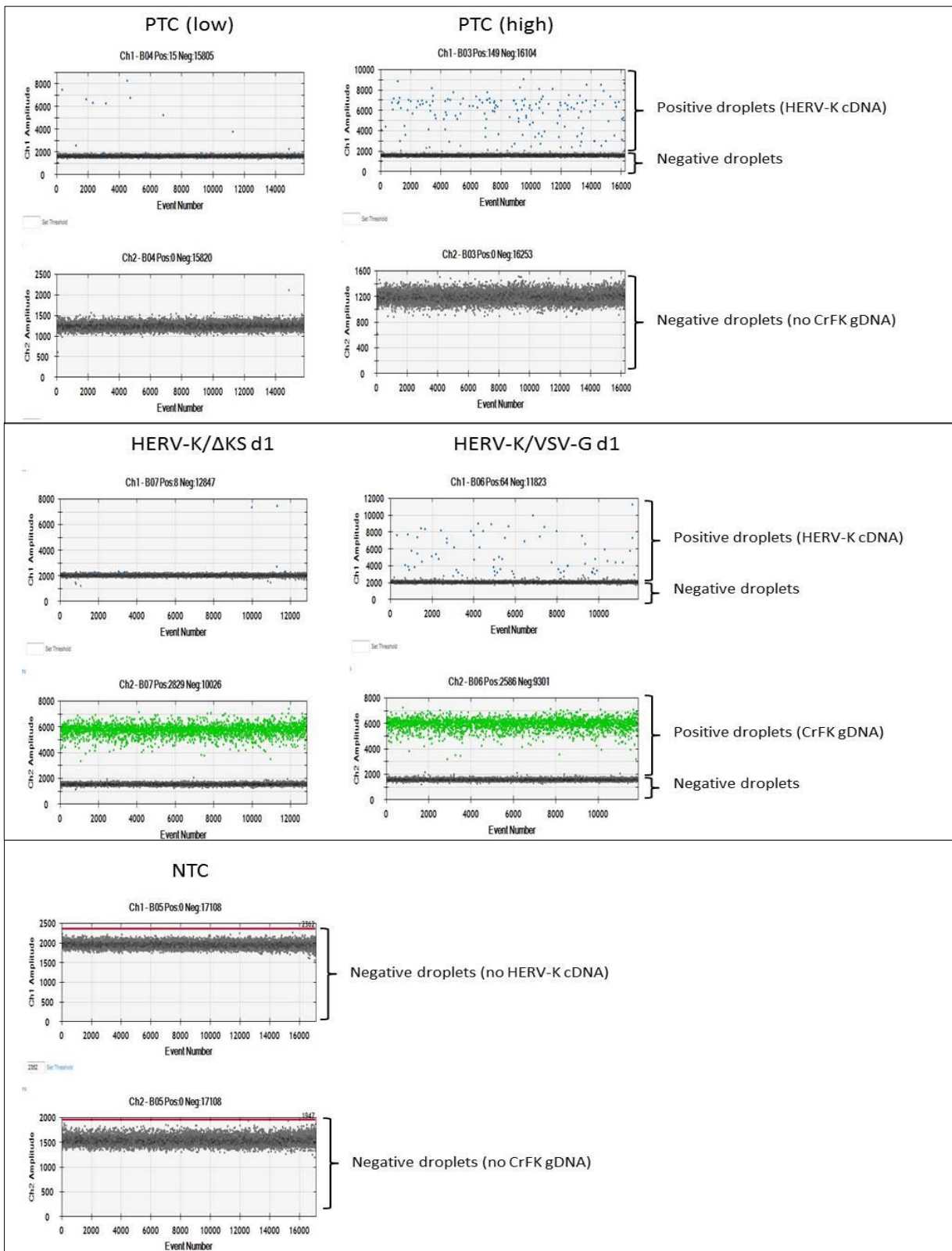


Figure 26: Fluorescence intensity vs. droplet number for ddPCR from CrFK genomic DNA after infection with pseudotyped HERV-K reporter viruses

D-plots showing single positive and negative droplets after ddPCR for Env VSV-G and HIV-1 Δ KS pseudotyped reporter viruses, high and low copy numbers of the positive template control (PTC) and the no template control (NTC). FAM=HERV-K DNA. HEX=CrFK genomic DNA

5. Discussion

5.1. Production and infectivity of plasmid-based HERV-K reporter viruses

While no naturally occurring infectious HERV-proviruses have been detected so far, engineered recombinant HERV-K(HML-2) proviruses have been shown to be infectious in various cell lines including human cells [95] [96]. In this work, HML-2-based luciferase reporter viruses which were mutated in the U3-region of their 3'LTR were used for infection of CrFK cells and isolated DNA screened for different RT products by real-time qPCR and ddPCR. Two subsequent infections showed that infection rate for mutated VSV-G-pseudotyped HML-2-based luciferase reporter viruses was comparable to non-mutated counterparts (s. figure 12), with however a decrease in infectivity in the second infection (not shown). Yet, infection rate for pseudotyped HIV-1 reporter viruses was 2-4 \log_{10} stages higher (s. figure 11). This could be due to the post-entry, pre-integration block which has been suggested for HERV-K(HML-2) and is absent from HIV-1 [64]. There is yet another explanation: the ELISA which has been performed prior to infection for normalization only measures the amount of viral capsid protein present in the sample, without distinction between capsid protein on infectious and non-infectious virus particles. It is thus not guaranteed that equal amounts of infectious virus particles were present in HIV-1 and HML-2-based luciferase reporter viruses. In order to ensure equal amounts of infectious virus particles, a Cavid assay could in future be performed instead of ELISA, since Cavid assays measure the RT activity present in a sample. A difference in infectivity could be observed between HIV-1 and HML-2-based luciferase reporter viruses with HERV-K(HML-2) showing a peak 24h post-infection and HIV-1 showing a peak 48h post-infection. This does not lie in line with what has been reported for HIV-1 by others, namely HIV-1 showing a peak in RT-activity 24h post-infection compared to HIV-2 showing a peak 48h post-infection) [101]. However, whereas monocyte-derived macrophages (MDMs) had been used as set-up in this paper, CrFK cells have been used in this work, which could account for the observed difference. In conclusion, it could be shown in this work, that a post-entry, pre-integration block impairs infectivity of HERV-K(HML-2) and that infection rate for HIV-1 is thus much higher. In order to validate this finding, infections should be repeated with prior normalization of infectious virus particles by means of a Cavid assay.

5.2. ACH-2 cells as valid models for measurement of HIV-1 viral DNA?

In a paper published by Mbisa *et al.* [63] different primer pairs were used in a real-time TaqMan qPCR assay to specifically detect RT-products of HIV-1 reporter viruses. An alternative method was tested in this work, replacing TaqMan probes with universally applicable SYBR Green dye I. As first set-up, HIV-1 latent ACH-2 cells containing one proviral copy of HIV-1, were compared to HIV-1-deficient C8166 cells. Real-time qPCR results showed that this set-up is suitable to detect differences in total amount of HIV-1 vDNA between the different cell lines. It is not known, if HIV-1 replication takes place in latent ACH-2 cells and therefore no predictions could be made concerning the presence of early and late RT products. However, 1- and 2-LTR-circles have been reported to be present in these cells [95] [96]. In this experiment, no or only slight differences could be seen between ACH-2 and C8166 cells regarding the amount of integrated provirus, 1- and 2-LTR-circles and positive CT-values were measured for all C8166-samples as well as the NTC. This emphasizes the need of specific probes to avoid redundant signals generated by primer-dimerization and unspecific binding.

5.3. Plasmid background prevents analysis of cDNA from pseudotyped HIV-1 reporter viruses in real-time SYBR Green duplex qPCR

In another real-time SYBR Green duplex qPCR assay, cellular DNA from CrFK cells infected with plasmid-based HIV-1 reporter viruses was analyzed using the same primer pairs as for the ACHS-2-assay. In contrast to HIV-1 latent ACH-2 cells, replication was clearly expected to occur within these cells upon infection. The drawback of this assay was the inevitable presence of pDNA contamination which provides a template for certain primer pairs. As could be seen for ACH-2 cells, redundant signals impaired evaluation of the experiment. This effect could be partly responsible for the effects observed with plasmid-based HIV-1 reporter viruses where no obvious differences in CT-values between samples from infectious (VSV-G-pseudotyped) and non-infectious (Δ KS-pseudotyped) viruses could be observed (s. figure 16). Correction for gDNA content showed negligible differences in vDNA-content between the samples (s. figure 17). Yet, the presence of pDNA in both samples from infectious and non-infectious samples clearly accounts for part of the signal, at least for early and late RT products and overall vDNA. As has been reported, total HIV vDNA in a cell consists largely of non-integrated linear DNA, followed by integrated provirus, 1-LTR-circles and at last 2-LTR [102] [103]. Full-length HIV vDNA is detectable already three to four hours after infection, one hour later integrated DNA starts to

form and eight to 12 hours post-infection circular HIV DNA starts to form [102]. It would have been interesting to compare these reported findings (which obviously depend on the several factors such as target cells) with own data for example with DNA isolated at various time-points after infection or from different target cells. However, specific probes would have been necessary for further studies. In conclusion, both real-time SYBR Green qPCRs have approved that SYBR Green dye I binds unspecific to all double-stranded DNA and promotes primer-dimerization which in turn leads to redundancy in signal. Especially when analyzing small amounts of DNA copies, this background impedes evaluation of the results.

5.4. Real-time duplex qPCR using TaqMan probes for detection of HERV-K(HML-2) cDNA

Although HML-2-based luciferase reporter viruses are known to be able to infect certain cell lines, there is no evidence of integration so far, implying a certain post-entry, pre-integration stop. It is, however, not known at which stage after cell entry this stop takes place. In contrast, other reconstituted HERV-K(HML-2) reporter constructs have been shown to integrate upon infection [97]. The aim of this work was to determine if reverse transcription takes place in HML-2-based luciferase reporter viruses upon cell-entry by measuring the newly produced cDNA content in infected cells. Real-time duplex qPCR was applied as this method has been shown in the past to successfully detect viral cDNA [97] [102]. The primer pairs used were designed to detect HERV-K(HML-2) total vDNA, 2-LTR-circles and the relocated mutation in the 5'LTR. There was the drawback of pDNA providing a template for primers detecting vDNA. In contrast to previous assays, TaqMan probes were used here to amplify only specific signals. While general vDNA could be measured in samples from infectious (VSV-G-pseudotyped) viruses 24h and 48h post-infection, the CT-values for 2-LTR-samples were completely negative (s. figure 19). The amount of HERV-K(HML-2) 2-LTR-circles has been reported to be around 8% of total vDNA-content of a cell [97] so at least some signal for 2-LTR-circles should have been detected (provided that indeed cDNA is responsible for the strong vDNA-signal). However, the most likely explanation is that the positive CT-values for vDNA largely result from pDNA and not cDNA.

In order to get rid of unwanted signal from p DNA and specifically detect newly produced viral cDNA, a mutation has been inserted in the U3-region of the 3'LTR of the CMVoriLuc-plasmid (termed CMVoriLuc_U3Tag2) used for production of HML-2-based luciferase reporter viruses. Due to intramolecular relocations during RT, this mutation duplicates and is present twice (in

each U3-region of both LTRs) in the cDNA. The reverse primer used for detection of this relocated mutation in the 5'LTR of the cDNA binds in the *gag* gene which lies just downstream of the 5'LTR. The forward primer binds in both mutated U3-regions. The combination of these two primers ensures that only the mutated 5'LTR and thus specifically cDNA is amplified. A PTC was used in real-time duplex qPCR in a serial dilution to evaluate the detection limit of this method. In parallel, isolated DNA from HERV-K(HML-2)-infected cells was analyzed. It could be shown, that detection limit of classic real-time qPCR is 1×10^2 plasmid copies in water (s. figure 25). CT-values for HERV-K(HML-2)-samples were completely negative. In connection with the previous results for 2-LTR-circles, these findings suggest that either no HERV-K(HML-2)-cDNA is formed or only very few copies of cDNA are formed and classic real-time qPCR applied is not sensitive enough for their detection.

5.5. Droplet digital PCR for detection of single HERV-K(HML-2) cDNA copy numbers

Droplet digital PCR fractionates a sample in 20'000 of water-oil droplets/20 μ l PCR mix, each containing one DNA copy. It has been shown to allow for measurement of HIV-1 DNA with a significantly increased precision and a lower detection limit compared to previous methods [106]. After classic PCR, each droplet is analyzed for positive signal which implies an amplification event. Since classic real-time qPCR did not provide evidence that cDNA is formed after HERV-K(HML-2) cell entry, ddPCR was used as an alternative method to measure cDNA content of the same samples. Again, the primer pair detecting the relocated mutation in the 5'LTR was used. 97 cDNA copies could be measured in infectious (VSV-G-pseudotyped) viruses. In contrast, only 18 cDNA copies could be measured in non-infectious (Δ KS-pseudotyped) viruses (s. table 24). In theory, no copies should have been detected in these samples and it is uncertain whether mere background signals account for this finding or whether there is yet another explanation. Nevertheless, the experiment overall showed, that reverse transcription is taking place after HERV-K(HML-2) cell entry. Interestingly, the results for the PTC show that the calculated copy numbers in the serial dilutions in fact deviate from the actual copy numbers present (s. table 24). This has implications for the newly calculated detection limit of classic real-time PCR, being now corrected to 243 copies. Considering that only 97 cDNA copies were present in samples from infectious HERV-K(HML-2), this explains why no cDNA was detected in these samples in classic real-time PCR. 97 copies of HERV-K(HML-2) cDNA are rather few when considering a total cell number of 6'503 present in the sample. It is not clear, whether this finding implies a generally low infection rate of HERV-K(HML-2) (which would question the

results from the luciferase assay) or whether optimized parameters for ddPCR would allow for more exact results. Either way, experiments have to be repeated and various parameters varied in order to find the best PCR protocol for ddPCR of HERV-K(HML-2) DNA.

5.6. Infection studies of HERV-K(HML-2) reporter viruses

This work has shown the necessity of good infections in order to obtain enough cells where reverse transcription takes place. No cDNA could be measured with classic real-time qPCR in this work; however, a paper published by Y. N. Lee *et al.* [96] clearly showed detection of HERV-K(HML-2) cDNA by classic PCR. In this paper, integration of certain viral genes into the host genome could be detected. These findings could not be reproduced in this work.

5.7. Outlook

Droplet digital PCR has shown that detection of HERV-K cDNA is possible. A further step would be the measurement of other RT products such as early and late RT products, 1- & 2-LTR-circles and integrated provirus.

Infection parameters should be optimized in order to obtain more cells where reverse transcription takes place. As could be shown by P. Kramer *et al.* [84], competition of HML-2-based luciferase reporter viruses with other reporter viruses considerably increases infection rate and could be applied in the future to obtain more infected cells. If higher copy numbers of cDNA are obtained, classic real-time qPCR could be reused to analyze DNA-samples. Overall, the experiments need to be repeated in order to draw final conclusions.

6. Supplement

Mutation in the U3-region of the 5'LTR with inserted *SacI*-restriction site

5'...TGTGGGGAAAAGCAAGAGAGATCAGATTGTTACTGTGTCTGTGTAGAAAGAAGTAGACATAGGAG
 ACTCCATTTTGTATGTACTAAGAAAAATTCTTCTGCCTTGAGATTCTGTTAATCTATGACCTTACCCC
 CAACCCCGTGCTCTCTGAAACATGTGCTGTGTCAACTCAGAGTTGAATGGATTAAGGGCGGTGCAGGA
 TGTGCTTTGTTAAACAGATGCTTGAAGGCAGCATGCTCCTTAAGAGTCATCACCCTCCCTAATCTCAA
 GTACCCAGGGACACAAAAACTGCGGAAGGCCGCAGGGACCTCTGCCTAGGAAAGCCAGGTATTGTCCA
 AGGTTTCTCCCATGTGATAGTCTGAAATATGGCCTCGTGGGAAGGGAAAGACCTGACCGTCCCCAGC
 CCGACACCCGTAAAGGGTCTGTGCTGAGGAGGATTAGTATAAGAGGAAGGAATGCCTCTTGCAGTTGA
 GACA**GAGCTC**AGGCATCTGTCTCCTCCCTGTCCCTGGGCAATGGAATGTCTCGGTATAAAACCCGATTG
 TATGCTCCATCTACT...3'

SacI-restriction site:

5'...GAGCTC...3'
 3'...CTCGAG...5'

Table 25: Primers and probes for HERV-K and HIV quantitative PCR

Type	Stage of reverse transcription	Name of oligonucleotide	Sequence
HERV-K	Control for HERV-K cDNA	HERV_U5-F	5'-TCCATATGCTGAACGCTGGT-3'
		HERV_U5_1777-R	5'-CACCTGTGGGTGTTTCTCG-3'
		HERV_U5-Probe	5'-F-TCCAAATCTCTCGTCCCACCTTACG-Q-3'
HERV-K	Control for DNA quantity	catGAPDH_44F	5'-GGTGATGCTGGTGCTGAGTAT-3'
		catGAPDH_45R	5'-TGGTTCACGCCCATCACAA-3'
		catGAPDH_Probe	
HERV-K	2-LTR-circles (with HERV_U5-Probe)	HERVU5_1649-1688_For	5'-TACTAAGGGAACCTCAGAGGC-3'
		HERVU3_9360-9383_Rev	5'-ATCTGATCTCTCTTGCTTTTCC-3'
HERV-K	Mutation in 5'LTR	U3tag2_F2	5'-CTTGCAGTTGAGACAGAGCT-3'
		U3tag2_R2	5'-CTAGAGAAAAGCCTCCACGTTGG-3'
		U3tag2-Probe	5'-FAM-CTCCTCCCTGTCCCTGGGCA-BHQ1-3'
HIV	Control for HIV cDNA [98]	MM_HIV1-For	5'-TACTGACGCTCTCGCACC-3'
		MM_HIV1-Rev	5'-TCTCGACGCAGGACTCG-3'
HIV	Integrated provirus	MH535	5'-AACTAGGGAACCCACTGCTTAAG-3'
		SB704	5'-TGCTGGGATTACAGGCGTGAG-3'
HIV	2-LTR-circles	SS-F4	5'-TGGTTAGACCAGATCTGAGCCT-3'
		LTR-R5	5'-GTGAATTAGCCCTTCCAGTACTGC-3'
HIV	Control for DNA quantity	catAlb_For	5'-GATGGCTGATTGCTGTGAGA-3'
		catAlb_Rev	5'-CCCAGGAACCTCTGTTTATT-3'
HIV	Early products	hRU5-F2	5'-GCCTCAATAAAGCTTGCCTTGA-3'
		hRU5-R	5'-TGACTAAAAGGGTCTGAGGGATCT-3'
HIV	Late products	MH531	5'-TGTGTGCCCGTCTGTTGTGT-3'
		MH532	5'-GAGTCCTGCGTCGAGAGATC-3'
HIV	1-LTR-circles	LA 1	5'-GCGCTTCAGCAAGCCGAGTCCT-3'
		LA 15	5'-CACACCTCAGGTACCTTTAAGA-3'
HIV	Control for cellular DNA [98]	CCR5-For	5'-CCAGAAGAGCTGAGACATCCG-3'
		CCR5-Rev	5'-GCCAAGCAGCTGAGAGGTTACT-3'

7. References

- [1] V. Ellerman und O. Bang, „Experimentelle Leukämie bei Hühnern,“ *Zentralbl. Bakteriol. Parasitenkd. Infektionskr. Hyg. Abt. I*, Nr. 46, pp. 595-609, 1908.
- [2] P. Rous, „A Sarcoma of the Fowl Transmissible by an Agent Separable from the Tumor Cell,“ *Journal of Experimental Medicine*, Bd. 4, Nr. 13, pp. 397-411, 1911.
- [3] J. J. Bittner, „Some Possible Effects of Nursing on the Mammary Gland Tumor Incidence in Mice,“ *Science*, Bd. 2172, Nr. 84, p. 162, 1936.
- [4] B. J. Poiesz und et al., „Detection and isolation of type C retrovirus particles from fresh and cultured lymphocytes of a patient with cutaneous T-Cell lymphoma,“ *PNAS*, Bd. 12, Nr. 77, pp. 7415-7419, 1980.
- [5] R. Gallo und et al., „Frequent detection and isolation of cytopathic retroviruses (HTLV-III) from patients with AIDS and at risk for AIDS,“ *Science*, Bd. 4648, Nr. 224, pp. 500-503, 1984.
- [6] H. M. Temin und S. Mizutani, „RNA-dependent DNA polymerase in virions of Rous sarcoma virus,“ *Nature*, Bd. 5252, Nr. 226, pp. 1211-1213, 1970.
- [7] M. Lu, S. C. Blacklow und P. S. Kim, „A trimeric structural domain of the HIV-1 transmembrane glycoprotein,“ *Nature Structural Biology*, Bd. 2, Nr. 12, pp. 1075-1082, 1995.
- [8] H. R. Gelderblom, „Fine structure of human immunodeficiency virus (HIV) and immunolocalization of structural proteins,“ *Virology*, Bd. 1, Nr. 156, pp. 171-176, 1987.
- [9] T. Gramberg, N. Sunseri und N. R. Landau, „Accessories to the crime recent advances in HIV accessory protein biology,“ *Current HIV/AIDS report*, Bd. 6, Nr. 1, pp. 6-42, 2009.
- [10] W. C. Greene, „The molecular biology of human immunodeficiency virus type 1 infection,“ *New England Journal of Medicine*, Bd. 324, Nr. 5, pp. 308-317, 1991.
- [11] A. J. Cann und J. Karn, „Molecular biology of HIV: new insights into the virus life cycle,“

- AIDS*, Bd. 3, pp. S19-34, 1989.
- [12] M. S. Gottlieb, „Pneumocystis pneumonia-Los Angeles. 1981,“ *American Journal of Public Health*, Bd. 6, Nr. 96, pp. 980-981, 2006.
- [13] A. Basavapathruni und K. S. Anderson, „Reverse transcription of the HIV-1 pandemic,“ *The FASEB Journal*, Bd. 14, Nr. 21, pp. 3795-3808, 2007.
- [14] S. L. Gilman, „AIDS and Syphilis: The Iconography of Disease,“ *The MIT Press*, Bd. 43, pp. 87-107, 1987.
- [15] J. Cohen, „Making Headway Under Hellacious Circumstances,“ *Science*, Bd. 313, Nr. 5786, pp. 470-473, 2006.
- [16] C. f. D. Control, „Update on aquired immune deficiency syndrome (AIDS) - United States,“ *MMWR Morb Mortal Wkly Rep.*, Bd. 31, Nr. 37, pp. 507-508, 513-514, 1982.
- [17] UNAIDS, *AIDS by the numbers 2015*, 2016.
- [18] F. Barre-Sinoussi und J. C. Chermann, „Isolation of a T-lymphotropic retrovirus from a patient at risk of acquired immune deficiency syndrome (AIDS),“ *Science*, Bd. 220, Nr. 4599, pp. 865-867, 1983.
- [19] F. Barre-Sinoussi, J. C. Chermann, F. Rey, M. T. Nugeyre, S. Chamaret, J. Gruest, C. Dauguet, C. Axler-Blin, F. Vezinet-Brun, C. Rouzioux, W. Rozenbaum und L. Montagnier, „Isolation of a T-lymphotropic retrovirus from a patient at risk for aquired immune deficiency syndrome (AIDS),“ *Science*, Bd. 220, Nr. 4599, pp. 868-871, 1983.
- [20] R. C. Gallo und P. S. Sarin, „Isolation of human T-cell leukemia virus in acquired immune deficiency syndrome (AIDS),“ *Science*, Bd. 220, Nr. 4599, pp. 865-867, 1983.
- [21] P. Hiltz, „U.S. Drops Misconduct Case Against an AIDS Researcher,“ *New York Times*, 1993.
- [22] R. Aldrich und G. Wotherspoon, *Who's who in contemporary Gay and Lesbian History: From World War II to the Present Day*, Bd. 2, Routledge, 2011.
- [23] T. N. P. i. P. o. M. 2008, „www.nobelprize.org,“ 18 December 2008. [Online].
- [24] a. staff, „A Timeline of AIDS,“ *aids.gov. U.S. Department of Health & Human Services*, 2014.

- [25] J. Pickrell, „Timeline: HIV & AIDS,“ *New Scientist*, 2006.
- [26] K. Wright, „AIDS therapy: First tentative signs of therapeutic promise,“ *Nature*, Bd. 283, Nr. 6086, 1986.
- [27] M. H. Katz und J. L. Gerberding, „Postexposure Treatment of People Exposed to the Human Immunodeficiency Virus through Sexual Contact or Injection-Drug Use,“ *New England Journal of Medicine*, Bd. 15, Nr. 336, pp. 1097-1100, 1997.
- [28] M. Worobey und P. A. Marx, „Island Biogeography Reveals the Deep History of SIV,“ *Science*, Bd. 329, Nr. 5998, p. 1487, 2010.
- [29] D. G. McNeil Jr., „Researchers Have New Theory on Origin of AIDS Virus,“ *The New York Times*, 13. June 2003.
- [30] M. L. Kalish, N. D. Wolfe, C. B. Ndongmo, J. McNicholl, K. E. Robbins, M. Aidoo, P. N. Fonjungo, G. Alemnji, C. Zeh, C. F. Djoko, E. Mpoudi-Ngole, D. S. Burke und T. M. Folks, „Central African hunters exposed to simian immunodeficiency virus,“ *Emerging Infectious Diseases Journal*, Bd. 11, Nr. 12, pp. 1928-1930, 2005.
- [31] P. A. Marx, P. G. Alcabes und E. Drucker , „Serial human passage of simian immunodeficiency virus by unsterile injections and the emergence of epidemic human immunodeficiency virus in Africa,“ *Philosophical Transactions of the Royal Society*, Bd. 356, Nr. 1410, pp. 911-920, 2001.
- [32] M. Worobey, M. Gemmel, D. E. Teuwen, T. Haselkorn, K. Kunstman, M. Bunce, J.-J. Muyembe, J.-M. M. Kabongo, R. M. Kalengayi, E. Van Marck, M. T. P. Gilbert und S. M. Wolinsky, „Direct evidence of extensive diversity of HIV-1 in Kinshasa by 1960,“ *Nature*, Bd. 455, pp. 661-664, 2008.
- [33] J. D. de Sousa, V. Müller, P. Lemey, A. M. Vandamme und D. P. Martin, „High GUD incidence in the early 20th century created a particularly permissive time window for the origin and initial spread of epidemic HIV strains,“ *PLOS ONE*, Bd. 4, Nr. 5, p. e9936, 2010.
- [34] P. J. Klasse, R. Bron und M. Marsh, „Mechanisms of enveloped virus entry into animal cells,“ *Advanced drug delivery reviews*, Bd. 1, Nr. 34, pp. 65-91, 1998.
- [35] K. J. Williams und L. A. Loeb, „Retroviral reverse transcriptases: error frequencies and mutagenesis,“ *Current topics in Microbiology and Immunology*, Nr. 172, pp. 165-180, 1992.

-
- [36] D. Derse, „Human T-cell leukemia virus type 1 integration target sites in human genome: comparison with those of other retroviruses,“ *Journal of Virology*, Bd. 81, Nr. 12, pp. 6731-6741, 2007.
- [37] M. Stevenson, „Integration is not necessary for expression of human immunodeficiency virus type 1 protein products,“ *Journal of Virology*, Bd. 5, Nr. 64, pp. 2421-2425, 1990.
- [38] O. Sued, M. I. Figueroa und P. Cahn, „Clinical challenges in HIV/AIDS: Hints for advancing prevention and patient management strategies,“ *Advanced Drug Delivery Reviews*, 2016.
- [39] F. M. Hecht, „Use of laboratory tests and clinical symptoms for identification of primary HIV infection,“ *AIDS*, Bd. 8, Nr. 16, pp. 1119-1129, 2002.
- [40] T. Elliott, A. Casey, P. A. Lambert und J. Sandoe, *Lecture Notes: Medical Microbiology and Infection*, Wiley, 2012.
- [41] J. Bennett, R. Dolin und M. Mandell, *Mandell, Douglas, and Bennett's Principles and Practice of Infectious Diseases 8th Edition*, Saunders, 2015.
- [42] A. Roulston, R. C. Marcellus und P. E. Branton, „Viruses and Apoptosis,“ *Annual Review of Microbiology*, Bd. 53, pp. 577-628, 1999.
- [43] N. Yan und Z. J. Chen, „Intrinsic Antiviral Immunity,“ *Nature Immunology*, Bd. 13, Nr. 3, pp. 214-222, 2012.
- [44] P. D. Zamore, T. Tuschl, P. A. Sharp und D. P. Bartel, „RNAi: double-stranded RNA directs the ATP-dependent cleavage of mRNA at 21 to 23 nucleotide intervalls,“ *Cell*, Bd. 101, pp. 25-33, 2000.
- [45] L. A. Marraffini und E. J. Sontheimer , „CRISPR interference: RNA-directed adaptive immunity in bacteria and archaea,“ *Nature Reviews Genetics*, Bd. 11, pp. 181-190, 2010.
- [46] C. A. Jenaway, P. Travers und M. Walport, *Immunobiology 6th edition*, B&T, 2005.
- [47] K. Ozato, D.-M. Shin, T.-H. Chang und H. C. Morse, „TRIM family proteins and their emerging roles in innate immunity,“ *Nature Reviews Immunology*, Bd. 8, pp. 849-860, 2008.
- [48] M. W. Yap, S. Nisole und J. P. Stoye, „A single amino acid change in the SPRY domain of human Trim5alpha leads to HIV-1 restriction,“ *Current Biology*, Bd. 15, Nr. 1, pp. 73-78,
-

- 2005.
- [49] S. Ohkura, M. W. Yap, T. Sheldon und J. P. Stoye, „All Three Variable Regions of the TRIM5alpha B30.2 Domain Can Contribute to the Specificity of Retrovirus Restriction,“ *Journal of Virology*, Bd. 80, Nr. 17, pp. 8554-8565, 2006.
- [50] D. L. Mallery, W. A. McEwan, S. R. Bidgood, G. J. Towers, C. M. Johnson und L. James, „Antibodies mediate intracellular immunity through tripartite motif-containing 21 (TRIM21),“ *PNAS*, Bd. 107, Nr. 46, pp. 19985-19990, 2010.
- [51] A. M. Sheehy, N. C. Gaddis, J. D. Choi und M. H. Malim, „Isolation of a human gene that inhibits HIV-1 infection and is suppressed by the viral Vif protein,“ *Nature*, Bd. 418, Nr. 6898, pp. 646-650, 2002.
- [52] A. M. Sheehy, N. C. Gaddis, J. D. Choi und M. H. Malim, „The antiretroviral enzyme APOBEC3G is degraded by the proteasome in response to HIV-1 Vif,“ *Nature Medicine*, Bd. 9, Nr. 11, pp. 1404-1407, 2003.
- [53] L. G. Holden, C. Prochnow, Y. P. Chang, R. Bransteitter, L. Chelico, U. Sen, R. C. Stevens, M. F. Goodman und X. S. Chen, „Crystal structure of the anti-viral APOBEC3G catalytic domain and functional implications,“ *Nature*, Bd. 456, Nr. 7218, pp. 121-124, 2008.
- [54] H. Lahouassa und et al., „SAMHD1 restricts the replication of human immunodeficiency virus type 1 by depleting the intracellular pool of deoxyxynucleoside triphosphates,“ *Nature Immunology*, Bd. 13, Nr. 3, pp. 223-228, 2012.
- [55] P. Stumptner-Cuvelette, S. Morchoisne, M. Dugast, S. Le Gall, G. Raposo, O. Schwartz und P. Benaroch, „HIV-1 Nef impairs MHC class II antigen presentation and surface expression,“ *PNAS*, Bd. 98, Nr. 21, pp. 12144-12149, 2001.
- [56] Z. Klase, F. Kashanchi und et al., „HIV-1 TAR miRNA protects against apoptosis by altering cellular gene expression,“ *Retrovirology*, Bd. 6, Nr. 18, p. 18, 2009.
- [57] k. Stopak und et al., „HIV-1 Vif blocks the antiviral activity of APOBEC3G by impairing both its translation and intracellular stability,“ *Molecular Cell*, Bd. 12, Nr. 3, pp. 591-601, 2003.
- [58] K. Muthumani und et al., „The HIV-1 Vpr and glucocorticoid receptor complex is a gain-of-function interaction that prevents the nuclear localization of PARP-1,“ *Nature Cell Biology*,

- Bd. 8, Nr. 2, pp. 170-179, 2011.
- [59] N. Laguette und et al., „Evolutionary and functional analyses of the interaction between the myeloid restriction factor SAMHD1 and the lentiviral Vpx protein,“ *Cell Host Microbe*, Bd. 11, Nr. 2, pp. 205-217, 2012.
- [60] S. J. Neil und et al., „An interferon-alpha-induced tethering mechanism inhibits HIV-1 and Ebola virus particle release but is counteracted by the HIV-1 Vpu protein,“ *Cell Host Microbe*, Bd. 2, Nr. 3, pp. 193-203, 2007.
- [61] K. Peng und et al., „Quantitative microscopy of functional HIV post-entry complexes reveals association of replication with the viral capsid,“ *eLIFE*, 2014.
- [62] N. Arhel, „Revisiting HIV-1 uncoating,“ *Retrovirology*, Bd. 7, Nr. 96, 2010.
- [63] J. L. Mbisa, „Real-Time PCR Analysis of HIV-1 Replication Post-entry events,“ *Methods in Molecular Biology*, pp. 485:55-72, 2009.
- [64] V. Lausch, *Etablierung eiens Verfahrens zur Kombination der Elektronenmikroskopie (EM) mit der Spitzenverstärkten RAMAN-Spektroskopie (TERS) sowie Untersuchungen zum Infektionsprozess und der Ultrastruktur des Humanen Endogenen Retrovirus K (HERV-K); Dissertation*, Berlin: Robert Koch Institute, 2013.
- [65] N. Bannert, O. Hohn und K. Hanke, „HERV-K (HML-2), the best preserved family of HERVs: endogenization, expression, and implications in health and disease,“ *Frontiers in Oncology*, Bd. 3, Nr. 246, 2013.
- [66] R. Lower, J. Lower und R. Kurth, „The viruses in all of us: characteristics and biological significance of human endogenous retrovirus sequences,“ *PNAS*, Bd. 93, Nr. 11, pp. 5177-5184, 1996.
- [67] J. F. Hughes und J. M. Coffin, „Human endogenous retrovirus K solo-LTR formation and insertional polymorphisms: implications for human and viral evolution,“ *PNAS*, Bd. 101, Nr. 6, pp. 1668-1672, 2004.
- [68] J. P. Stoye, „Endogenous retroviruses: still acitve after all these years?,“ *Current Biology*, Bd. 11, Nr. 22, pp. R914-916, 2001.

- [69] R. Van Nie, A. A. Verstraeten und J. De Moes, „Genetic transmission of mammary tumour virus by GR mice,“ *International Journal of Cancer*, Bd. 19, Nr. 3, pp. 383-390, 1977.
- [70] N. de Parseval und T. Heidmann, „Human endogenous retroviruses: from infectious elements to human genes,“ *Cytogenetic and Genome Research*, Bd. 110, Nr. 1-4, pp. 318-332, 2005.
- [71] S. S. Kalter und et al., „Brief communication: C-type particles in normal human placentas,“ *Jorunal of National Cancer Institute*, Bd. 50, Nr. 4, pp. 1081-1084, 1973.
- [72] D. Bierwolf und et al., „[C-type-like particles in normal human placentas (author's translation)],“ *Archiv Geschwulstforschung*, Bd. 45, Nr. 7, pp. 628-633, 1975.
- [73] F. Arnaud und et al., „Coevolution of endogenous betaretroviruses of sheep and their host,“ *Cell Molecular Life Sciences*, Bd. 65, Nr. 21, pp. 3422-3432, 2008.
- [74] N. Bannert und R. Kurth, „The Evolutionary Dynamics of Human Endogenous Retroviral Families,“ *Annual Review of Genomics and Human Genetics*, Bd. 7, pp. 149-173, 2006.
- [75] N. Bannert, N. Beimforde, K. Hanke, I. Ammar und R. Kurth, „Molecular cloning and functional characterization of the human endogenous retrovirus K113,“ *Virology*, Bd. 371, Nr. 1, pp. 216-225, 2008.
- [76] . R. P. Subramanian, J. H. Wildschutte, C. Russo und J. M. Coffin, „Identification, characterization, and comparative genomic distribution of the HERV-K (HML-2) group of human endogenous retroviruses,“ *Retrovirology*, pp. 8 - 90, 2011.
- [77] R. Belshaw, V. Pereira, A. Katzourakis, G. Talbot, J. Paces, A. Burt und M. Tristem, „Long-term reinfection of the human genome by endogenous retroviruses,“ *PNAS*, Bd. 101, Nr. 14, pp. 4894-4899, 2004.
- [78] Turner und et al., „Insertional polymorphisms of full-length endogenous retroviruses in humans,“ *Current Biology*, Bd. 11, Nr. 19, pp. 1531-1535, 2001.
- [79] P. Perot, N. Mugnier, C. Montgiraud, J. Gimenez, M. Jaillard, B. Bonnaud und et al., „Microarray-based sketches of the HERV transcriptome landscape,“ *PLoS One*, Bd. 7, Nr. 6, 2012.

- [80] K. Boller, K. Schonfeld, S. Lischer, N. Fischer, A. Hoffmann, R. Kurth und et al., „Human endogenous retrovirus HERV-K113 is capable of producing intact viral particles,“ *Jornal of General Virology*, Bd. 89, Nr. 2, pp. 567-572, 2008.
- [81] W. Li, A. Nath und et al., „Human endogenous retrovirus-K contributes to motor neuron disease,“ *Science Translational Medicine*, Bd. 7, Nr. 307, 2015.
- [82] A. Serafino, E. Balestrieri, P. Pierimarchi, C. Matteucci , G. Moroni, E. Oricchio und et al., „The activation of human endogenous retrovirus K (HERV-K) is implicated in melanoma cell malignant transformation,“ *Experimental Cell Research*, Bd. 315, Nr. 5, pp. 849-862, 2009.
- [83] K. Iramaneerat, P. Rattanatunyong, N. Khemapech, S. Triratanachat und A. Mutirangura, „HERV-K hypomethylation in ovarian clear cell carcinoma is associated with a poor prognosis and platinum resistance,“ *International Journal of Gynecological Cancer*, Bd. 21, Nr. 1, pp. 51-57, 2011.
- [84] P. Kramer, V. Lausch, A. Volkwein, K. Hanke, O. Hohn und N. Bannert, „The human endogenous retrovirus K (HML-2) has a broad envelope-mediated cellular tropism and is prone to inhibition at a post-entry, pre-integration step,“ *Virology*, Bd. 487, Nr. 0, pp. 121-128, 2016.
- [85] K. Hanke, P. Kramer, S. Seeher, N. Beimforde, R. Kurth und N. Bannert, „Reconstitution of the Ancestral Glycoprotein of a Human Endogenous Retrovirus-K and Modulation of its Functional Activity by Truncation of the Cytoplasmic Domain,“ *Journal of Virology*, Bd. 83, Nr. 24, pp. 12790 - 12800, 2009.
- [86] U. Linz, U. Delling und H. Rubsamen-Waigmann, „Systematic studies on parameters influencing the performance of the polymerase chain reaction,“ *Journal of clinical chemistry and clinical biochemistry*, Bd. 4, Nr. 3, pp. 5-13, 1990.
- [87] S. Palmer, A. P. Wiegand und F. Maldarelli, „New real-time reverse transcriptase-initiated PCR assay with single-copy sensitivity for human immunodeficiency virus type 1 RNA in plasma,“ *Journal of Clinical Microbiology*, pp. 4531-4536, 2003.
- [88] J. L. Mbisa, „Real-Time PCR Analysis of HIV-1 Replication Post-entry Events,“ *Methods in Molecular Biology*, Nr. 485, pp. 55-72, 2009.

- [89] P. Kramer, „Untersuchungen zum Hüllprotein und dem Tropismus des humanen endogenen Retrovirus K,“ Robert Koch-Institut, Berlin, 2011.
- [90] J. Ongradi, J. Szilagyi, H. Laird, A. Horvath und M. Bendinelli, „Unique morphological alterations of the HTLV-1 transformed C8166 cells by infection with HIV-1,“ *Pathology and Oncology Research*, Nr. 6, pp. 27-37, 2000.
- [91] R. Behrendt, U. Fiebig, S. Norley, L. Gurtler, R. Kurth und J. Denner, „A neutralization assay for HIV-2 based on measurement of provirus integration by duplex real-time PCR,“ *Journal of Virology Methods*, Bd. 159, Nr. 1, pp. 40-46, 2009.
- [92] T. Okimoto, T. Friedmann und A. Miyanochara, „VSV-G envelope glycoprotein forms complexes with plasmid DNA and MLV retrovirus-like particles in cell-free conditions and enhances DNA transfection,“ *Molecular Therapy*, Bd. 4, Nr. 3, pp. 232-238, 2001.
- [93] P. Kramer, *Untersuchungen zum Hüllprotein und dem Tropismus des humanen endogenen Retrovirus K (Disputation)*, Berlin: Robert Koch-Institut, 2011.
- [94] M. S. Malnati, G. Scarlatti, F. Gatto, F. Salvatori, G. Cassina, T. Rutigliano, R. Volpi und P. Lusso, „A universal real-time PCR assay for the quantification of group-M HIV-1 proviral load,“ *Nature Protocols*, Bd. 3, pp. 1240-1248, 2008.
- [95] T. C. Pierson, T. L. Kieffer, C. T. Ruff, C. Buck, S. J. Gange und R. F. Siliciano, „Intrinsic Stability of Episomal Circles Formed during Human Immunodeficiency Virus Type 1 Replication,“ *Journal of Virology*, Bd. 76, Nr. 8, pp. 4138-4144, 2002.
- [96] S. L. Butler, E. P. Johnson und F. D. Bushman, „Human Immunodeficiency Virus cDNA Metabolism: Notable Stability of Two-Long Terminal Repeat Circles,“ *Journal of Virology*, Bd. 76, Nr. 8, pp. 3739-3747, 2002.
- [97] T. Brady, Y. N. Lee, K. Ronen, N. Malani, C. C. Berry, P. D. Bieniasz und F. D. Bushman, „Integration target site selection by a resurrected human endogenous retrovirus,“ *Genes & Development*, Bd. 23, pp. 633-642, 2009.
- [98] M. Langenegger, *Generation of a HERV-K (HML-2) reporter construct with a unique mutation in the U3-region of the 3'LTR (project work)*, Berlin: Humboldt-Universität zu Berlin, 2016.

-
- [99] M. Dewannieux und et al., „Identification of an infectious progenitor for the multiple-copy HERV-K human endogenous retroelements,“ *Genome Research*, Bd. 16, Nr. 12, pp. 1548-1556, 2006.
- [100] Y. N. Lee und P. D. Bieniasz, „Reconstitution of an infectious human endogenous retrovirus,“ *PLoS Pathogens*, Bd. 3, Nr. 1, p. 10, 2007.
- [101] D. Marchant, S. J. D. Neil und A. McKnight, „Human immunodeficiency virus type 1 and 2 have different replication kinetics in human primary macrophage culture,“ *Journal of General Virology*, Bd. 87, pp. 411-418, 2006.
- [102] S. L. Butler, M. S. Hansen und F. Bushman, „A quantitative assay for HIV DNA integration in vivo,“ *Nature Medicine*, Bd. 7, pp. 631-634, 2001.
- [103] S. Y. Kim, R. Byrn, J. Groopman und D. Baltimore, „Temporal aspects of DNA and RNA synthesis during human immunodeficiency virus infection: evidence for differential gene expression,“ *Journal of Virology*, Bd. 63, pp. 3708-3717, 1989.
- [104] A. Meyerhans, T. Breinig, J.-P. Vartanian und S. Wain-Hobson, „Forms and Function of Intracellular HIV DNA,“ [Online]. Available: www.hiv.lanl.gov/content/index.
- [105] D. Dube, R. Contreras-Galindo, S. He, S. R. King, M. J. Gonzalez-Hernandez, S. D. Gitlin, M. H. Kaplan und D. M. Markovitz, „Genomic Flexibility of Human Endogenous Retrovirus Type K,“ *Journal of Virology*, Bd. 88, Nr. 17, pp. 9673-9682, 2014.
- [106] M. C. Strain, S. M. Lada, T. Luong, S. E. Rought, S. Gianella, V. H. Terry, C. A. Spina, C. H. Woelk und D. D. Richman, „Highly Precise Measurement of HIV DNA by Droplet Digital PCR,“ *PLOS One*, Bd. 8, Nr. 4, 2013.
- [107] G. H. R., *Electron microscopy of HIV-1*, Robert Koch-Institute.
- [108] F. Barre-Sinoussi und et al., „Isolation of a T-lymphotropic retrovirus from a patient at risk for acquired immune deficiency syndrome (AIDS),“ *Science*, Bd. 4599, Nr. 220, pp. 868-871, 1983.
- [109] „New, aggressive strain of HIV discovered in Cuba,“ *CBS News*, 2015.
- [110] N. Yan und Z. J. Chen, „Intrinsic antiviral immunity,“ *Nature Immunology*, Bd. 13, Nr. 3, pp. 214-222, 2012.
-

-
- [111] K. A. Matreyek und A. Engelman, „Viral and cellular requirements for the nuclear entry of retroviral preintegration nucleoprotein complexes,“ *Viruses*, Bd. 5, pp. 2483-2511, 2013.
- [112] Z. Ambrose und C. Aiken, „Hiv-1 uncoating: connection to nuclear entry and regulation by host proteins,“ *Virology*, Bde. %1 von %2454-455, pp. 371-379, 2014.
- [113] L. Hilditch und G. J. Towers, „A model for cofactor use during HIV-1 reverse transcription and nuclear entry,“ *Current Opinion in Virology*, Bd. 4, pp. 32-36, 2014.
- [114] D. McDonald, M. A. Vodicka, G. Lucero, T. M. Svitkina, G. G. Borisy, M. Emerman und T. J. Hope, „Visualization of the intracellular behavior of HIV in living cells,“ *The Journal of Cell Biology*, Bd. 159, pp. 441-452, 2002.
- [115] M. Lusic, B. Marini, H. Ali, B. Lucic, R. Luzzati und M. Giacca, „Proximity to PML nuclear bodies regulates HIV-1 latency in CD4+ T cells,“ *Cell Host + Microbe*, Bd. 13, pp. 665-677, 2013.
- [116] I. Solovei und M. Cremer, „3D-FISH on cultured cells combined with immunostaining,“ *Methods in molecular biology*, Bd. 659, pp. 117-126, 2010.
- [117] J. Tilton und et al., „A combination HIV reporter virus system for measuring post-entry event efficiency and viral outcome in primary CD4+ T cell subsets,“ *Journal of Virology Methods*, Bd. 195, pp. 164-169, 2014.
- [118] M. d. M. Gutierrez, M. G. Mateo, F. Vidal und P. Domingo, „The toxicogenetics of antiretroviral therapy: the evil inside,“ *Current Medicinal Chemistry*, Bd. 18, pp. 209-219, 2011.
- [119] D. Nolan, „Metabolic complications associated with HIV protease inhibitor therapy,“ *Drugs*, Bd. 63, pp. 2555-2574, 2003.
- [120] D. O. Hohn, *Retroviren: Gefährten, Revoluzzer und Massenmörder (Presentaion)*, Berlin: Robert Koch-Institut, Zentrum für HIV und Retrovirologie - FG 18, 2011.
- [121] P. Bremer, *Etablierung und Validierung von Methoden zur Quantifizierung der proviralen HIV-1-DNA in humanen CD4+-T-Gedächtniszellen (Masterarbeit)*, Berlin: Robert Koch-Institut, 2016.
-

-
- [122] „ACADEMIC - Academic dictionaries and encyclopedias,“ [Online]. Available: <http://de.academic.ru/dic.nsf/dewiki/1468054>. [Zugriff am 10th July 2016].
- [123] J. M. Carr, K. M. Cheney, C. Coolen, A. Davis, D. Shaw, W. Ferguson, G. Chang, G. Higgins, C. Burrell und P. Li, „Development of Methods for Coordinate Measurement of Total Cell-Associated and Integrated Human Immunodeficiency Virus Type 1 (HIV-1) DNA Forms in Routine Clinical Samples,“ *Journal of Clinical Microbiology*, Bd. 45, Nr. 4, pp. 1288-1297, 2007.

Acknowledgement

My sincere thanks and gratitude go to Prof. Dr. Norbert Bannert for giving me the opportunity to accomplish my Master's thesis in his research group at the Robert Koch-Institute. I would like to thank Prof. Dr. Peter Hegemann and Prof. Dr. Norbert Bannert for assessing my Master's thesis. My deepest gratefulness belongs to Dr. Oliver Hohn for his supervision and advice during my time at the institute. Many thanks also go out to all members of the department for their help and company- work would only have been half as fun without you!

Declaration of Authorship

The work underlying this thesis has been accomplished at the Robert Koch-Institute in Berlin between 1st January 2016 and 20th July 2016.

I hereby declare that I have written this thesis without the assistance of any other person, using only the sources indicated.

Berlin, 21st July 2016

Signature

Mirjam Yasemine Langenegger